SOUND TRANSIT LINK LIGHT RAIL PROJECT

North Link
Hi-Lo Mitigation EMI Report

Prepared by:

LTK Engineering Services

Document Number: ***LTK.ST.0406.001***
April 2006

TABLE OF CONTENTS

TABLES

FIGURES

APPENDICES

1 FOREWORD

This report presents the results of investigations of the sources of stray magnetic fields ("B-fields") likely to be caused by the North Link rail transit line operating through the University of Washington campus in Seattle. It makes recommendations for design techniques and operational procedures for minimizing the levels of those fields. This report summarizes the results of a number of earlier reports, analyses, studies, and tests completed by numerous individuals, including the author of this report, Dr. F. Ross Holmstrom. Additional inputs were provided by Dr. Luciano Zaffanella of Enertech; Dr. David Fugate of ERM, Inc.; Dr. T. Dan Bracken, EMI consultant to the UW; Chris Fassero, James Irish, Tracy Reed, and Steve Proctor of Sound Transit; and LTK systems engineers.

2 EXECUTIVE SUMMARY

While offering many potential benefits, North Link has the potential to affect research activities at a number of UW laboratories. Magnetic fields, arising from the propulsion currents measured in the thousands of amperes flowing from power substations to the electrically powered trains, could disrupt sensitive apparatus. Perturbation to Earth's magnetic field, caused by the motion of steel bodied rail cars passing near laboratories, is another potential source of magnetic field disruption.

Magnetic field strength due to propulsion currents is referred to as B_{prop} in this report, and magnetic field strength due to geomagnetic field perturbations is referred to as B_{ptb}. Both are collectively referred to as "stray B-fields", and are stated in units of gauss (G) or milli-gauss (mG). In the SI system of units widely used for scientific and technical work magnetic field strength is stated in units of tesla (T). One T equals 10^4 G. By way of orienting the reader to B-field magnitudes, note that in the northern US Earth's B-field has a magnitude of approximately 0.6 G. And a straight conductor carrying 1000 amperes of current will produce a B-field circulating around it with a strength of 0.16 G at a distance of one meter (3.28 ft). Because of their time varying nature, stray B-fields with levels as small as 0.1 mG, or one six thousandth of Earth's B-field level, could compromise the accuracy of some of the UW's most sensitive research equipment.

If no special techniques are employed to attenuate B_{prop} field levels, they will form the predominant part of stray B-fields. Through careful design of the traction power system, B_{prop} fields can be greatly reduced, leaving the B_{ptb} fields to predominate. The only practical way of dealing with the B_{ptb} fields is to allow sufficient distance between tracks and sensitive laboratories.

General practice in the transit field to date has been to not employ techniques to attenuate B_{prop} fields. The only tool used to provide acceptable field levels at sensitive laboratory sites has been to locate laboratories and transit tracks far enough apart. One manufacturer of sensitive lab equipment similar to that employed at the UW specifies a separation of 800 ft (244 meters) between rail transit tracks and the equipment.

Without mitigation, the thousands of amperes of propulsion current flowing in the loops of conductor formed by the overhead contact wire and running rails with LRVs traversing the area, would lead to B_{prop} field levels that would exceed UW specs practically everywhere on campus, no matter where on campus North Link were located. The B_{prop} fields from these large loops have strength proportional to the height of the loops times current carried, and inversely proportional to the square of the distance from the track.

To mitigate B_{prop} fields, North Link is considering a technique, locally dubbed "Hi-Lo mitigation", that is essentially the same as that employed by a light rail line in Bielefeld, Germany running past the University of Bielefeld, in operation for a number of years; and another presently in planning for the Cross County extension of the St. Louis

MetroLink, to run past the main campus of Washington University in St. Louis, expected to commence service in 2006.

The UW and Sound Transit are considering a route for North Link through the UW campus. The route and approximate limits of mitigation are shown in Figure 2.1.

The following assumptions are used in this report as a basis for calculations:

- Four car trains operating at full current of 2800 Amps, one train in each direction in EMI Mitigation area, one train in each direction north of and one train in each direction south of EMI mitigation area
- Contact wire wear of 30% from new condition
- Special considerations to minimize wire splice contact resistance
- Minimizing stray current loss through ground paths

A special technique for measuring the health of rail-to-ground resistance is being used for Central Link Light Rail and will be utilized for North Link. The health of the rail-to-ground resistance is a major deterrent to stray current propagation. Specialized equipment will be located at trackside near traction power substations that will remotely monitor the integrity of the insulation properties of the running rail fasteners.

Table 2.1 gives the UW requested stray B-field levels at critical laboratories, the B-field levels that would result if no special B-field mitigation techniques were employed and stray B-field levels predicted to be achieved by Hi-Lo B-field mitigation. As can be seen from the table, UW desired stray B-field levels can be met at all but Wilcox and Roberts Halls and the ME Building and Annex. These failing locations and B-field values are highlighted in bold in Table 2.1. Without B-field mitigation it is seen that stray B-field level(s) exceed the UW thresholds at practically all critical lab locations.

B-field levels resulting from employment of Hi-Lo B-field mitigation are shown two ways in Table 2.1; first assuming that the geographical extent over which Hi-Lo mitigation techniques are employed is infinite; and again assuming that the Hi-Lo mitigation region extends north only as far as a point on the North Link right of way just SW of the intersection of University Way and NE 45th St., and south for a distance of approx. 450 meters (1500 ft) from the southern end of the University of Washington station. The stray B-field values resulting from the finite extent of Hi-Lo mitigation include contributions from trains operating north of the NE 45th St. station and south of the University of Washington station simultaneously with trains running northbound and southbound through the UW campus.

Two additional mitigation measures that could be used if necessary are limiting maximum power draw of trains passing under the University campus and limiting light rail operations to only one train under the campus at a time. However, Sound Transit has indicated that both of these measures would be used only if absolutely necessary to reduce impacts to the most sensitive buildings. This is because they would restrict the

ability of the system to carry higher passenger loads in the future and during special events at Husky Stadium and make operations more difficult overall.

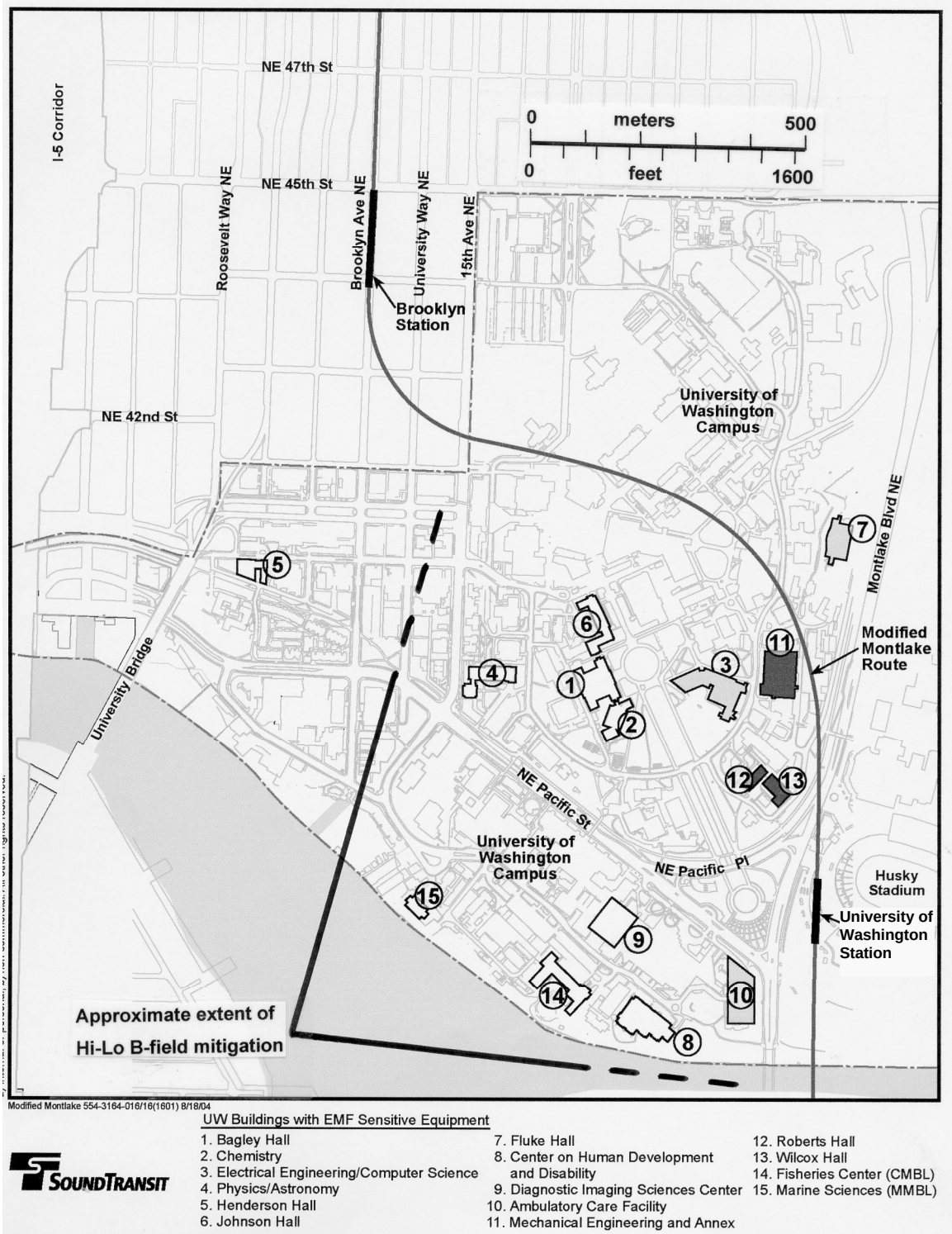

Figure 2.1 UW campus map showing laboratory buildings with critical stray B-field requirements, the North Link right-of-way, and the approximate required extent of Hi-Lo B-field mitigation

Table 2.1 Mitigated and unmitigated North Link stray B-field levels at critical UW labs.

Lab	UW B-field spec levels, mG	Unmitigated B-field mG	Infinite-extent Hi-Lo mitigated B-field mG*	Finite-extent Hi-Lo mitigated B-field mG***
Bagley Hall	0.1	**0.562**	0.033	0.076
Chemistry Bldg.	0.1	**0.530**	0.032	0.066
EE-CS	5.0	3.98	0.184	0.217
Physics-Astron.	0.5	0.376	0.017	0.070
Johnson Hall	5.0	1.144	0.059	0.110
Fluke Hall	0.3	**4.27**	0.223	0.256
ME Bldg.	0.2	**18.75**	**0.875**	**0.907**
ME Rm. 135	0.2	**6.37**	**0.300**	**0.332**
ME Annex	0.2	**36.3**	**1.598**	**1.630**
Roberts Hall	0.1	**6.01**	**0.284**	**0.319**
Wilcox Hall	0.1	**17.29**	**0.810**	**0.846**
Henderson**	**	0.370	0.016	0.142
CHDD	0.3	**0.948**	0.056	0.183
Diagn. Imaging	5.0	0.494	0.030	0.087
Surgery Pavilion	1.0	**5.44**	0.344	0.471
Fisheries Ctr.	0.1	**0.315**	0.019	0.093
Marine Science	1.0	0.089	0.005	0.045
Roberts-W. half	0.1	**4.37**	**0.199**	**0.234**

Notes: *Hi-Lo mitigated B-field was calculated with 30 percent overhead contact wire wear.

**At Henderson Hall UW spec is |dB,tot/dt| Ò0.2 mG/sec.

***Includes B-fields from trains operating north and south of campus.

Levels shown in bold in Table 2.1 are levels that exceed UW spec B-field levels at the respective labs. Lab names shown in bold indicate that Hi-Lo mitigated B-field levels at the respective labs do not meet UW specs. Note that for the Hi-Lo mitigation endpoints chosen for this modeling the labs that passed the UW spec limits for the case of Hi-Lo mitigation of infinite extent also passed when the extent was made finite.

The specific results for B-fields mitigated by a Hi-Lo mitigation region of finite extent given in Table 2.1 depend strongly on the chosen Hi-Lo mitigation endpoints as well as on the assumptions of worst-case train currents locations for trains operating north and south of the campus.

The final northern and southern ends of the Hi-Lo mitigation will be determined at the time of final design and will include refined estimates of worst case train currents and locations for trains on campus and north and south of the campus. With the above endpoints the Hi-Lo mitigation region stretches approx. 1800 meters (5900 ft) along the curved North Link right of way. However, more refined modeling could result in the estimate of required length decreasing to approximately 1500 meters (5000 ft).

The B-field modeling reported here for the Hi-Lo B-field mitigated case has been done assuming that the overhead contact wire wear had reduced its cross sectional area by 30 percent from its initial value.

Table 2.2 gives the value of a Hi-Lo mitigation "compliance factor" CF for each of the four most critical laboratories. Based on a combination of UW spec level and location, of the labs at which UW spec B-field levels can be met, these labs are Bagley Hall, the Chemistry Bldg., Fluke Hall and the Fisheries Center. CF is the number by which calculated northbound plus southbound propulsion B-fields arising from currents in the Hi-Lo mitigated region must be multiplied to bring total stray B-field up to the UW specified level. The factor must have a value greater than 1 for total stray B-fields to meet the UW requested thresholds. This factor serves as an overall indication of the degradation from modeled behavior that can occur before overall stray B-fields fail to

Table 2.2 Values of Hi-Lo mitigation compliance factor CF for four critical UW labs.

Lab	CF
Bagley Hall	2.0
Chemistry Bldg.	2.3
Fluke Hall	1.3
Fisheries Center	2.0

comply with the UW limits. A larger factor indicates less sensitivity and greater leeway. CF was calculated by arbitrarily multiplying calculated Hi-Lo mitigated propulsion B-fields by a factor before adding those fields to the others to produce the overall totals, and then by increasing the value of the factor until the stray B-field totals equaled the UW spec limits. The minimum CF recommended to comply with UW specified B-field limits and allow a sufficient factor of safety is 2.0.

The purpose of the extensive modeling performed to yield the results summarized in Table 2.1 is to document the prediction that Hi-Lo B-field mitigation can produce greatly reduced propulsion B-field levels where needed. In practice at most critical laboratories the peak levels of propulsion B-field that actually occur will be due to the distances from those labs to the endpoints of Hi-Lo mitigation near the north and south ends of the campus.

The effectiveness of Hi-Lo B-field mitigation depends upon the avoidance of propulsion currents leaking into the ground. A special technique for measuring the health of rail-to-ground resistance is being used for Central Link Light Rail and will be utilized for North Link. The health of the rail-to-ground resistance is a major deterrent to stray current propagation. Specialized equipment will be located at trackside near traction power substations that will remotely monitor the integrity of the insulation properties of the running rail fasteners.

The calculations summarized in Table 2.1 were performed assuming conductor sizes and positions as given in the circuit design presently regarded as the most likely one to be implemented. Whereas prior modeling of stray B-fields was performed to assess the feasibility of various routes and B-field mitigation techniques, the modeling for this report was performed including the effects of the industry standard value of 30 percent maximum contact wire wear. Consequently the total stray B-field values are larger than those previously published.

The Hi-Lo mitigation technique uses a large diameter cable buried beneath the center of each track to carry most of the current from substation to train, while the remaining fraction of current will flow in the overhead contact wire. Current will flow in one sense around the loop formed by overhead contact wire, train and running rails, and in the opposite sense around the loop formed by the buried cable, train and running rails. Since these loops are located close together, their magnetic fields will be nearly equal in spatial variation and their field lines will point in practically opposite directions.

If the product of overhead contact wire height above the rails times its electrical conductance equals the product of buried cable depth below the rails times its conductance, the B_{prop} fields from the top and bottom loops will be nearly equal in magnitude and opposite in direction, and they will largely cancel. The degree of reduction of B_{prop} fields depends on the precision with which the fields from the top and bottom loops can be made to cancel.

An array of "riser cables" spaced tens of meters apart down the track will carry train current from the buried cable up to the overhead contact wire at points very near the train. Currents in the risers nearest the train will lead to additional B_{prop} fields of a very localized nature that are smaller and fall off more rapidly with distance than the original unmitigated B_{prop} fields.

At points on the right-of-way well away from critical laboratories standard propulsion circuitry will be used, with currents flowing to trains through the normal overhead messenger and contact wires. The locations of the end points of Hi-Lo mitigation depend upon B-fields caused by semi-infinite current carrying loops of full contact wire height falling off sufficiently with distance so that maximum stray B-field levels at critical labs are not exceeded. The end of Hi-Lo mitigation at the north end of campus is set by required distance from Bagley Hall, and at the south end by required distance from the Fisheries Center. The approximate required extent of Hi-Lo B-field mitigation is noted in Figure 2.1. A final determination of the extent of Hi-Lo mitigation will be made at the time of final design.

In November 2003, measurements were made on the UW campus to assess the existing magnetic field environment at locations near sensitive laboratories. These results are summarized in this report. Existing stray B-field levels on the UW campus arising from geomagnetic field perturbations caused by motor vehicles were examined and measured in order to obtain information on the presently existing stray B-field environment on the campus. The focus of measurements was on B_{ptb} levels arising from the passage of articulated diesel transit buses with a length of approx. 60 ft (18 m). These ply Stevens Way and certain connecting roads in large number, especially during rush hours, and are among the largest of vehicles to be found routinely on the campus.

It was found that the Mechanical Engineering Bldg. is so close to Stevens way that existing B_{ptb} levels from the buses already exceed the UW stray B-field specs throughout much of the building. Other buildings are farther from Stevens Way but have adjacent parking lots. Cars, vans and light trucks in these parking lots were found to yield B_{ptb} levels considerably higher than the UW stray B-field specs at the exterior walls of Fluke, Roberts and Wilcox Halls. Similar B-field levels could be expected in the ME Annex. While it is true that the B_{ptb} fields arising from cars, vans and light trucks fall off with distance much more rapidly than those from large transit buses, these results nonetheless indicate inconsistency in the establishment of the UW's stray B-field specs. If researchers envision the flexibility to locate the most B-field sensitive instruments anywhere in the interior of many UW buildings, changes will have to be made to traffic and parking nearby these buildings.

Although the purpose of this report is to provide technical information and not make recommendations, the author will discuss a number of implications of the results given in Table 2.1. Given the alignment of the North Link right-of-way considered in this report, North Link B_{ptb} field levels by themselves will exceed the UW spec limits for overall stray B-fields in Wilcox Hall, the ME Annex, and that part of the ME Bldg. closest

to the North Link right-of-way. Bus traffic on Stevens Way already causes B_{ptb} levels above the total UW B-field spec limits in the remainder of the ME Bldg.

If the present and future B-field sensitive research activities in ME, ME Annex, Wilcox, and Roberts are moved elsewhere, UW B-field specs could be met at all critical UW labs. The lab with the lowest B_{prop} compliance factor would then be Fluke Hall, with a factor of 1.3, meaning that an increase in B_{prop} levels by that factor would bring overall stray “B-fields to that level at Fluke Hall.

The long-term effectiveness of the program to mitigate B_{prop} fields will depend specifically on the ability to achieve and maintain cancellation of the B_{prop} fields from the upper and lower loops in the Hi-Lo B-field mitigation circuit. The wear of the overhead contact wire will be the chief predictable cause of variation of B_{prop} field levels over time. Possible unpredictable causes include current imbalances caused by propulsion currents leaking through electrically degraded rubber rail cushions into the ground, and the deterioration of electrical cable splices, leading to increased values of contact resistance, and leading in turn to changes in current flow patterns.

Assurance of the long term effectiveness of stray B-field mitigation will require an effective long term preventive and corrective maintenance program. Small problems will best be dealt with before they can worsen and become disruptive. Monitoring of stray B-fields will serve as one important input to the maintenance program. The monitoring could employ permanently installed magnetic field sensors, coupled to interface computers to send the data over the internet to a centralized point. As an alternative, periodic B-field monitoring using portable B-field sensors could be employed as well when more flexibility is needed. Data analysis of the type used during testing for this program, but more automated, could provide output for assessment of B-field mitigation performance on either a continuous, real-time basis or periodic basis. The B -field sensors might be housed in suitable corners of existing UW buildings. Final development of the B-field monitoring program will require an analysis of potential monitoring sites, both permanent and temporary, on the UW campus, existing and future locations of sensitive lab equipment, and the existing and future non-North Link sources of stray B-fields that could interfere with monitoring.

We believe that with careful testing, analysis, design and construction, coupled with long term diagnosis and maintenance, the objectives for North Link stray B-field mitigation can be met.

3 PROPULSION B-FIELD MITIGATION

To develop the Hi-Lo B-field mitigation system, design concepts were employed based on the magnetic fields produced by currents flowing in conducting circuits with simple standard shapes such as infinitely long straight pairs of conductors, small conducting loops, and others described in Sec. 3.2 below. The resulting designs were analyzed by performing rigorous numerical analysis to obtain spatially varying B-fields from propulsion currents. The elements of current-caused B-field behavior are presented below, together with the techniques of numerical analysis used to calculate B-fields resulting from the Hi-Lo mitigation design. The numerical B-field results are also given.

3.1 B-Fields From Straight Finite-Length Conducting Segments

The starting point for calculation of B-fields due to currents is the Law of Biot and Savart, also attributed to Ampère, that states that in free space, a short straight incremental segment of conductor carrying current I for vector distance **dL** causes an incremental vector B-field, at a vector distance **d** from the conductor segment, as given by the relation

$$\mathbf{dB} = \frac{\mu_o I}{4\pi d^2}\mathbf{dL}\times\mathbf{a}_d = \frac{\mu_o I}{4\pi d^3}\mathbf{dL}\times\mathbf{d} \qquad (3.1)$$

as shown in Figure 3.1 [Ref. 1]. Vectors are shown in bold, magnitudes of vectors are shown in normal type, i.e., d = |**d**|, and the magnetic permeability of free space = μ_o = $4\pi \times 10^{-7}$ henries/meter. The vector $\mathbf{a}_d$ is the unit vector that points in the direction of **d**, i.e., $\mathbf{a}_d = \mathbf{d}/d$.

In the above relation, current is in amperes (A) and B-field in teslas (T). In transit applications it is useful to work in units of kilo-amperes (kA) for current and gauss (G) for B-field. Since 1 T = 10^4 G and 1 kA = 10^3 A, the above relation written using kA and G units is

$$\mathbf{dB} = \frac{I}{d^2}\mathbf{dL}\times\mathbf{a}_d = \frac{I}{d^3}\mathbf{dL}\times\mathbf{d} \qquad (3.2)$$

Magnetic field **dB** points in a direction perpendicular to the plane containing **L** and **d**. Where θ is the angle between vectors **L** and **d**, the magnitude of **dB** is given by the relation

$$dB = \frac{I dL}{d^2}\sin\theta \qquad (3.3)$$

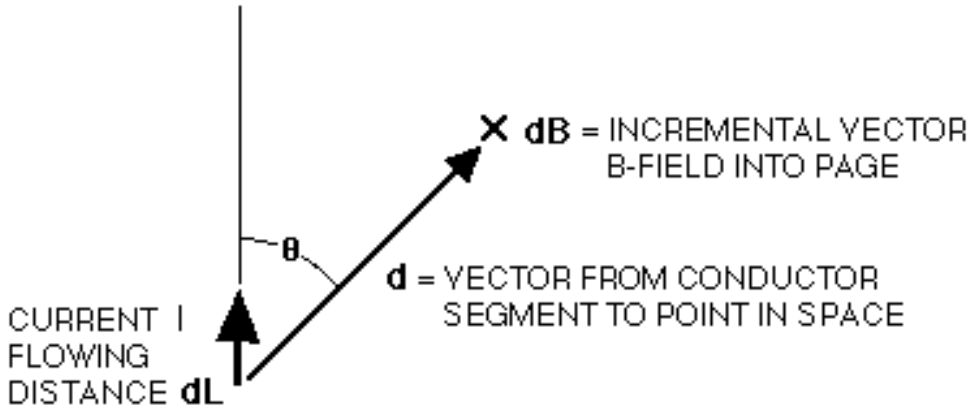

Figure 3.1 Conductor of incremental vector length dL carrying current I and creating magnetic field dB at the point indicated. The "X" is at the point where the incremental vector field dB is defined. The "X" symbol denotes that at that point vector dB points directly into the page. A "•" symbol would denote dB pointing out of the page.

Integration over the length of a straight finite-length conducting segment carrying current I from point $\mathbf{r}_1$ to point $\mathbf{r}_2$ yields the following relation for net magnetic field at point **r** in space, as pictured in Fig. 3.2:

$$\mathbf{B}(\mathbf{r}) = \frac{I}{d}(\cos\theta_1 - \cos\theta_2)\mathbf{a}_B \tag{3.4}$$

The above equation uses units of kA and G. Unit vector $\mathbf{a}_B$ points in a direction perpendicular to both **L** and $\mathbf{d}_1$. The following relations apply:

$$\mathbf{d}_1 = \mathbf{r} - \mathbf{r}_1 \quad \text{and} \quad \mathbf{d}_2 = \mathbf{r} - \mathbf{r}_2$$

$$\mathbf{L} = \mathbf{r}_2 - \mathbf{r}_1$$

$$\cos\theta_1 = \frac{\mathbf{L}\bullet\mathbf{d}_1}{Ld_1} \quad \text{and} \quad \cos\theta_2 = \frac{\mathbf{L}\bullet\mathbf{d}_2}{Ld_2} \tag{3.5}$$

$$\mathbf{a}_B = \frac{\mathbf{L}\times\mathbf{d}_1}{|\mathbf{L}\times\mathbf{d}_1|} = \frac{\mathbf{L}\times\mathbf{d}_2}{|\mathbf{L}\times\mathbf{d}_2|}$$

$$d = \frac{|\mathbf{L}\times\mathbf{d}_1|}{L} = \frac{|\mathbf{L}\times\mathbf{d}_2|}{L}$$

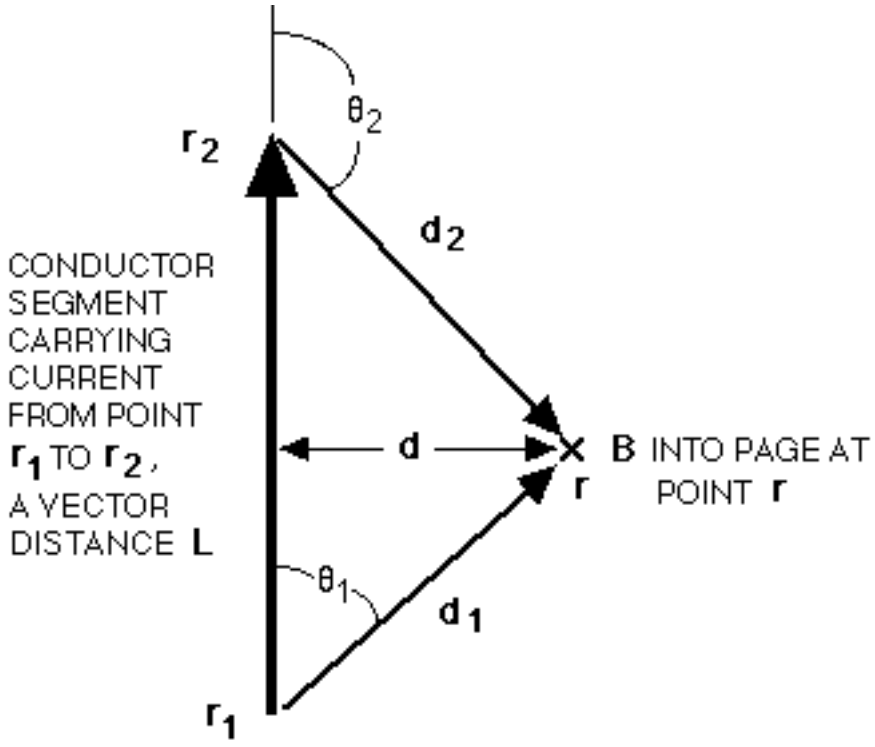

Figure 3.2 Conductor vector length L carrying current I from r1 to r2 and creating magnetic field B at point r.

For computation of B-fields it is straightforward if tedious to express locations and vectors in Cartesian (x, y, z) coordinates.

Expressions for B-fields due to finite-length current conducting segments oriented parallel to the x-, y- or z-axis are very useful. For instance, a conducting segment running parallel to the x-axis, conducting current I from point (x_1, y_1, z_1) to point (x_2, y_1, z_1) will cause B-field components at the point (x, y, z) given as follows: Define

$$d^2 = \left[(y - y_1)^2 + (z - z_1)^2\right]$$

$$d_1 = \left[(x - x_1)^2 + (y - y_1)^2 + (z - z_1)^2\right]^{1/2} \qquad (3.6)$$

$$d_2 = \left[(x - x_2)^2 + (y - y_1)^2 + (z - z_1)^2\right]^{1/2}$$

Then,

$$B_x(x,y,z) = 0$$

$$B_y(x,y,z) = +I \bullet \frac{(z-z_1)}{d^2} \left(\frac{(x-x_2)}{d_2} - \frac{(x-x_1)}{d_1} \right) \qquad (3.7)$$

$$B_z(x,y,z) = -I \bullet \frac{(y-y_1)}{d^2} \left(\frac{(x-x_2)}{d_2} - \frac{(x-x_1)}{d_1} \right)$$

Similar expressions for the B-field components due to currents in segments oriented parallel to the y-axis can be written by changing x to y, y to z, and z to x in the above relations. Then this process can be repeated to obtain expressions for B-field components arising from conductor segments parallel to the z-axis.

3.2 B-Fields From Long Straight Conductors and Loops

The B-field in the vicinity of an infinitely long straight conductor can be found by letting $\theta_1 = 0$ and $\theta_2 = 180^o$ in Eqn. 3.4, yielding the result

$$\mathbf{B}(d) = \frac{2I}{d}\mathbf{a}_\phi \qquad (3.8)$$

where unit vector $\mathbf{a}_\phi$ points in the azmuthal direction according to the right-hand rule. Note that field strength falls off as 1/d. Lines of magnetic flux are shown in Fig. 3.3

Two very long straight parallel conductors distance a apart, carrying the same current I in opposite directions give rise to B-fields at points much farther from the conductors than distance a, given by the relation

$$B(d) = \frac{2Ia}{d^2} \qquad (3.9)$$

The B-field arising from the two parallel conductors is called a 2-dimensional dipole field. Magnetic flux lines are shown in Fig. 3.4. Note that strength is proportional to conductor spacing, and it falls off as $1/d^2$. The field strength from the two conductors is smaller than that from the single conductor by a factor of (a/d).

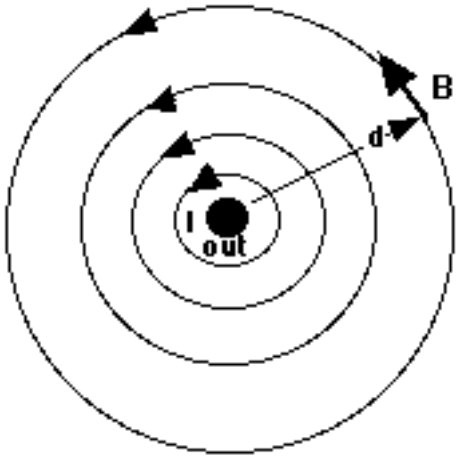

Figure 3.3 B-field lines in the vicinity of a long straight conductor carrying current I out of the page

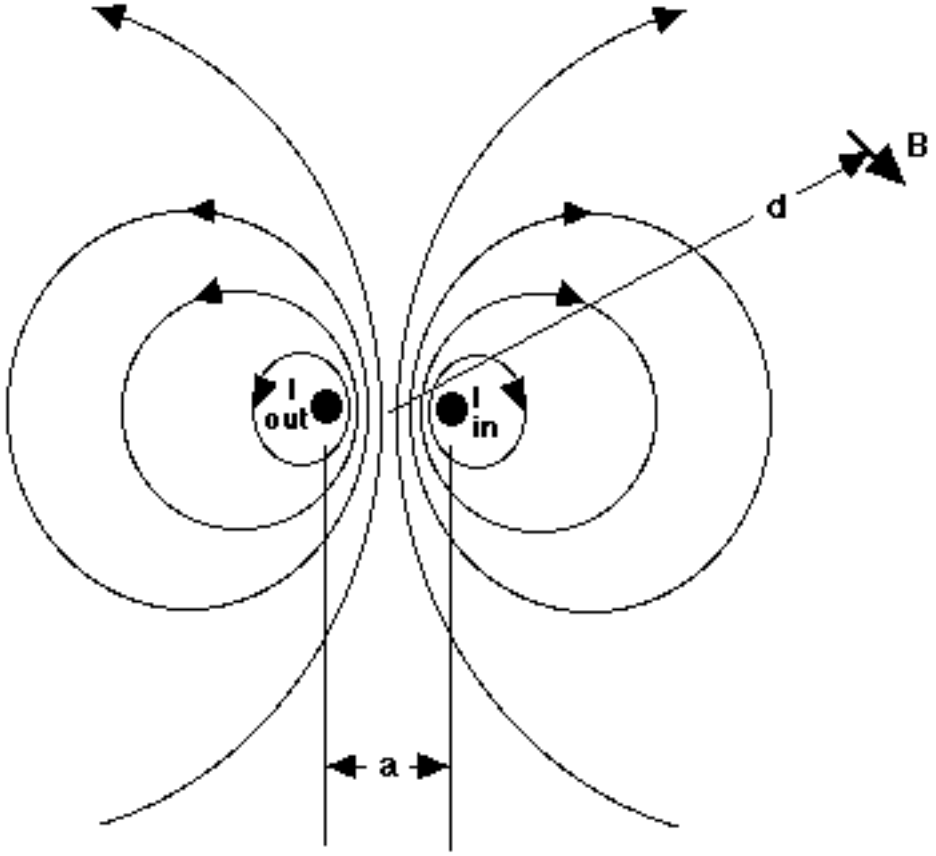

Figure 3.4 B-field lines in the vicinity of two parallel long straight conductors, one carrying current I in direction out of the page, the other carrying current I in direction into the page.

This figure also shows the approximate behavior of B-field lines on the plane containing the axis of a circular loop carrying current I out at the left and in at the right, with the axis of the loop running up the page in the center of the figure.

Four long straight parallel conductors each conducting current I and intersecting a normal plane at the corners of a square of side a as seen in Fig. 3.5 give rise to a two-dimensional magnetic field which at great distance from the conductors obeys the relation for a two-dimensional quadrupole field

$$B(d) = \frac{4Ia^2}{d^3} \qquad (3.10)$$

Note that here B falls off as $1/d^3$. And note that the fields from this four wire case are smaller than those of the previous two-wire case by a factor of (2a/d).

A conducting loop with area A gives rise to magnetic fields which far from the loop have the approximate field strength (with exact field strength depending on location relative to the axis through the center of the loop)

$$B(d) = \frac{2IA}{d^3} \qquad (3.11)$$

where d is the distance from the center point of the loop and is much greater than the distance across the loop. The loop can be any shape as long as it is in a plane. This is a 3-dimensional dipole field. Note that it falls off as $1/d^3$. Figure 3.4 also serves to show the behavior of magnetic flux lines for this case, with $A = \pi a^2/4$. At distances much greater than the loop diameter a the B-field approximates that of an ideal 3-dimensional dipole field.

At points very near a current conducting loop formed of two very long straight closely spaced conductors connected at their ends, B-fields behave according to Eqn. 3.9 for long straight conducting pairs. However, at distances much greater than the loop length, B-fields behave according to Eqn. 3.11 for conducting loops

Two coaxial circular loops each with the same product (IA) of current times area, one carrying current clockwise and the other counterclockwise, with distance a between centers, yield an approximate 3-dimensional quadrupole magnetic field strength at great distances of

$$B(d) = \frac{4IaA}{d^4} \qquad (3.12)$$

Note that here falloff with distance is as $1/d^4$, and resulting field strength is smaller than the previous single loop case by a factor of (2a/d). Fig. 3.5 also serves approximately to picture the magnetic flux lines for this case, with $A = \pi a^2/4$.

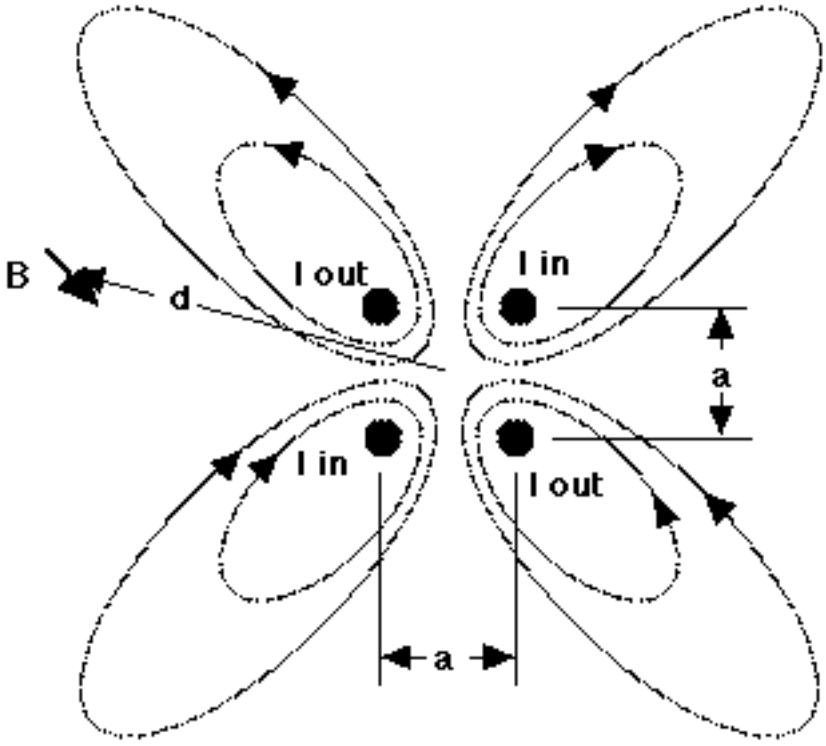

Figure 3.5 B-field lines in the vicinity of four long straight conductors carrying currents I into and out of the page.

This figure also shows the approximate behavior of B-field lines on the plane containing the axis of two circular loops, the upper one carrying current I out at the left and in at the right, and the lower one carrying current in the opposite direction, with the axis of the two loops running up the page in the center of the figure.

Inspection of these relationships shows that magnetic fields due to closely spaced conductors carrying equal and opposite currents will diminish in magnitude with increasing distance much more rapidly than those of single conductors. And fields due to loops or matched pairs of loops will fall off with successively greater rate as distance increases.

3.3 Unmitigated North Link Propulsion B-Fields

If standard DC propulsion circuitry were to be used for North Link, in the UW campus area propulsion currents would flow in the 4.3 meter high overhead contact wire from the University of Washington substation to the train cars, downward through the cars, and back to the substation through the running rails. Because of the upgrade from Montlake and Pacific to 45th and University, northbound trains are expected to draw nearly maximum current nearly all the way. Maximum current will be 2.8 kA when trains reach their ultimate length of 4 cars.

According to Eqn. 3.9, B-fields at slant distances d away from the northbound track would be as large as

$$B(d) = \frac{2 \bullet 2.8 \bullet 4.3}{d^2} = \frac{24}{d^2} \text{ gauss} \qquad (3.13)$$

Solution of the above equation for d as a function of B shows that for maximum stray B-fields in the 0.1 to 0.5 mG range specified for a number of UW laboratories, the corresponding minimum distance d ranges from 220 to 490 meters (720 to 1600 ft). Inspection of the map in Fig.2.1 shows that there is not enough space between critical lab buildings to locate a route going from near the Montlake Bridge to the corner at 45th Ave. NE and University Way.

3.4 The Hi-Lo Propulsion B-field Mitigation Design

The prime task of the Hi-Lo B-field mitigation design is to eliminate the 4.3 meter high loops carrying propulsion current from substation to trains, and thus eliminate a tremendous amount of stray B-field. As indicated by Eqn. 3.9, B-fields arising from current in very long conducting loops is directly proportional to the height or width of the loops. In the Hi-Lo design the arrangement of conductors carrying current to and from trains produces a greatly reduced net effective loop height.

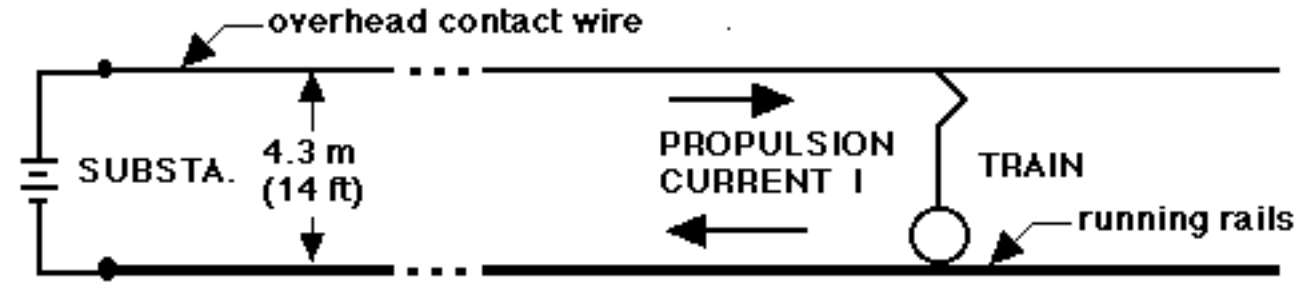

a. Un-mitigated propulsion circuit with tall, long current-carrying loop.

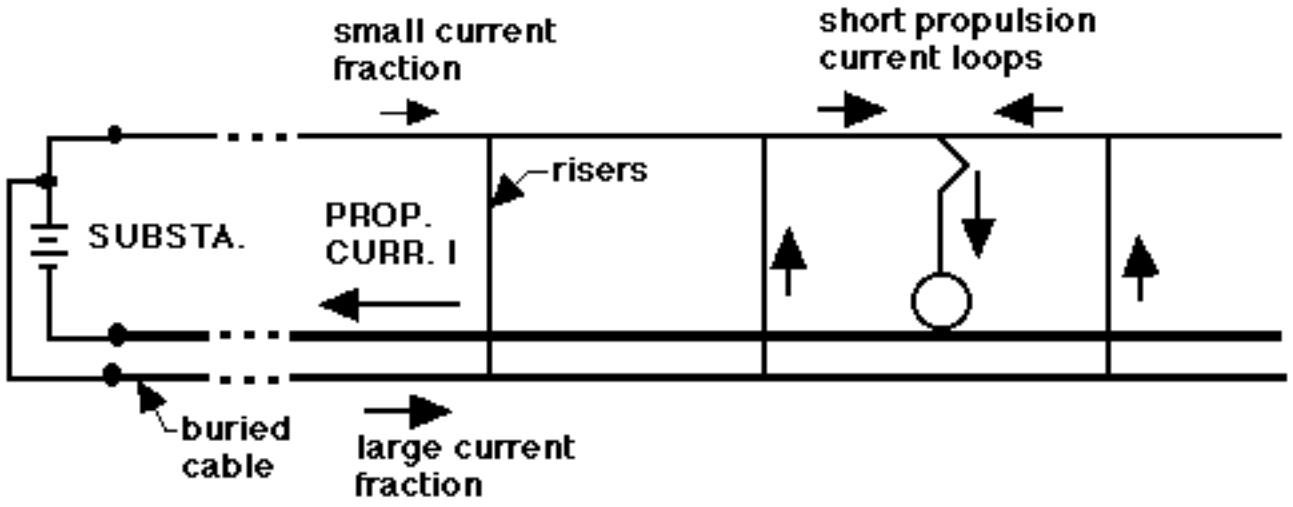

b. Hi-Lo mitigated propulsion circuit.

Figure 3.6 Unmitigated and Hi-Lo mitigated propulsion circuits for electric transit. The Hi-Lo mitigated propulsion circuit replaces the long tall current loops with an effective pair of much shorter loops. The effective height of majority of current loop from substation to train is nearly zero. Result is much lower B-field production.

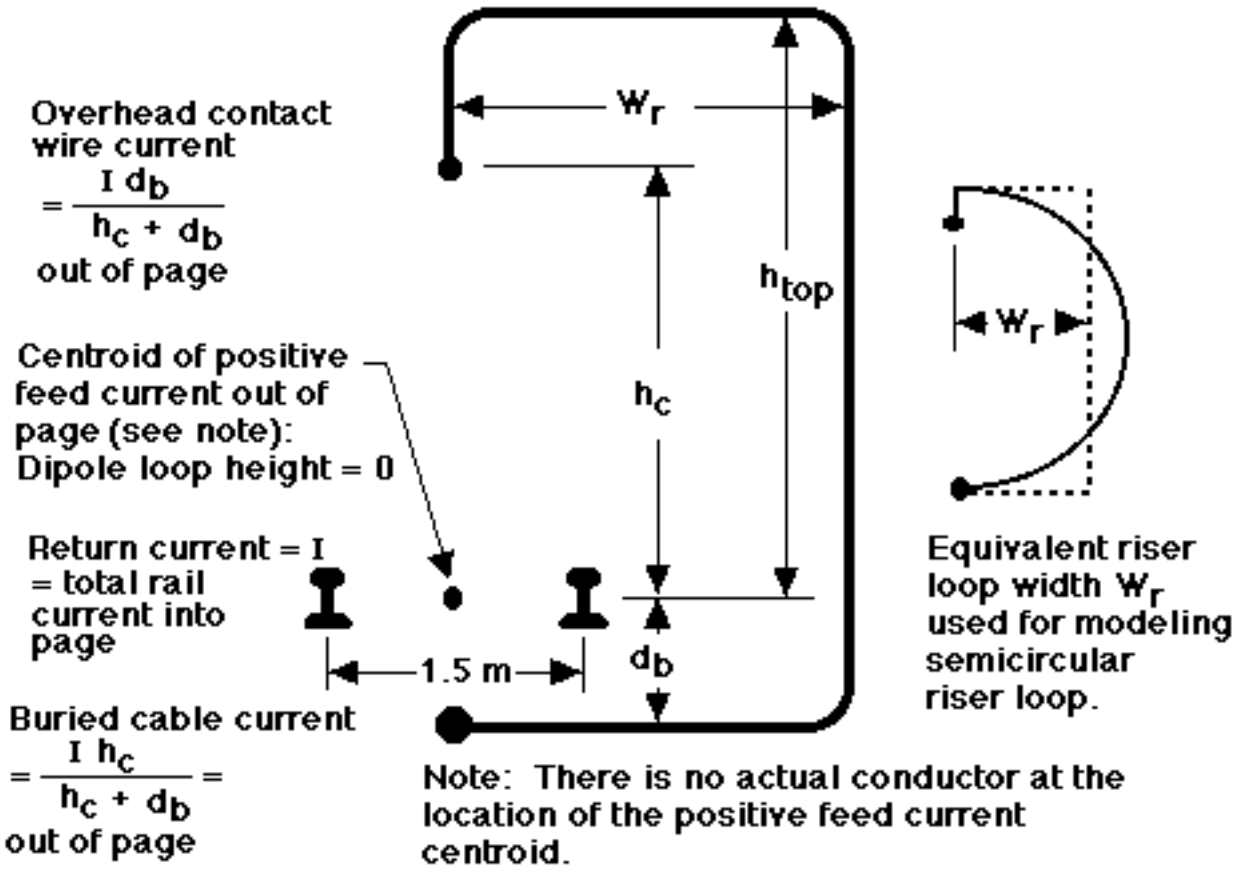

Figure 3.7 Conductors in the Hi-Lo B-field mitigation circuit shown in end view, with relations for ideal buried cable depth vs. contact wire height. Effective width of the rectangular riser loop modeled yields loop area equal to that of actual semicircular loop.

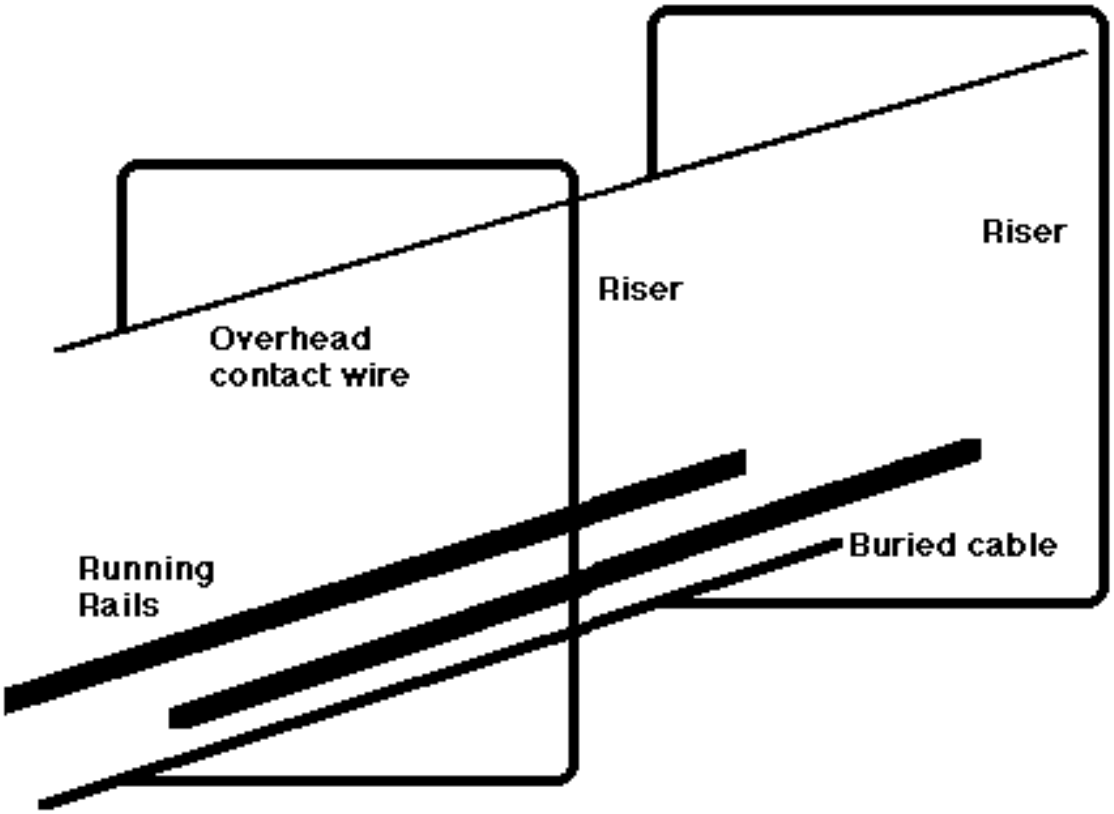

Figure 3.8 Conductors in the Hi-Lo B-field mitigation circuit shown in oblique view.

The arrangement of conductors in the Hi-Lo design is shown in Fig's 3.6 and 3.7. To carry most propulsion current from substation to train the Hi-Lo design uses a cable of large cross section buried 0.3 to 1 m (approx 1 to 3 ft) deep, immediately below the center line of each track, i.e., centered between the two running rails and down a fraction of a meter. An overhead contact wire, with which the rail car pantographs make contact, has much smaller cross section. As will be seen the overhead contact wire only carries a large fraction of propulsion current to the train for the last 10 to 20 meters (33 to 66 ft) on its way to the train.

Where

d_b = buried cable depth

h_c = overhead contact wire height

R_b = buried cable resistance per meter (dimensions of Ω/m)

R_c = contact wire resistance per meter (dim's Ω/m)

G_b = buried cable conductance (dim's siemens•meters) = 1/ R_b

G_c = contact wire conductance (dim's siemens•meters) = 1/ R_c

the relation between the parameters in the Hi-Lo design is

$$h_c G_c = d_b G_b, \quad \text{or} \quad h_c / R_c = d_b / R_b \tag{3.14a}$$

When contact wire and buried cable are connected in parallel to the positive substation supply to send total current I_o to a distant train, they will conduct buried cable current I_b and contact wire current I_c according to the relations

$$I_b = \frac{I_o G_b}{G_b + G_c} \quad \text{and} \quad I_c = \frac{I_o G_c}{G_b + G_c} \quad \text{or,}$$

$$I_b = \frac{I_o R_c}{R_b + R_c} \quad \text{and} \quad I_c = \frac{I_o R_b}{R_b + R_c} \tag{3.14b}$$

Then the products of vertical dimension times current will be equal for the contact wire-running rail loop and the buried cable-running rail loop. From Eqn's 3.14a and 3.14b it follows that

$$I_b d_b = I_c h_c \tag{3.15}$$

According to Eqn. 3.9, at considerable distance from the conductors the B-fields produced by each loop will be nearly equal in magnitude. Since currents flow around the corresponding loops in opposite sense, the B-fields caused by one loop will point in exactly the opposite direction relative to that from the other loop.

Consequently, the net B-field will have a very small value. In actuality, there will be a two-dimensional quadrupole B-field with magnitude vs. distance behavior given by a relation similar to Eqn. 3.10, that indicates a smaller B-field, falling off as $1/d^3$ with distance, and still smaller higher-order multipole fields that will fall off with distance even faster.

"Riser" cables of cross section intermediate between that of the buried cable and overhead contact wire are periodically spaced down the track to connect buried cable to overhead contact wire. As will be seen shortly, for a train at a considerable distance from the substation, currents will divide between buried cable and overhead contact wire according to Eqn. 3.14b, maintaining the condition given in Eqn. 3.15, up to a few riser spacings from the train. The buried cable component of train current will not flow upward to the contact wire until it reaches risers very near or at the train.

Furthermore, calculations will show that in a typical case, some of the buried cable current will actually flow past the train and up risers near and past the end of the train farthest from the substation. In side view one sees loops comprised of risers providing upward current path, contact wire, and cars providing downward current path. To yield the smallest area of these loops, thus minimizing their resulting B-fields according to Eqn. 3.11, one wants upward currents to flow as close to the cars as possible. This end can be achieved by making the risers of larger cross section and spacing them closer together.

Magnetic field behavior of the Hi-Lo design depends upon the relations between positions of the conductors and the currents they carry, which depend in turn upon the relative conductor resistivities and the lengths and orientation of conducting segments. The B-field modeling described in this report has been performed using the set of parameters matching the present estimate of those to be used in the final design. The parameters are given in Table 3.1. Note that cable and overhead contact wire cross sections may change in the final design. In such case the relation $h_c/R_c = d_b/R_b$ will be maintained.

Figure 3.7 identified the "centroid" of current flow from substation to train, and indicates that if the ratios of currents and dimensions are correct, then this centroid will be located at a point directly between the running rails, which happens to be the centroid of current flow from train back to substation. If the ratios of currents and dimensions are not correct, then the centroid of positive current flow will be offset above or below the centroid of return current flow. Taking the elevation of the centroid for return current flow as the reference level, the elevation of the centroid for positive current flow is given by the relation

$$h_d = \frac{I_c h_c - I_b d_b}{I_c + I_b} = \frac{R_b h_c - R_c d_b}{R_c + R_b} \quad \text{since} \quad \frac{I_c}{I_b} = \frac{R_b}{R_c} \tag{3.16}$$

The centroid elevation is defined as h_d because it represents the height of an effective 2-dimensional dipole conductor pair carrying current I_o that will cause a B-field that falls off with distance as $2I_o h_d / d^2$ as given by Eqn. 3.9. It will be shown that in order to meet the UW's B-field requirements it will be necessary to hold the magnitude of h_d within limits in the 10's of cm range.

Table 3.1 Presumed final Hi-Lo design dimensions and electrical parameters.

Buried cable (see Note 1)	2000 kCmil soft annealed copper, 1.675×10^{-5} Ω/m
Contact wire (see Note 1)	4/0 hard-drawn copper, 1.655×10^{-4} Ω/m
Riser cable	1000 kCM soft annealed copper, 3.35×10^{-5} Ω/m
Riser-to-riser spacing	20 meters (65.6 ft)
Riser cable length	9.73 meters (32 ft)
Buried cable riser-to-riser resistance R_b	0.335 mΩ
Riser cable resistance R_r	0.326 mΩ = 0.973 R_b
Contact wire riser-to-riser resistance R_c	3.31 mΩ = 9.88 R_b
Buried cable depth d_b	45.7 cm (1.5 ft)
Contact wire height h_c	4.3 meters (14.1 ft) = 9.4 d_b
Riser loop dimensions	2.31 m wide x 5.26 m high (7.68 x 17.25 ft)
Contact wire lateral offset for modeling	25 cm (9.8 in)
Contact wire zig-zag	Limits are 9 in (23 cm) right to 9 in left of center
Pantograph spacing	27 meters (88.6 ft)
Rail center spacing	1.5 meters = 4' $8^1/_2$" gauge + one rail head width
Train current	4 cars x 0.7 kA/car = 2.8 kA/train

Note 1: Buried cable and overhead contact wire cross sections may change in final design. In such case the relation hc/Rc = db/Rb will be maintained.

3.5 Current Flow in the Hi-Lo Conductors

The behavior of the Hi-Lo circuit design in constraining riser currents to those risers closest to a pantograph is shown in Figures 3.9 - 3.11. Figure 3.9 shows the electrical circuit containing a single car with the pantograph contacting the contact wire at a riser location. Currents in the different conductor branches are shown in the figure. Figure 3.10 shows a similar diagram when the car's pantograph contacts the contact wire midway between two risers. Figure 3.11 is for the case of the contact point being one quarter of the way from one riser to the next.

For the example of Figures 3.9 - 3.11 the resistance ratios used were $R_c/R_b = 15$ and $R_r/R_b = 1.44$, compared to the respective values of 9.88 and 0.973 from Table 3.1. However, as will finally be seen, the behavior of currents in the circuits in the example is nearly identical to those expected if cable resistances were chosen from Table 3.1.

In the case of each circuit in the figures it is observed that for the ratios of R_c/R_b and R_r/R_b used, as one moves in either direction away from the contact point on the contact wire, riser currents get smaller, with a ratio of current in a given riser to that in the riser next nearest the contact point equal to $\gamma = 0.077$.

A relation for the ratio γ in terms of the resistance ratios will now be derived. Consider the circuit shown in Figure 3.12, which represents a portion of a ladder circuit many riser intervals long. The currents in the nth riser, contact wire segment and buried cable segment are defined as $I_{r,n}$, $I_{c,n}$ and $I_{b,n}$ respectively.

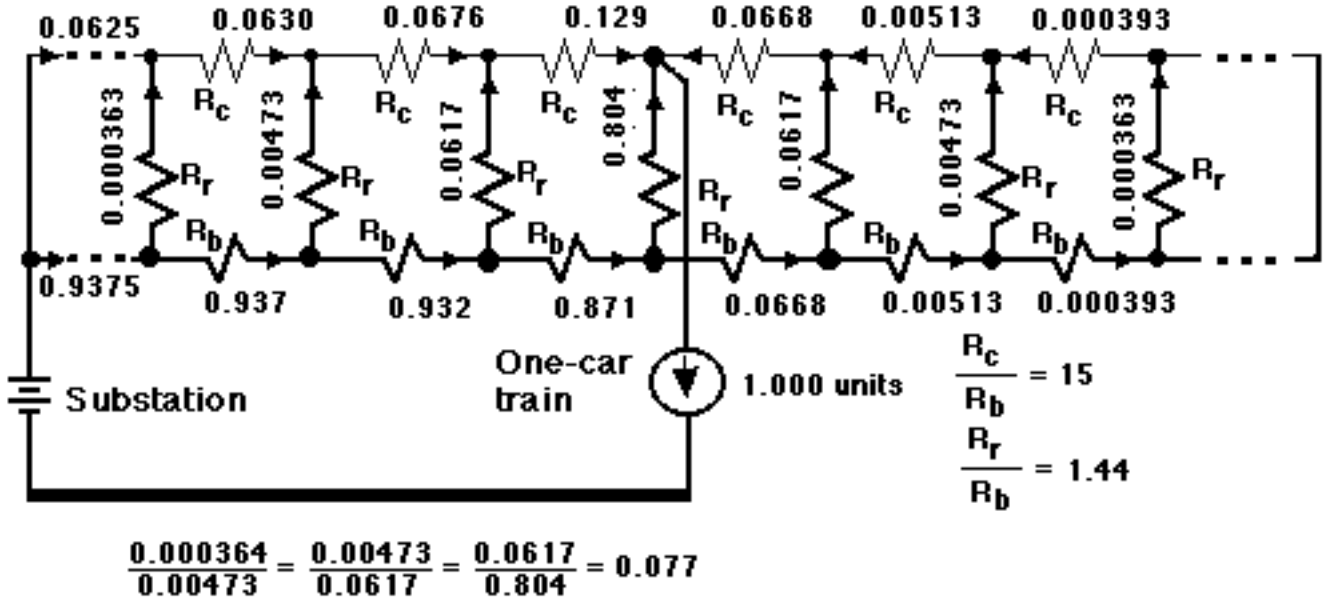

Figure 3.9 The DC power feed circuit many riser sections long with the pantograph of a single car contacting the contact wire at a riser location. The contact wire is the top horizontal conductor with the buried cable at the bottom. The running rails (not shown) conduct train current back to the substation. Risers periodically connect the buried cable with overhead contact wire. The train conducts 1.0 arbitrary units of current. Proportional units of current flowing in each branch of the circuit are shown. Ratios of currents in adjacent risers are given. Risers conducting negligibly small currents (less than 10-4 units) have been omitted from the drawing.

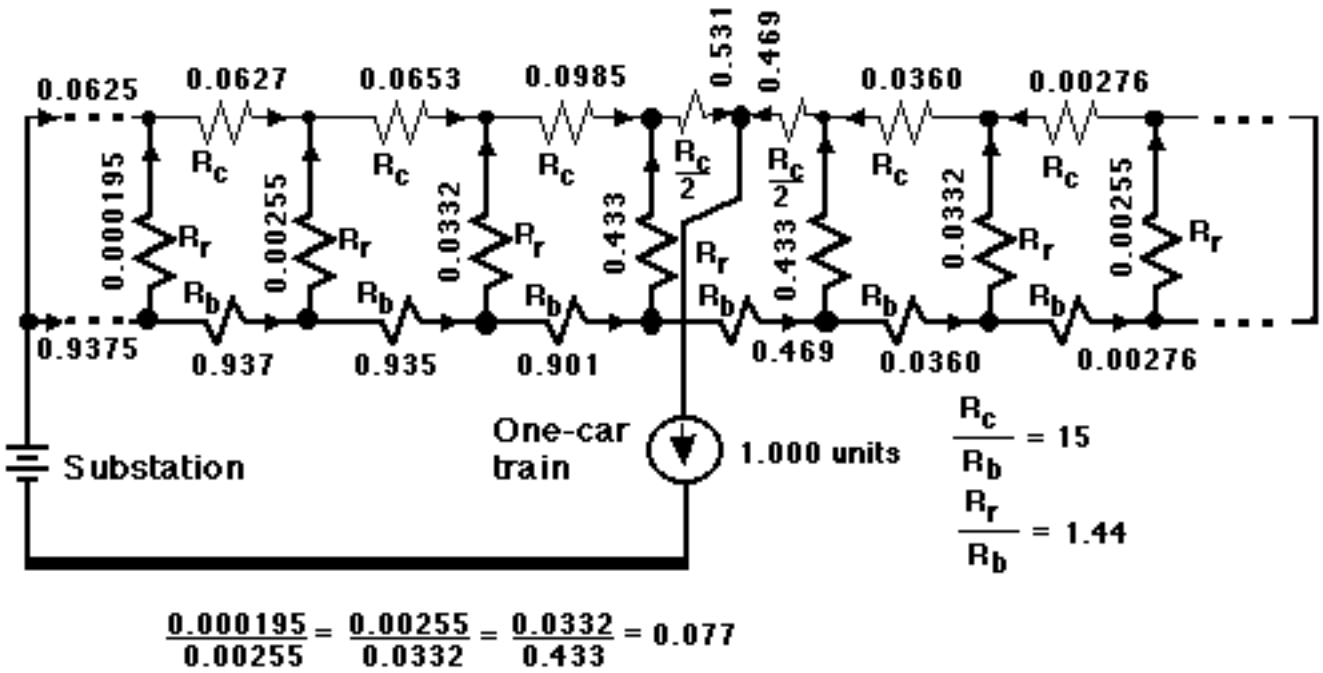

Figure 3.10 The DC power feed circuit many riser sections long with the pantograph of a single car contacting the contact wire at a location midway between risers. See caption of Figure 3.9 for explanation**.**

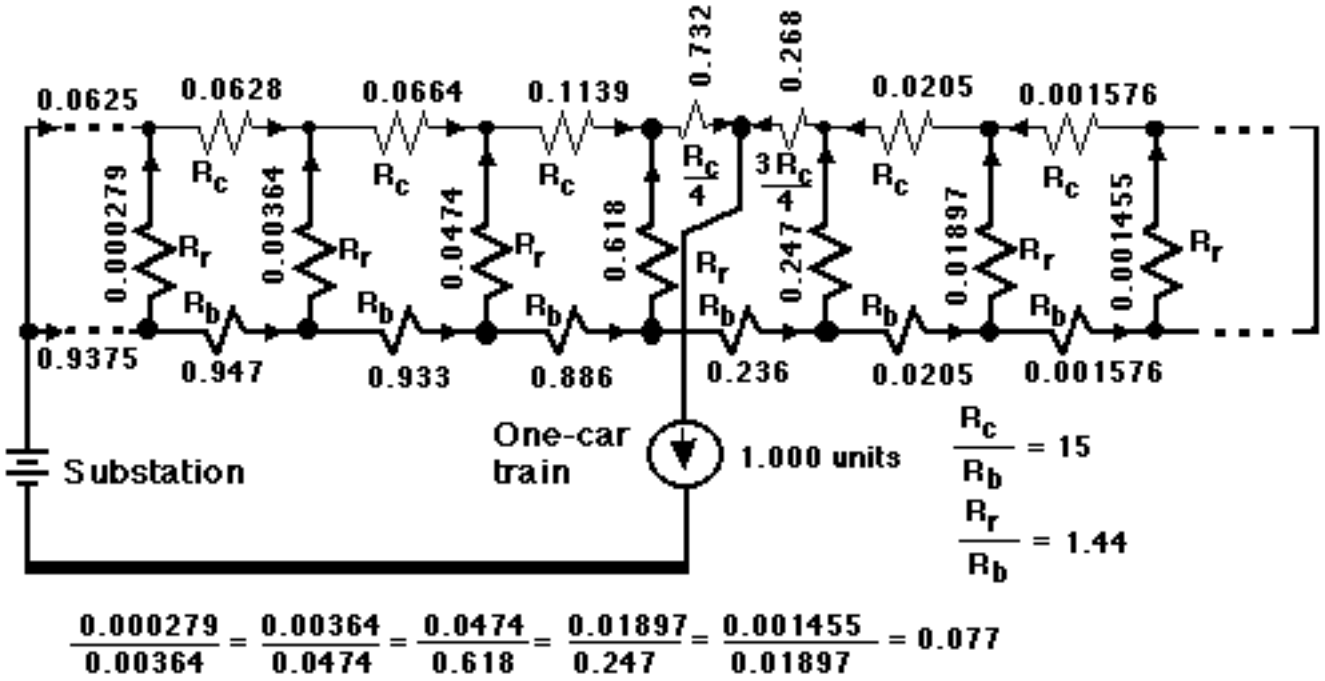

Figure 3.11 The DC power feed circuit many riser sections long with the pantograph of a single car contacting the contact wire at a location one quarter of the way to the next riser. See caption of Figure 3.9 for explanation.

It is assumed that the entire circuit is long enough for the initial values of contact wire and buried cable currents at the left hand end of the circuit to be determined by resistance ratios and to have the values

$$I_{co} = \frac{I_o R_b}{R_c + R_b}$$
$$I_{bo} = \frac{I_o R_c}{R_c + R_b} \qquad (3.17)$$

For the case in which

$$I_{r,n-1} = \gamma I_{r,n}, \quad I_{r,n-2} = \gamma^2 I_{r,n}, \quad I_{r,n-3} = \gamma^3 I_{r,n}, \quad \text{etc.} \qquad (3.18)$$

$I_{c,n}$ can be written in terms of I_{co} plus riser currents as follows:

$$\begin{aligned} I_{c,n} &= I_{co} + I_{r,n-1} + I_{r,n-2} + I_{r,n-3} + \ldots \\ &= I_{co} + \gamma I_{r,n} + \gamma^2 I_{r,n} + \gamma^3 I_{r,n} + \ldots \\ &= I_{co} + I_{r,n}(\gamma + \gamma^2 + \gamma^3 + \ldots) \\ &= I_{co} + \frac{\gamma}{(1-\gamma)} I_{r,n} \end{aligned} \qquad (3.19)$$

It is important to note that $\gamma < 1$ in the above expressions. Likewise,

$$I_{b,n} = I_{bo} - \frac{\gamma}{(1-\gamma)} I_{r,n} \qquad (3.20)$$

The (I x R) voltage drops along paths ABD and ACD now can be set equal to obtain the expression

$$I_{b,n} R_b + I_{r,n} R_r = I_{r,n-1} R_r + I_{c,n} R_c, \quad \text{or}$$
$$\left(I_{bo} - \frac{\gamma}{(1-\gamma)} I_{r,n}\right) R_b + I_{r,n} R_r = \gamma I_{r,n} R_r + \left(I_{co} + \frac{\gamma}{(1-\gamma)} I_{r,n}\right) R_c \qquad (3.21)$$

The equality $I_{bo}R_b = I_{co}R_c$ can be subtracted out of the above expression, and the $I_{r,n}$'s can be cancelled to yield, after some manipulation,

$$(\gamma - 1)^2 = \rho\gamma, \quad \text{where} \quad \rho = \frac{R_c + R_b}{R_r}, \quad \text{or}$$
$$\gamma^2 - (2 + \rho)\gamma + 1 = 0 \qquad (3.22)$$

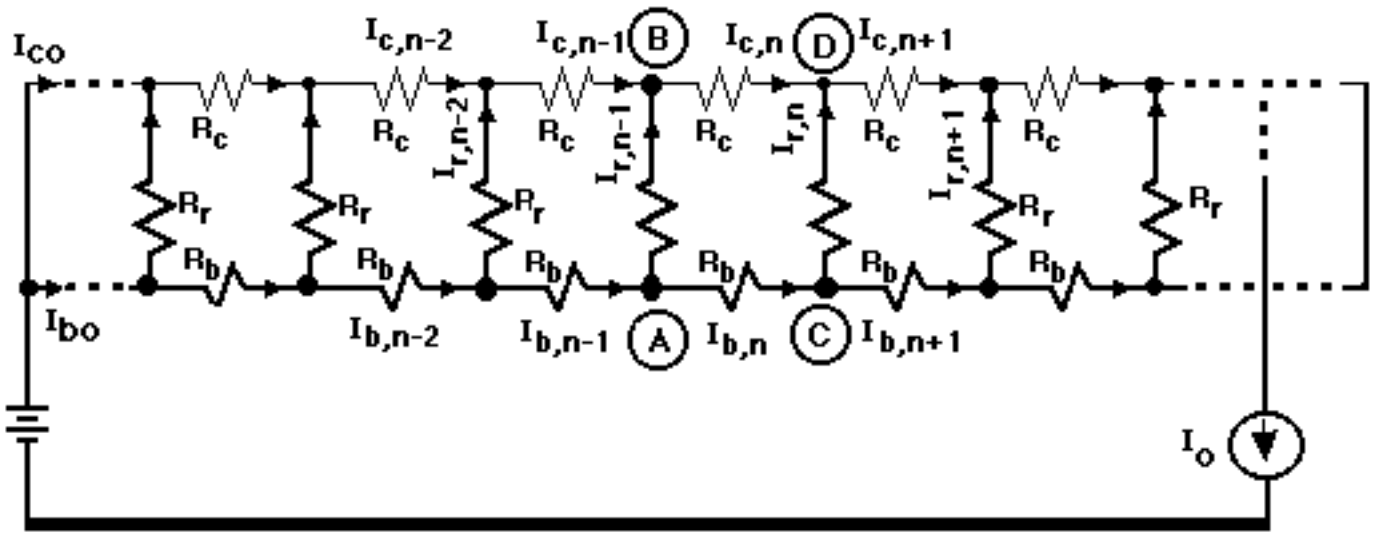

Figure 3.12 A portion of a Hi-Lo riser circuit many riser intervals long, at a point to the left of the train. Riser currents are greater near the right end of the circuit, and become very small near the left end of the circuit.

The quadratic equation above has solutions

$$\gamma = \left(1+\frac{\rho}{2}\right) - \sqrt{\left(1+\frac{\rho}{2}\right)^2 - 1} < 1, \quad \text{and} \quad \left[\left(1+\frac{\rho}{2}\right) - \sqrt{\left(1+\frac{\rho}{2}\right)^2 - 1}\right]^{-1} > 1 \tag{3.23}$$

The second solution can also be obtained by putting a (+) sign in front of the square root term in the expression for the first solution, as some algebra will show.

The resistance ratios $R_c/R_b = 15$ and $R_r/R_b = 1.44$ yield

$$\rho = \frac{R_c + R_b}{R_r} = \frac{100}{9} = 11.1 \tag{3.24}$$

When the first expression above for γ as a function of ρ is evaluated for this value of ρ, the resulting value is $\gamma = 0.077$, which is the same value found from calculations performed using the electronic circuit analysis program SPICE. Similar means can be used to derive the same expressions for the values of γ for the right-hand end of the circuit beyond the location of the pantographs.

Incidentally, the resistance ratios used in the actual Hi-Lo circuits modeled for this report, namely $R_c/R_b = 9.88$ and $R_r/R_b = 0.973$, yield resistance ratio

$$\rho = \frac{R_c + R_b}{R_r} = \frac{9.88 + 1}{0.973} = 11.2$$

essentially the same as the value of 11.1 in the circuits of the examples. The corresponding value of γ is 0.076. Thus current division between the risers in circuits with parameters from Table 3.1 should be virtually identical to that arising in the circuits of the examples.

In portions of Hi-Lo DC power feed circuits only a few sections long, in which the number of sections N is not great enough to yield $\gamma^N << 1$, currents in successive risers ahead or behind a train will have to be written as sums of partial solutions that get smaller going to the right plus ones that get smaller going to the left. Or the currents can be calculated using SPICE (Simulation Program with Integrated Circuit Emphasis - see Appendix C for a description).

The most important aspect of the above relation for γ is that it shows how γ depends on the resistance ratios. For the case in which resistance ratio $\rho >> 1$, the first solution to Eqn. 3.23 above can be approximated by $\gamma \approx 1/(\rho + 2)$.

The results of the analysis presented above serve as an intuitive tool. The application SPICE was used to find currents in actual multi-car circuits in which the current contributions from each car add by superposition. In a practical situation the riser-to-riser distances will be shorter in the direct vicinity of sensitive labs and longer farther away.

3.6 B-Field Calculations for the Hi-Lo Design

To assess the effectiveness of the Hi-Lo design reducing propulsion B-fields numerical calculations of resulting propulsion B-fields were made. These were performed assuming that a single train conducting the maximum train current of 2.8 kA was passing by the various labs in question.

For all circuit configurations SPICE was used to calculate the values of currents in each circuit branch. Then these currents were entered in the Microsoft Excel spreadsheet programmed to calculate B-fields individually due to each straight segment of each current carrying branch, and then add them up. Appendix C shows an example of a simplified physical circuit layout, the SPICE input file and currents calculated, and the spreadsheet used to calculate B-fields.

B-field levels are most problematical when labs are nearest to the transit route. Both Hi-Lo mitigated propulsion B-fields and perturbation B-fields have been found to fall off rapidly away from trains in all directions. Maximum North Link train length will be approx. 108 meters. An inspection of Fig. 2.1 shows that as the transit route progresses northward from the ship canal it stays straight past Wilcox and Roberts Halls. North of that point the westward curve is of such great radius that over the distance of a train length all four cars of a maximum length train will be in approximately straight alignment. Therefore, the propulsion B-fields for the Hi-Lo mitigation design were calculated assuming that the train and tracks were aligned in a straight line parallel to a principal axis in a Cartesian coordinate system.

As shown in Fig. 3.13, the origin of the Cartesian coordinate system was taken at a point midway between the northbound running rails, at rail height, at the University of Washington Substation feed point. From that point, x was measured west, y up, and z north. Whatever the conceptual cost is of having a principal axis pointing leftward, a benefit accrues from all labs but one having x-values > 0.

To take account of the variation in contact wire lateral location and to allow testing of the effects of positional tolerances of the buried cable, provision for easily varying the lateral and vertical positions of buried cables and overhead contact wires from their ideal locations was included in the spreadsheets used for computation. To avoid wear in one spot on the pantographs the contact wire will zig-zag between a 9 inch (23 cm) lateral offset one way and the same distance the other way. Since modeling showed that the extreme offset in the direction away from the labs produced

the highest B-field levels, a standard offset away from the labs of 23 cm plus 2 cm tolerance allowance for a total of 25 cm was used in practically all modeling.

Figure 3.14 shows the z-coordinates of cars and conductors in one of the circuits that was modeled. Riser currents also are shown. Only three risers past each end of a train carry current of appreciable magnitude. Currents in the overhead contact wire segments and buried cable segments can be calculated from the riser and car currents.

Car currents were assumed to divide equally between the two running rails, with the currents from car to rails flowing through conductor segments located at y = 0 and z = car location. Early modeling verified that use of this very simple model for current flow in cars did not change overall results.

For the circuit shown in Fig. 3.14, the pantograph of the first car is located directly at a riser location. Since riser currents and the B-fields that they cause will depend on the location of the pantographs, in order to be sure that modeling replicated a near worst case, four additional circuits were analyzed, with the leftmost car's pantograph located at distances of 4, 8, 12 and 16 meters to the right of a riser, with succeeding cars positioned at 27 meter intervals.

To determine worst-case Hi-Lo B-fields for a particular lab, the lab's x-, y- and z-coordinates were entered at the appropriate places in the spreadsheets, and then the entire collection of cars and risers was moved by varying z_{offset} to find the worst-case value for the magnitude of B. In initial modeling this process was repeated for each circuit. It eventually became clear that one or two of the circuits generally always produced the worst case.

Note that in these circuit models all conductors run in either the x-, y- or z direction. This fact allowed spreadsheets for B-field computation to be prepared in which the x-, y- and z-directed portions of the various conducting segments were entered separately. Then B-fields from conducting segments oriented in each principal-direction were calculated separately using Eqn. 3.7 for x-direction currents and similar equations for y- and z-direction currents as discussed in Sec. 3.1.

As can be seem from Fig. 2.1, Bagley and Johnson Halls and the Chemistry Building are near the center of the northwestward going curve of the right-of-way. To calculate propulsion B-fields a spreadsheet was programmed with relations derived from Eqn's 3.4 and 3.5 allowing calculation of B-fields from straight conducting segments arbitrarily positioned in 3-dimensional space. The procedure followed is detailed in Appendix C.

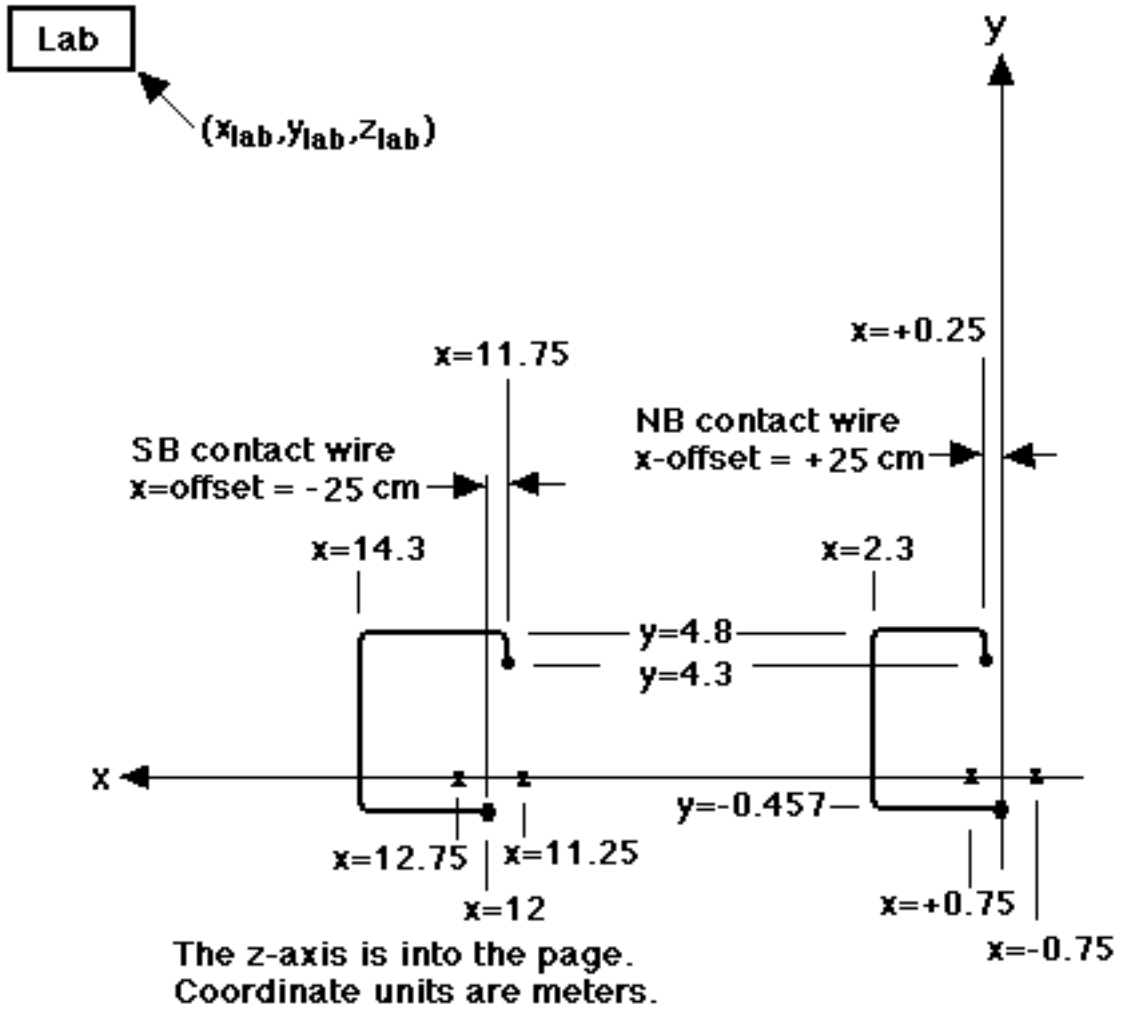

Figure 3.13 X-Y coordinates of conductors in the Hi-Lo B-field mitigation scheme. In the example shown both sets of risers are shown looping toward the lab, while one overhead contact wire is offset toward the lab and the other away from the lab, whereas for worst-case computations both overhead contact wires were offset 25 cm away from the labs.

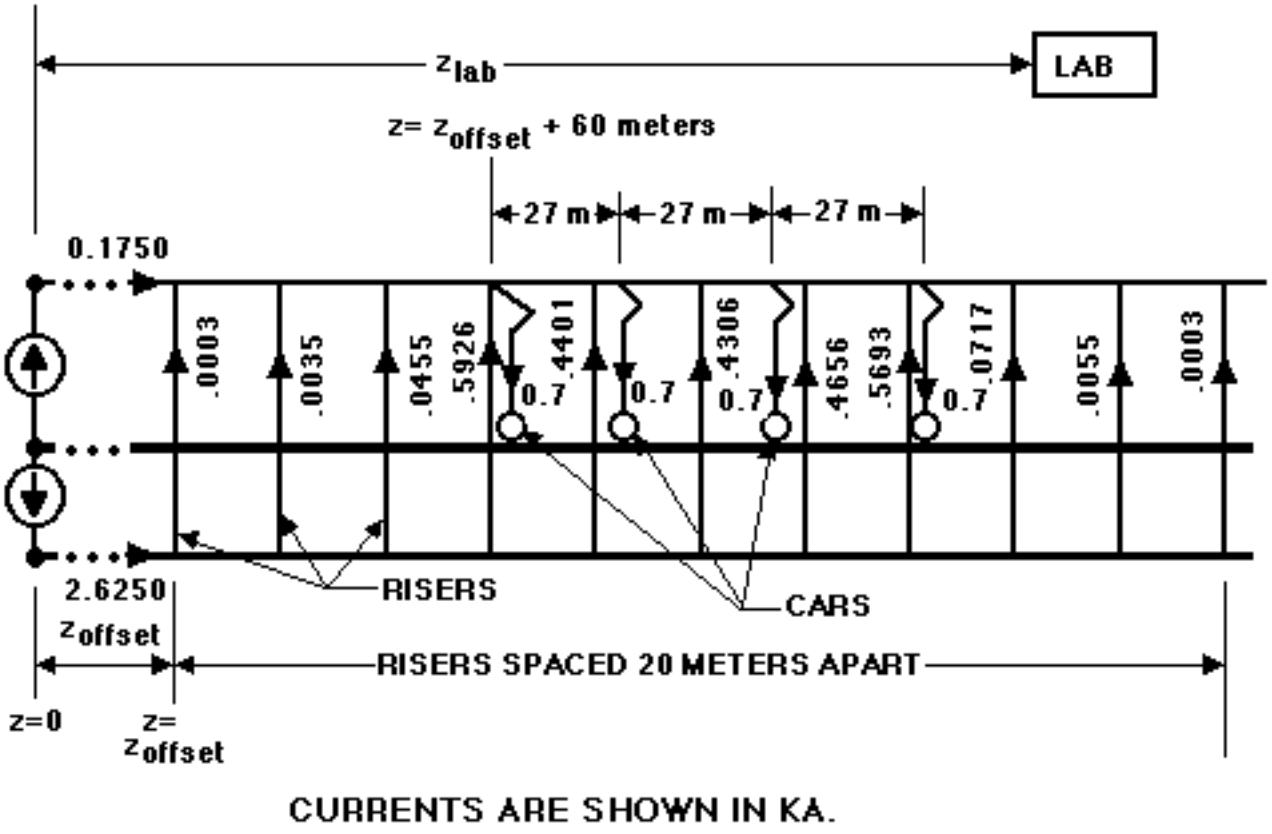

Figure 3.14 Z-coordinates of conductors and rail car current pickups in the Hi-Lo B-field mitigation scheme for the case where the southernmost car's current pantograph is directly at a riser location. Currents in buried cable segments and overhead contact wire segments are derivable from riser currents shown in units of kA. Risers conducting current of less than 0.1 A = 10-4 kA are omitted from the circuit and are neglected when calculating B-fields.

To summarize the computational process, as shown in Appendix C, the spatial coordinates of the ends of each principal-direction portion of each conducting segment were determined. The currents in all the conducting segments were determined. The three spatial coordinates of the lab in question were entered. And then equations like Eqn. 3.7, etc., were used to calculate the B-fields at the lab location for each principal-direction portion of each conducting segment. Finally, all the B_X's, B_Y's and B_Z's for the entire circuit were added up to determine total B_X, B_Y, B_Z and |B| at the lab location. The z_{offset} distance was varied to obtain worst-case |B| resulting from each of the five circuits with different riser-current pickup patterns.

In the process of developing the computational spreadsheets some simple examples that could be checked by hand were calculated, to be sure that the spreadsheets were yielding valid answers. Since the Hi-Lo system performs a balancing act in which B-fields caused by one part of the circuit are almost entirely offset by those caused by another, practically any error in initial data entry resulted in an unexpectedly large value of computed B-field.

3.7 Stray B-field Modeling Results

Tables 3.3 and 3.4 present the major results for B-field modeling when Hi-Lo B-field mitigation is used and when it is not. Results of additional modeling to compare cases of zero percent vs. 30 percent overhead contact wire wear are presented here.

Table 3.2 gives predicted propulsion B-field levels for the Hi-Lo design employing the parameters from Table 3.1 for the critical labs, for a single train drawing 2.8 kA on the nearest track. Results for three cases are compared: the first for 0 percent overhead contact wire wear and the risers on the lab-side tunnel wall, the second for 0 percent wear and the risers on the tunnel wall opposite the lab, and the third for the case of 30 percent overhead contact wire wear and the risers on the lab-side tunnel wall. For the case of 30 percent overhead contact wire wear the value of contact wire resistance is 1/(1-0.3) = 1.43 times its initial value, and nearly all circuit currents are different than in the case of zero wear. For all three cases the overhead contact wire location was laterally displaced 25 cm (9.8 in) away from the lab from its centered position, since as previously noted it was found that this location the produced worst-case B_{prop} for any location between 25 cm offset toward or away from the lab. B-field levels failing the UW B-field specs are shown in bold.

With zero percent overhead contact wire wear, incorporation of the Table 3.1 parameter values into Eqn. 3.16 yields a nearly ideal elevation for the centroid of positive current flow to the train, namely 2 cm (0.8 in) below the height of the running rail centroids. Comparison of B_{prop} values at the various labs shows the existence of slightly lower levels for the case with risers on the tunnel wall nearest the labs.

Table 3.2 Predicted attainable propulsion B-field levels for the Hi-Lo design employing the parameters from Table 3.1 for the critical labs in Table 2.1, for three cases. A single train drawing 2.8 kA is on the nearest track.

		distances					un-mitigated		Hi-Lo mitig, 0% wear, risers toward lab		Hi-Lo mitig, 0% wear, risers away from lab		Hi-Lo mitig, 30% wear, risers twd lab	
	UW stray B-field limit, mG	z,lab m	x, lab m	y,lab m	r slant m	1-train B,ptb mG	B,prop mG	B,tot mG	B,prop mG	B,tot mG	B,prop mG	B,tot mG	B,prop mG	B,tot mG
Bagley Hall	0.1	750	298	30	300	0.007	0.288	0.296	0.005	0.012	0.004	0.011	0.013	0.020
Chemistry Bldg.	0.1	685	307	35	309	0.007	0.272	0.28	0.004	0.011	0.004	0.011	0.013	0.020
EE-CS	5.0	450	103	34	108	0.067	2.160	2.23	0.022	0.089	0.033	0.099	0.076	0.143
Physics-Astronomy	0.5	1200	366	6.7	366	0.005	0.192	0.20	0.002	0.006	0.002	0.006	0.007	0.011
Johnson Hall	5.0	815	206	19	207	0.016	0.595	0.61	0.011	0.027	0.009	0.025	0.023	0.039
Fluke Hall	0.3	670	102	26	105	0.072	2.320	2.39	0.025	0.097	0.035	0.107	0.083	0.155
CHDD	0.3	220	230	21	231	0.013	0.487	0.50	0.004	0.017	0.004	0.016	0.017	0.030
Diagn. Imaging	5.0	100	296	32	298	0.007	0.250	0.26	0.002	0.009	0.002	0.009	0.008	0.016
Surgery Pav.-1st fl.	1.0	150	88	33	94	0.091	2.930	3.02	0.030	0.121	0.050	0.141	0.101	0.192
Surgery Pav.-pkng	1.0	150	88	24	91	0.097	3.130	3.23	0.033	0.131	0.052	0.149	0.111	0.208
ME Bldg.	0.2	430	32	37	49	**0.385**	10.800	11.19	0.139	**0.524**	0.359	**0.744**	0.289	**0.674**
ME Bldg. Rm. 135	0.2	440	70	47	84	0.116	3.500	3.62	0.039	0.155	0.077	0.193	0.114	**0.231**
ME Annex	0.2	517	2.7	38	38	**0.685**	19.300	19.99	0.468	**1.153**	0.539	**1.224**	0.358	**1.043**
Roberts Hall	0.1	255	78	38	86	**0.110**	3.300	3.41	0.038	**0.148**	0.068	**0.178**	0.115	**0.225**
Wilcox Hall	0.1	255	34	38	51	**0.351**	9.900	10.25	0.133	**0.484**	0.319	**0.670**	0.266	**0.616**
Fisheries Ctr.	0.1	150	379	20	379	0.004	0.159	0.16	0.001	0.005	0.001	0.005	0.005	0.010
Marine Sci. Bldg.	1.0	100	666	15	666	0.001	0.044	0.05	0.0003	0.002	0.0003	0.002	0.002	0.003
Henderson Hall	see note	1500	368	-4.3	368	0.005	0.188	0.19	0.002	0.006	0.002	0.006	0.007	0.011
Roberts-W. half	0.1	255	97	38	104	0.073	2.370	2.44	0.024	0.097	0.038	**0.111**	0.082	**0.155**

Note 1: The UW stray B-field specification for Henderson Hall is based on the time rate of change of B,tot(t): $|dB,tot/dt| \leq .2$ mG/sec.

Note 2: For all calculations in this table overhead contact wires were offset 25 cm away from the labs.

Table 3.3 UW specified and predicted stray B-field levels at critical UW labs for the modified Montlake alignment, with Hi-Lo B-field mitigation and with 30 percent overhead contact wire wear. Levels failing UW thresholds are in bold.

Routes & Labs	Long. Dist.	Horiz. & Vert. Distances			Transverse Slant Dist's		<----------B, mG---------->							
Mitigated Montlake Alignment	z_{lab} m	NB dX m	SB dX m	y_{lab} m	r,NB m	r, SB m	NB B_{ptb}	NB B_{prop}	NB B_{tot}	SB B_{ptb}	SB B_{prop}	SB B_{tot}	NB + SB B_{tot}	UW Stray B-field limit
UW Labs North of NE Pacific St.: SB B_{tot} = max[(SB B_{prop}) , (SB B_{ptb})]														
Bagley Hall	750	310	298	30.0	311.4	299.5	0.007	0.013	0.020	0.007	0.013	0.013	0.033	0.1
Chem Bldg.	685	319	307	35.0	320.9	309.0	0.006	0.013	0.019	0.007	0.013	0.013	0.032	0.1
EE-CS	450	115	103	34.0	119.9	108.5	0.053	0.06	0.116	0.067	0.076	0.068	0.184	5.0
Physics-Astron. [2]	1200	378	366	6.7	378.1	366.1	0.004	0.01	0.010	0.005	0.007	0.006	0.017	0.5
Johnson Hall	815	218	206	19.0	218.8	206.9	0.014	0.02	0.037	0.016	0.023	0.023	0.059	5.0
Fluke Hall	670	102	114	26.0	105.3	116.9	0.071	0.083	0.155	0.054	0.068	0.068	0.223	0.3
ME Bldg. [2]	430	44	32	37.0	57.5	48.9	0.269	0.222	**0.491**	0.384	0.289	**0.384**	**0.875**	**0.2**
ME Rm. 135 [2]	440	82	70	47.0	94.5	84.3	0.090	0.094	**0.184**	0.116	0.114	**0.116**	**0.300**	**0.2**
ME Annex [2]	517	14.7	2.7	38.0	40.7	38.1	0.574	0.358	**0.932**	0.665	0.355	**0.665**	**1.598**	**0.2**
Roberts Hall [2]	255	90	78	38.0	97.7	86.8	0.084	0.091	**0.175**	0.109	0.115	**0.109**	**0.284**	**0.1**
Wilcox Hall	255	46	34	38.0	59.7	51.0	0.248	0.212	**0.460**	0.350	0.266	**0.350**	**0.810**	**0.1**
Henderson Hall	1500	380	368	-4.3	380.0	368.0	0.004	0.006	0.010	0.005	0.006	0.007	0.017	Note 1
Roberts-W half	255	109	97	38.0	115.4	104.2	0.058	0.067	**0.125**	0.073	0.074	0.074	**0.199**	**0.1**
UW Labs South of NE Pacific St.: SB B_{tot} = (SB B_{prop}) + (SB B_{ptb})														
CHDD	220	242	230	21.0	242.9	231.0	0.011	0.015	0.026	0.013	0.017	0.030	0.056	0.3
Diagn. Imaging	100	308	296	32.0	309.7	297.7	0.007	0.008	0.014	0.007	0.008	0.016	0.030	5.0
Surgery Pav-1st fl., [2]	150	100	88	33.00	105.3	94.0	0.071	0.081	0.152	0.091	0.101	0.192	0.344	1.0
Surgery PavPkng. [2]	150	100	88	24.0	102.8	91.2	0.075	0.088	0.163	0.097	0.111	0.209	0.371	1.0
Fisheries Ctr.	150	391	379	20.0	391.5	379.5	0.004	0.005	0.009	0.004	0.005	0.010	0.019	0.1
Marine Science	100	678	666	15.0	678.2	666.2	0.001	0.001	0.003	0.001	0.002	0.003	0.006	1.0

Note 1: UW stray B-field spec for Henderson Hall is |dB/dt| < 0.2 mG/sec.
Note 2: See Section 4. Traffic effects could cause other perturbations.
Note 3: For calculations in this table overhead contact wires are offset 25 cm away from labs, and risers are on walls of tunnels toward labs.

Table 3.4 UW specified and predicted stray B-field levels at critical UW labs for the modified Montlake alignment, for the case in which Hi-Lo mitigation is not used. Levels failing UW thresholds are in bold.

Routes & Labs	Long. Dist.	Horiz. & Vert. Distances			Transverse Slant Dist's		<----------B, mG---------->							
Modified Montlake Alignment	z_{lab} m	NB dX m	SB dX m	y_{lab} m	r,NB m	r, SB m	NB B_{ptb}	NB B_{prop}	NB B_{tot}	SB B_{ptb}	SB B_{prop}	SB B_{tot}	NB + SB B_{tot}	UW Stray B-field limit
UW Labs North of NE Pacific St.: SB B_{tot} = max[(SB B_{prop}) , (SB B_{ptb})]														
Bagley Hall	750	310	298	30.0	311.4	299.5	0.007	0.267	**0.274**	0.007	0.288	**0.288**	**0.562**	**0.1**
Chem Bldg.	685	319	307	35.0	320.9	309.0	0.006	0.252	**0.258**	0.007	0.272	**0.272**	**0.530**	**0.1**
EE-CS	450	115	103	34.0	119.9	108.5	0.053	1.770	1.823	0.067	2.16	2.16	3.98	5.0
Physics-Astron. [2]	1200	378	366	6.7	378.1	366.1	0.004	0.180	0.184	0.005	0.192	0.192	0.376	0.5
Johnson Hall	815	218	206	19.0	218.8	206.9	0.014	0.535	0.549	0.016	0.595	0.595	1.144	5.0
Fluke Hall	670	102	114	26.0	105.3	116.9	0.071	2.32	**2.39**	0.056	1.880	**1.880**	**4.27**	**0.3**
ME Bldg. [2]	430	44	32	37.0	57.5	48.9	0.269	7.68	**7.95**	0.384	10.80	**10.80**	**18.75**	**0.1**
ME Rm. 135 [2]	440	82	70	47.0	94.5	84.3	0.090	2.78	**2.87**	0.116	3.50	**3.50**	**6.37**	**0.1**
ME Annex [2]	517	14.7	2.7	38.0	40.7	38.1	0.574	16.50	**17.07**	0.665	19.30	**19.30**	**36.3**	**0.1**
Roberts Hall	255	90	78	38.0	97.7	86.8	0.084	2.63	**2.71**	0.109	3.30	**3.30**	**6.01**	**0.1**
Wilcox Hall [2]	255	46	34	38.0	59.7	51.0	0.248	7.14	**7.39**	0.350	9.90	**9.90**	**17.29**	**0.1**
Henderson Hall	1500	380	368	-4.3	380.0	368.0	0.004	0.177	0.181	0.005	0.188	0.188	0.370	Note 1
Roberts-W half	255	109	97	38.0	115.4	104.2	0.058	1.940	**1.998**	0.073	2.37	**2.37**	**4.37**	**0.1**
UW Labs South of NE Pacific St.: SB B_{tot} = (SB B_{prop}) + (SB B_{ptb})														
CHDD	220	242	230	21.0	242.9	231.0	0.011	0.437	**0.448**	0.013	0.487	**0.030**	**0.948**	**0.3**
Diagn. Imaging	100	308	296	32.0	309.7	297.7	0.007	0.230	0.237	0.007	0.250	0.016	0.494	5.0
Surgery Pav-1st fl [2]	150	100	88	33.00	105.3	94.0	0.071	2.35	**2.42**	0.091	2.93	**0.192**	**5.44**	**1.0**
Surgery Pav-Pkng [2].	150	100	88	24.0	102.8	91.2	0.075	2.47	**2.54**	0.097	3.13	**0.209**	**5.77**	**1.0**
Fisheries Ctr.	150	391	379	20.0	391.5	379.5	0.004	0.148	**0.152**	0.004	0.159	**0.010**	**0.315**	**0.1**
Marine Science	100	678	666	15.0	678.2	666.2	0.001	0.043	0.044	0.001	0.044	0.003	0.089	1.0

Note 1: UW stray B-field spec for Henderson Hall is |dB/dt| < 0.2 mG/sec.
Note 2: See Section 6. Traffic effects could cause other perturbations.

This result, while perhaps counterintuitive, can only occur because of the specific manner in which the B-fields arising from riser currents add vectorally to those from other currents to produce the overall B-fields in the two cases.

With 30 percent wear and contact wire resistance increased to 1.43 times its original value, the centroid of positive current flow to the train is pushed downward to an elevation 14.2 cm below that of the running rail centroids. This departure from nearly ideal Hi-Lo circuit behavior results in a sizeable increase in the levels of B_{prop}. However, given the specific B-fields calculated at the labs and the UW B-field specs at those labs, there is no lab where the assumption of 30 percent contact wire wear pushes the total stray B-field level from compliance to noncompliance with the UW stray B-field specs.

At least one seeming anomaly appears in Table 3.2, evident when comparing the B_{prop} values for the ME Annex for the cases of zero percent and 30 percent overhead contact wire wear with the risers toward the lab. The value for zero percent wear is greater than that for 30 percent wear. This might be explained by the fact that the ME Annex site is practically directly over the southbound track for which computations were made at an elevation of 38 meters above rail height, at which the percentage difference in distance to overhead contact wire and buried cable is 12 percent. As the overhead contact wire wears the current it carries decreases over most of its length, shifting some of its positive current down to the buried cable that is farther away. In the direct vicinity of the conductors this could be expected to reduce B_{prop}. Repeating the calculations after increasing the vertical distance to 100 meters, a distance for which the percentage difference in distances to overhead contact wire and buried cable is only 4.5 percent, yields B_{prop} values of 0.016 mG for the zero percent wear case and 0.066 mG for the 30 percent wear case, a difference more in tune with intuition.

Table 3.3 shows the values for B_{prop} and total stray B-field $B_{tot} = (B_{prop} + B_{ptb})$ for northbound and southbound trains operating separately, and for simultaneous operation. For southbound trains north of NE Pacific St., peak values of B_{prop} and B_{ptb} will not occur simultaneously. At a lab location near the ROW in the central campus there will be a brief B_{prop} pulse as a southbound train starts south from NE 45th St., after which B_{prop} is reduced to nearly zero as the train travels the downgrade through campus in dynamic braking. As the southbound train passes the lab there will be a brief B_{ptb} pulse. Therefore, the maximum value of total stray B-field attained due to a southbound train will be the greater of the peak B_{prop} or B_{ptb} values.

In Table 3.3 bold typeface in used to highlight stray B-field levels that exceed the UW spec limits and B_{ptb} levels that by themselves exceed the UW spec limits. Note that at the ME Bldg., ME Annex, and Wilcox and Roberts Halls the B_{ptb} values by themselves exceed the UW spec limits. To actually achieve stray B-field levels in the ME Bldg. that anywhere fall below the UW spec limits would require closing Stevens Way to large transit buses and other vehicles of equivalent size, as is noted in Sec. 4 of this report. Additionally, Sec. 4 notes that parking next to sensitive lab buildings probably would have to be eliminated.

Figure 3.15 shows a representative calculated B_{prop} vs. train location along the track at a hypothetical lab located 64 meters west and 32 meters above the northbound track (slant distance = 72 meters), at a distance 255 meters in the northern z-direction from the University of Washington Substation propulsion feed point. The 72 meter slant distance is equivalent to that from the northbound track to a point between Roberts and Wilcox Halls, or to a point in the middle of the ME Bldg. proper. This example is for the case of 30 percent overhead contact wire wear, with the risers located on the tunnel wall away from the lab and the overhead contact wire offset from center 25 cm away from the lab. The longitudinal or z-direction is north. The lateral or x-direction is west, and the vertical or y-direction is up. The z values are given in meters north of the University of Washington Substation power feed point, and denote the location of the longitudinal center of the train.

Note that in this example the vertical or y-component of B_{prop} attains greater magnitude than the x- or z-components is the largest, and accounts for nearly all of the steady final value of |B| after the train has passed. With the passage of the train B_x, B_y and B_z all go through oscillations of larger period as the various current carrying loops associated with the train pass by, and oscillations of smaller period on the scale of the 20 meter riser-to-riser spacing.

The small ripples on the B vs. z waveforms apparently are caused by the time variations in the risers nearest the lab coupled by motion of the car current pickup points. Other computations have shown that as distance from the track increases, the relative magnitude of the ripples decreases.

B-field characteristics of the optimized Hi-Lo design are only a fraction albeit an important one of the overall story. As long as the Hi-Lo design can be employed to reduce propulsion B-fields to levels considerably below those due to perturbations of the geomagnetic field, it has done its job.

Figure 3.16 compares the |B| vs. train center location plot from Fig. 3.15 with those from three other cases: 0 percent contact wire wear, risers on tunnel wall toward and away from lab; and 30 percent contact wire wear, risers toward lab.

Inspection of the curves in Figures 3.15 and 3.16 shows that for some combinations of overhead contact wire wear and riser location maximum B_{prop} occurs when the train is in the vicinity of the lab, while for other combinations it occurs as an asymptotic value when the train is well past the lab. This fact was taken into account while performing the calculations to determine the worst case B_{prop} levels given in this report. For such calculations train location was swept from well before the lab to several thousand meters past the lab to assure that the worst-case B_{prop} value was caught.

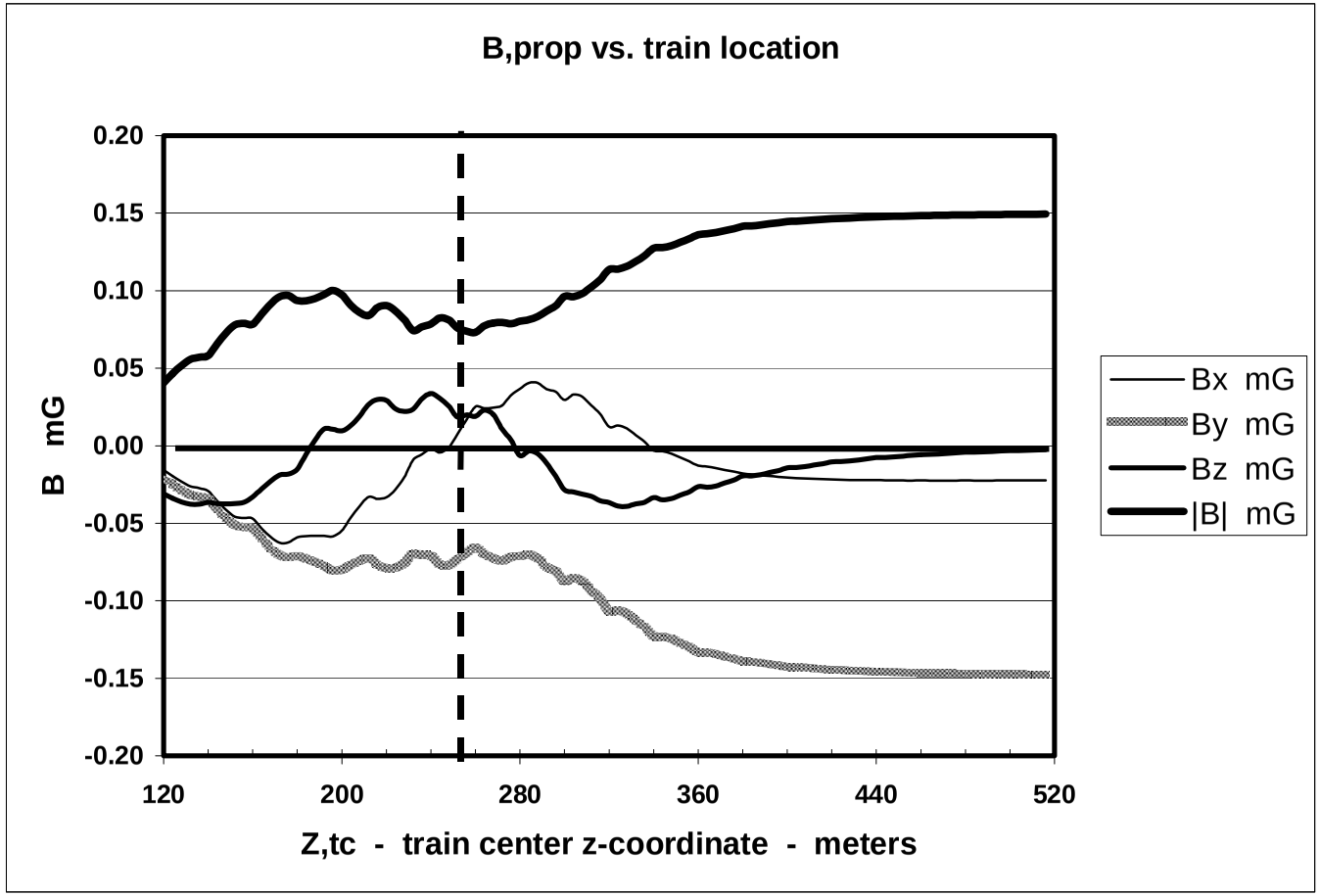

Figure 3.15 Spatial components and magnitude of B_{prop} vs. the location of the longitudinal center of a train conducting 2.8 kA passing a hypothetical lab located 64 meters west and 32 meters above the northbound track (slant distance = 72 meters). Distances correspond to a point between Roberts and Wilcox Halls 255 meters north of the University of Washington Substation feed point where z=0. For this case overhead contact wire wear is 30 percent, risers are located on the tunnel wall away from the lab, and overhead contact wire is offset 25 cm away from the lab.

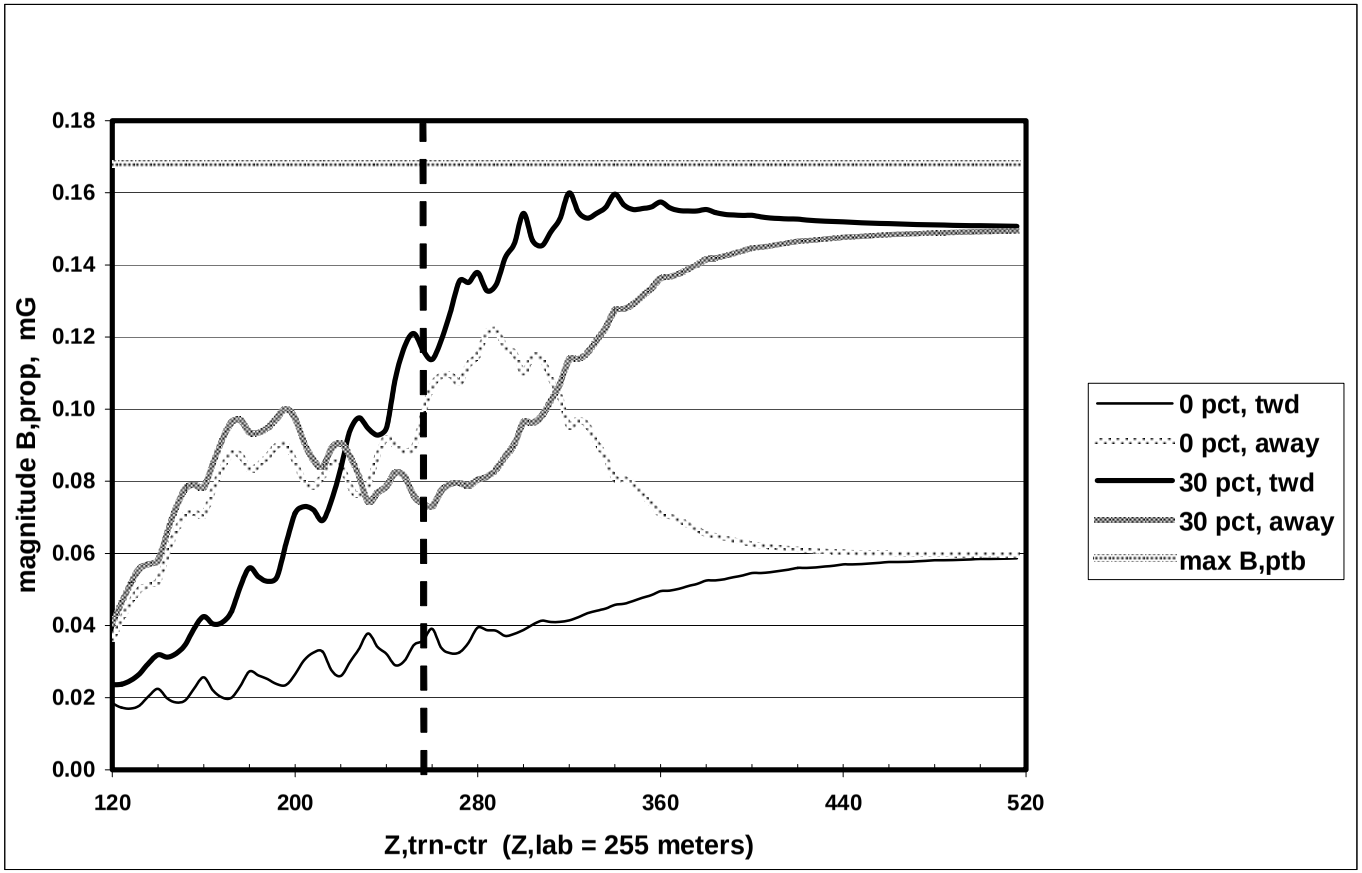

Figure 3.16 $|B_{prop}|$ vs. train location near a hypothetical lab located 64 meters west and 32 meters above the northbound track (slant distance = 72 meters), 255 meters north of the University of Washington Substation propulsion feed point where z = 0. Distances correspond to a point between Roberts and Wilcox Halls. Data for four cases are given, combining 0 percent and 30 percent contact wire wear, and risers on tunnel wall toward and away from lab. Overhead contact wire was offset 25 cm away from lab.

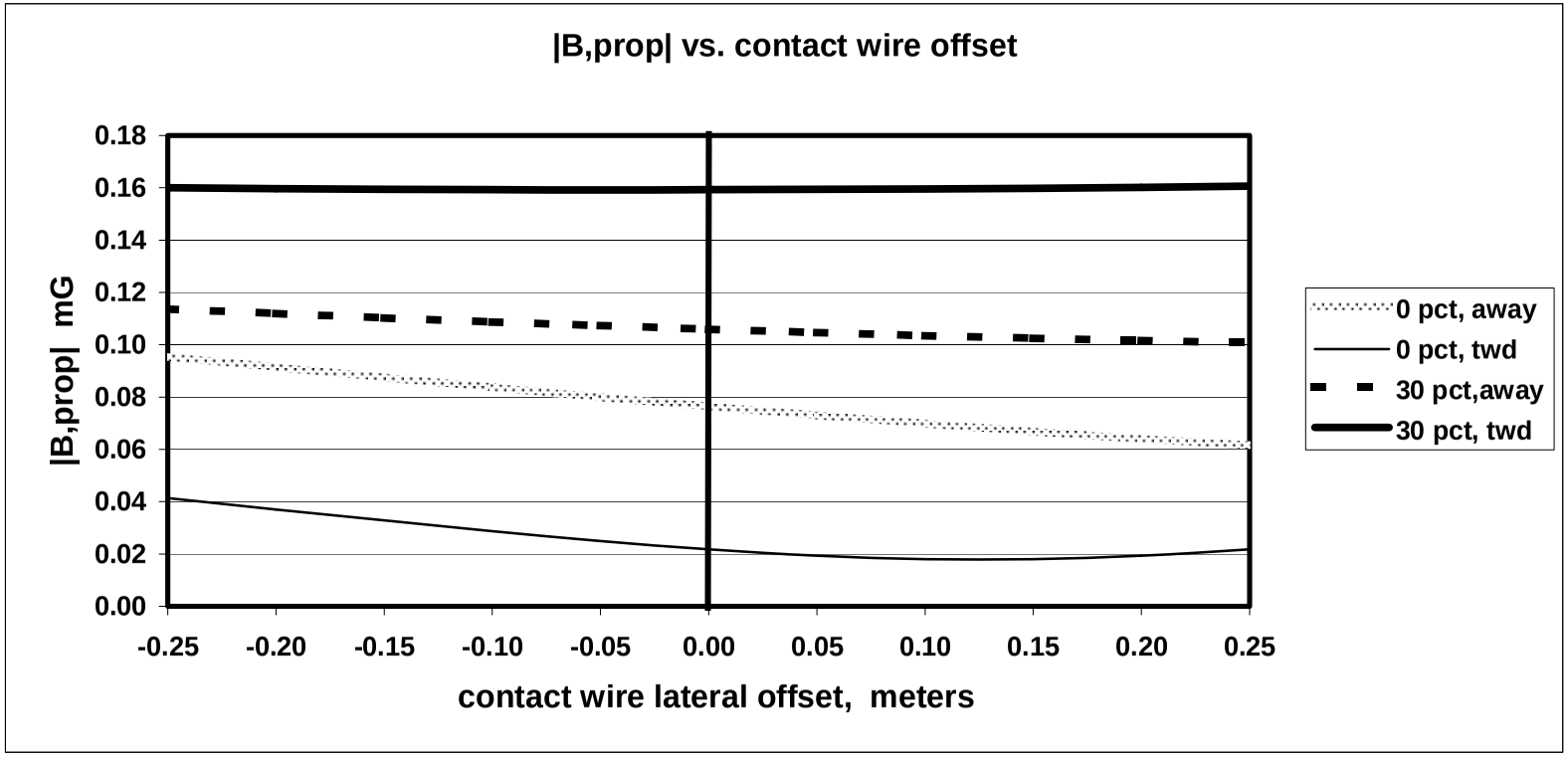

Figure 3.17 $|B_{prop}|$ vs. contact wire lateral offset for the four cases of Figures 3.16 at a fixed Z,trn distance of 320 meters. Lateral offsets < 0 are away from lab and offsets > 0 are toward lab. The fact that worst-case offsets in each case are away from lab explains why lateral offsets of 25 cm away from lab were used when calculating worst-case B_{prop} values.

Note that for 30 percent contact wire wear the choice of riser location makes little difference in the maximum value of |B| reached during train passage. However, if one were willing to take aggressive measures to minimize $|B_{prop}|$ and the resulting $|B_{tot}|$ at a lab relatively near the tracks one would mount the risers on the tunnel wall nearest the lab in question and then replace the overhead contact wire frequently in that vicinity to keep the maximum amount of wear low. This would achieve an approx. factor of 2.5 reduction in $|B_{prop}|$ relative to the 30 percent wear levels, but only a factor of 1.4 reduction in the $|B_{tot}|$ levels resulting from adding in the maximum $|B_{ptb}|$ value in each case.

Figure 3.17 shows the variation in $|B_{prop}|$ levels vs. contact wire lateral offset for the four cases of Fig. 3.16 for a fixed train location value of 320 meters. The range of offsets from -0.25 to +0.25 meters (-9.8 to +9.8 in) is slightly greater than the range to be used in practice. The evident small variations in $|B_{prop}|$ levels across this range indicate that the contact wire stagger employed to minimize pantograph wear should not create problems with Hi-Lo B-field mitigation.

Inspection of the curves in Fig. 3.17 does show that over the range of contact wire lateral offset covered the worst case B_{prop} levels occur for an overhead contact wire lateral offset of 25 cm away from the lab. Therefore, this value for contact wire lateral offset was used when calculating the worst case B_{prop} levels for this report.

3.8 Effect of Variation of Hi-Lo Mitigation Circuit Parameters From the Modeled Design

The choice of Hi-Lo mitigation circuit parameters for the final North Link design may differ from the Table 3.1 values. The choice of the family of parameters is determined by a variety of factors. One factor is the given overhead contact wire height, which has a minimum value based on the height of cars with their pantographs. For North Link, the maximum and minimum buried cable depths are determined by the characteristics of the tunnel structure and the roadbed structure respectively. Likewise, the dimensions of the riser loops are predicated by tunnel structure in the North Link case.

Ideally, a very shallow buried cable of very large cross section would yield the greatest insensitivity to variation in the elevation of the primary propulsion current centroid with contact wire wear.

Increasing the spacing between risers increases the length of the current loops formed by the first riser ahead and behind the train, the contact wire and pantographs. This would tend to increase B_{prop} values. At locations on the right-of-way relatively far from sensitive laboratories such an increase probably will be employed.

Inspection of the value of the riser-to-riser current attenuation coefficient γ leads to the consideration that it might be needlessly small. Decreasing the cross section of

risers by a factor of 1.5 to 2 would increase γ by a similar factor while not altering the fact that after the first riser ahead of or behind a train very little riser current flows.

To conclude, within a range of parameters constrained for a number of reasons, during final design, parameter variations will be investigated that offer the potential for greater economy or operational flexibility while still meeting the UW specs for stray B-field levels.

3.9 Traction Power Substation Cabling

In general the cables carrying multi-kA DC currents between rectifier banks and tracks should be run in closely spaced pairs to avoid the creation of large loops. During the process of developing layout plans for substations and cabling B-field modeling will have to be done to evaluate adequacy of designs for minimizing stray B-fields. Designs may have to depart from standard practices employed when stray B-fields are not an issue.

4 FINITE EXTENT OF THE HI-LO MITIGATION REGION AND OVERALL WORST CASE B-FIELDS

4.1 B-field Values Resulting from Finite Extent of Hi-Lo Mitigation

The Hi-Lo mitigation region must extend past all the B-field critical labs at the UW. For points on the North Link ROW sufficiently far north or south normal propulsion circuit design will be used, with currents flowing from substation to trains through the overhead contact wire and returning via the running rails. This normal propulsion circuitry results in the existence of current loops of 4.3 meter height drawing a maximum train current of 2.8 kA per train. The distance from each critical lab on campus to the nearest 4.3 meter high loop must be sufficiently great that the B-field from the conducting loop, when added to B-fields arising from currents in rails and contact wire near the lab, do not exceed the UW spec limit for the lab.

Provided Hi-Lo mitigation does not extend north to the end of the section of track powered by the University of Washington Station substation, each track will have a 4.3 meter high loop of some length just south of the Brooklyn Station capable of conducting 2.8 kA max train current. At critical labs, B-fields from these loops, generated when trains are present in them, pose an alternate hazard to that of the propulsion and perturbation B-fields arising when trains are nearby. In other words, B-fields from trains in the 4.3 meter high loops near Brooklyn have to be accommodated, as do perturbation B-fields from trains nearby, but not accommodated simultaneously.

The 4.3 meter high conducting loops on the campus are not the only consideration. North and south of the campus currents to trains also will flow in 4.3 meter high loops. These loops might extend in length more than a mile north and south of the campus. B-fields from currents in these loops also must be considered when determining how far north and south of the locations of critical labs Hi-Lo mitigation must be extended.

To determine the required extent of Hi-Lo mitigation a spatially distributed model was created containing three separate circuits and extending from approximately 3,000 meters (9,800 ft) north of NE 45thSt. to approximately 3000 meters south of the University of Washington Substation. Figure 4.1 shows the course followed by these circuits, following the North Link ROW through campus and extending north and south beyond the campus. Figure 4.1 also shows the coordinates of building corners and points on the ROW used for a series-of-straight-lines approximation to the ROW for this modeling. Coordinates are given in meters north and west of the point (0 W, 0 N) which is positioned in the middle of the ROW at the south end of the University of Washington Station.

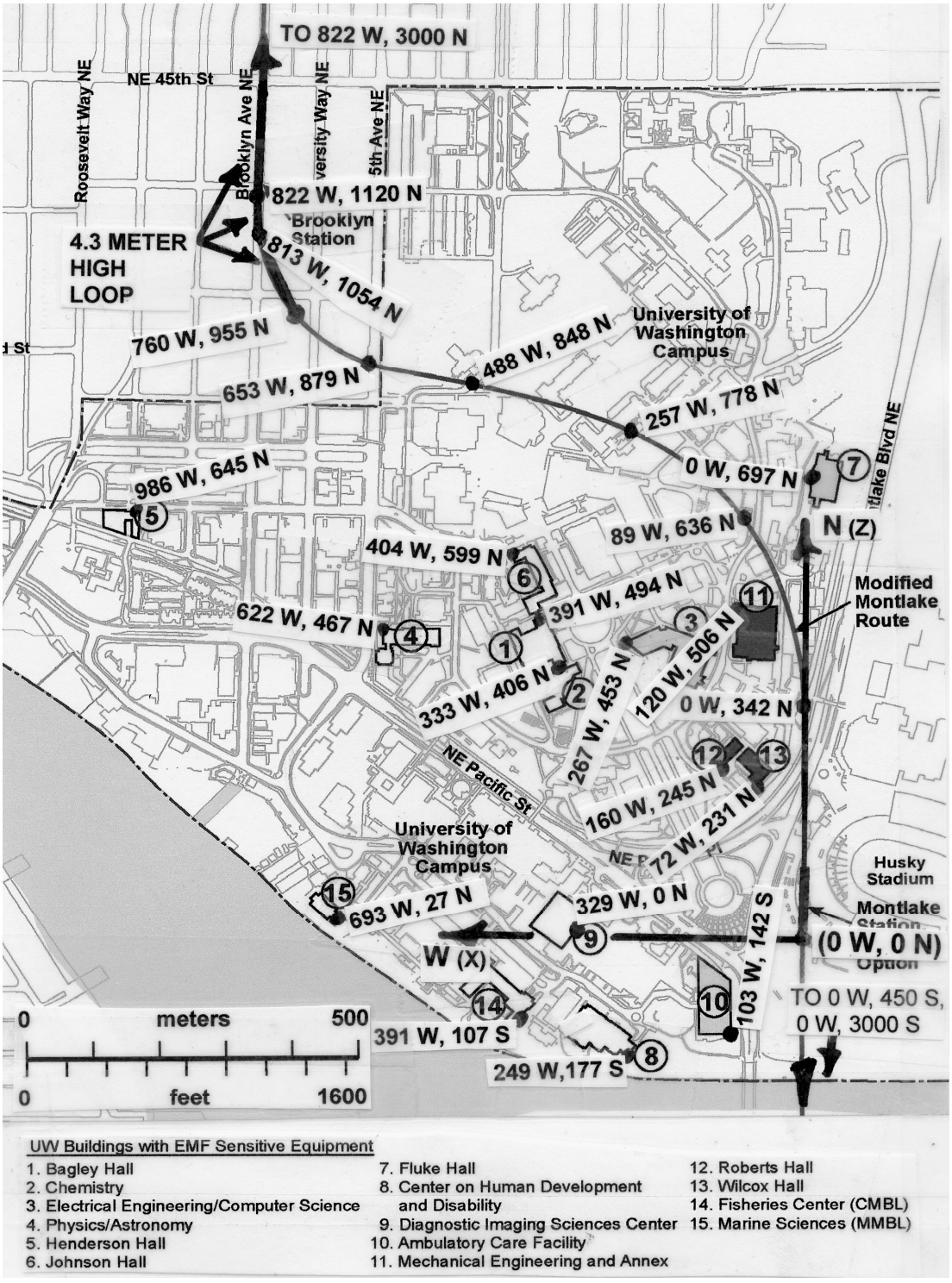

Figure 4.1 UW campus map showing coordinates in meters of building corners closest to Hi-Lo mitigation endpoints and of ends of series-of-straight-lines segments used for B-field modeling. An additional piecewise linear ROW point at (28 W, 516 N) has been omitted from the map above.

The first of the three electrical circuits in the model, named the Central circuit consists of a conductor carrying positive current northward from (0 W, 0 N) at a distance below rail height corresponding to the depth of the centroid of positive current flow which is depressed below rail height due to overhead contact wire wear. This depth was given extreme values of 0 or 15 cm. The depressed conductor carries current along the approximate piecewise linear ROW to the point (760 W, 955 N), the assumed northern end of Hi-Lo mitigation. At this point, approx. 100 meters SW of the intersection of NE 42nd and University Way, the positive conductor makes an abrupt transition upward to an elevation of 4.3 meters above rail height, and continues northward along the final two straight sections of modeled ROW to the northern end at (822 W, 1120 N), at the intersection of NE 43rd and Brooklyn Ave. NE. At this point, the conductor bends straight downward to rail height, and then follows the ROW at rail height back to (0 W, 0 N), where the loop is closed.

The second of the three electrical circuits, named Roosevelt, consists of a loop with lower conductor at rail height upper conductor 4.3 meters above. This loop extends from end of the first circuit at (822 W, 1120 N) 3,000 meters (9,800 ft) northward

The third electrical circuit named South of Montlake, is in the form of a two-conductor loop, with the positive conductor depressed 0 or 15 cm below the rail-height return conductor, running due south from (0 W, 0 N) a distance of 450 meters. At (0 W, 450 S) the positive current conductor makes a transition to +4.3 meter elevation. The 4.3 meter high loop continues southward to its endpoint at (0 W, 3000 S).

To model two trains in the Central loop just south of the NE 45th Street station conducting max propulsion current of 2.8 kA each, Central loop current was set at 5.6 kA. Likewise, to model two trains in the Roosevelt loop drawing max current from a rectifier bank at NE 45th, current in this loop was set at 5.6 kA. Note that if the two Roosevelt trains were near NE 45th and drawing their current from the Roosevelt substation, the current, and the B-fields generated, would have opposite polarity.

And finally, to model two trains in the South of Montlake loop, current was set at 5.6 kA. Two trains drawing max positive current in this loop is probably outside the realm of possibility. One train drawing 2.8 kA max current will be the usual case every time a train heads south from University of Washington Station up the north side of Capitol Hill. A second train traveling northbound probably would be in regenerative braking mode and would yield a net loop current less than 2.8 kA. However, for the sake of showing that 5.6 kA of current in the South of Montlake loop could be accommodated if it ever were to occur, that value was used.

Vector summation of all the B-fields from all parts of all three loops leads to a potentially time consuming process to determine the maximum possible propulsion B-field at a given lab. The parts of loops with depressed positive conductors tend to generate B-fields that point oppositely to the B-field from parts of loops with 4.3 meter high positive conductors. The result, for instance, is that at some labs in the central campus, B-fields from the central loop have greater magnitude when the depressed loop is depressed by a zero amount, whereas at other labs greater magnitude occurs with 15 cm depression.

Meaningful assumptions for modeling are that the Central loop has zero current, 5.6 kA current with zero positive conductor depression, or 5.6 kA current with 15 cm positive conductor depression. Meaningful assumptions for modeling the South of Montlake loop are the same. For the Roosevelt loop meaningful assumptions are + 5.6 kA, 0 or –5.6 kA. Thus in general, theoretically there are (3 x 2 x 3) – 1 = 17 possible conditions to search through to find worst-case vector B-field magnitude at each lab (the global zero-current condition has been subtracted out). To avoid this labor for the moment, the strategy used to check for compliance with UW B-field specs at each lab was to determine the worst-case magnitude of B-field from each loop at that lab and then sum the three magnitudes.

For each lab Table 4.1 gives the worst-case magnitude B-field from each of the three circuits in the model, and also gives the sum of the magnitudes, representing the maximum B-field due to the finite extent of Hi-Lo mitigation.

The table also repeats the Table 3.2 values of max Hi-Lo mitigated B-fields for two trains operating simultaneously in the central region. And, the table gives the sum of B-field magnitudes from the Roosevelt plus South of Montlake circuits.

The worst-case maximum overall B-field at each lab is then found by summing the contributions from the Roosevelt and South of Montlake loops with the greater of Central loop B-field or Hi-Lo mitigated B-field. This overall maximum B-field is shown in the last column of Table 4.1.

Overall max B-field levels exceeding UW spec limits are shown in bold in Table 4.1. Note that the spec limits are exceeded only in the ME area and at Roberts and Wilcox Halls.

The specification for Henderson Hall that stray B-fields |dB/dt| must be less than 0.2 mG/sec requires special consideration. Peak values of |dB/dt| will depend on peak rates of change of propulsion currents. Propulsion currents should change slowly enough for the Henderson |dB/dt| spec to be met as trains accelerate southbound from Brooklyn and ease over the start of the downgrade, and as northbound trains drawing max current on the upgrade ease onto the flat and then prepare to stop at Brooklyn.

Table 4.1 Stray B-fields due to the finite extent of Hi-Lo mitigation. B-fields from Hi-Lo mitigation are given with B-fields due to 2 max current trains at the north end of the central loop, 2 max current trains in the Roosevelt loop and 2 max current trains in the South of Montlake loop. Labs and overall B-field levels exceeding UW spec levels are highlighted in bold.

Lab	UW B-field spec levels, mG	Hi-Lo mitig. B-field mG*	B_{cent} mG	B_{roos} mG	B_{som} mG	B_{roos} + B_{som} mG *	Max. overall B-field, mG
Bagley Hall	0.1	0.033	0.039	0.025	0.012	0.037	0.076
Chemistry Bldg.	0.1	0.032	0.031	0.019	0.015	0.034	0.066
EE-CS	5.0	0.184	0.044	0.020	0.013	0.033	0.217
Physics-Astron.	0.5	0.017	0.032	0.026	0.012	0.038	0.070
Johnson Hall	5.0	0.059	0.066	0.034	0.010	0.044	0.110
Fluke Hall	0.3	0.223	0.111	0.025	0.0087	0.033	0.256
ME Bldg.	0.2	0.875	0.238	0.020	0.012	0.032	**0.907**
ME Rm. 135	0.2	0.300	0.238	0.020	0.012	0.032	**0.332**
ME Annex	0.2	1.598	0.238	0.020	0.012	0.032	**1.630**
Roberts Hall	0.1	0.284	0.069	0.012	0.023	0.035	**0.319**
Wilcox Hall	0.1	0.810	0.304	0.011	0.025	0.036	**0.846**
Henderson**	Note 1	0.016	0.085	0.050	0.007	0.057	0.142
CHDD	0.3	0.056	0.030	0.006	0.121	0.127	0.183
Diagn. Imaging	5.0	0.030	0.020	0.008	0.049	0.057	0.087
Surgery Pavilion	1.0	0.344	0.157	0.006	0.121	0.127	0.471
Fisheries Ctr.	0.1	0.019	0.014	0.007	0.067	0.074	0.093
Marine Science	1.0	0.005	0.008	0.009	0.028	0.037	0.045
Roberts-W. half	0.1	0.199	0.069	0.012	0.023	0.035	**0.234**

Notes: *Hi-Lo mitigated B-field was calculated with 30 percent overhead contact wire wear.

**At Henderson Hall UW spec is |dB,tot/dt| Ò0.2 mG/sec.

Jerk limiting action of each train's propulsion control system will assure an approx. 1 sec. minimum transition time for transitions between max accel. and coast. However the operational conditions noted above should make actual transition times several times longer, resulting in max |dB/dt| values well within the UW specs.

One other factor affecting values of |dB/dt| will be the formation of current conducting loop of full contact wire height every time a northbound train passes the boundary of Hi-Lo mitigation. However, since these loops will grow in length from an initial length of zero the resulting B-fields will grow slowly. The values of |dB/dt| resulting from trains making a transition from propulsion to coast or braking at the top of the grade as they approach the NE 45th St. station will be greater.

Note that the B-field levels resulting from the finite extent of Hi-Lo mitigation and the overall max B-field levels depend specifically on the chosen Hi-Lo mitigation endpoints. The critical consideration for locating the northern end of Hi-Lo mitigation is the resulting B-field at Bagley Hall. Placement of the northern end at (653 W, 879 N) yielded an overall B-field level at Bagley Hall of 0.1 mG, exactly at the UW spec limit. To allow for some margin, the position chosen for these computations was moved approx. 120 meters (390 ft) along the ROW and farther from Bagley to the point (760 W, 955 N). Future fine-tuning of all the assumptions going into the model may allow a final point for the northern end of Hi-Lo mitigation to be located between these two points.

Likewise, the critical consideration for locating the southern end of Hi-Lo mitigation is the resulting B-field at the Fisheries Center. If it can be demonstrated that max propulsion current in the South of Montlake loop has a value less than 5.6 kA then the southern end of Hi-Lo mitigation could be moved northward. For a 2.8 kA max current the southern end could be located approx. 150 meters (490 ft) farther north to (0 W, 300 S).

4.2 B_{prop} Compliance Factor

Based on considerations of UW B-field spec levels and distances from the North Link right of way the four laboratories most sensitive to increased B-field due to errors in performance of Hi-Lo mitigation are Bagley Hall, the Chemistry Bldg., Fluke Hall and the Fisheries Center. For these four labs the question was asked, by what factor does Hi-Lo mitigated B_{prop} have to increase to just bring overall B-fields as given in Table 4.1 up to the UW spec limit?

Errors in the performance of Hi-Lo mitigation could be expected to increase the height of the effective dipole current loop in the Hi-Lo mitigated region. This would increase the predicted B-field levels arising from the finite extent of Hi-Lo mitigation in Table 4.1. Such errors also would increase the values for B_{prop} given in Tables 3.2 and 3.3 and lead to an increase in the overall B-field levels given in Table 4.1.

To determine the increase in the dipole loop height that could be tolerated the maximum B-fields due to finite Hi-Lo mitigation extent were re-calculated with new dipole loop heights for each of the four labs in question, and factors by which increase in loop heights brought total B-fields to the UW spec levels were recorded.

To determine the increase in B_{prop} level that could be tolerated at each lab the B_{prop} value given in Table 3.3 was multiplied by a factor greater than 1, with the resulting increased values of Hi-Lo mitigated B-field then entered in Table 4.1. The value of this factor for which the max overall B-field in Table 4.1 reaches the UW spec limit was also determined.

These multiplicative factors, defined as “compliance factors” for each case, are recorded in Table 4.2 for the four labs.

Table 4.2 Compliance factors for Hi-Lo mitigation for the four most sensitive labs.

	CF determined by increasing dipole loop height	**CF determined by increasing B_{prop} values**
Bagley Hall	2.0	2.15
Chemistry Bldg.	2.5	2.3
Fluke Hall	2.4	1.3
Fisheries Ctr.	2.0	2.0

The above analysis appears to predict that if the Hi-Lo mitigation system were to degrade that the first lab to suffer would be Fluke Hall where overall maximum B-field levels would increase to the UW spec limit when B_{prop} levels had increased by 30 percent.

The smaller of the two CF values for each lab have been included in Table 2.2.

5 SENSITIVITY OF HI-LO PROPULSION B-FIELD MITIGATION TO PARAMETER VARIATIONS

The North Link light rail line must not only provide acceptable stray B-field performance when designed, but also when built and operated. For that reason the effect of various design parameters departing from their ideally assumed values must be examined. Some departures will be time-independent. Others could vary with time. One particular parameter, the conductivity of the overhead contact wire, will be certain to vary with time as the contact wire wears through its normal service life. Comparison of the effects of all likely parameter tolerances or variation leads to the conclusion that contact wire wear will be the one of overriding importance.

The Hi-Lo propulsion B-field mitigation scheme is designed to balance the effects of specific currents against each other. For instance, propulsion current flowing to a train are supposed to divide between overhead contact wire and buried cable in a manner that puts the centroid of positive current flow at a point directly between the running rails. Similarly, return current flowing from a train back to the substation is supposed to divide equally between the running rails so that the centroid of return current also lies directly between the running rails, at the same point as the positive current centroid.

The effects of current imbalances caused by parameter variation to increase propulsion B-fields above the design values are characterized below by the manner in which they cause the centroids of primary propulsion current or return current in the rails to be displaced from each other. This displacement will give rise to the existence of an effective dipole current loop. The width or height that this loop must have to produce appreciable effects can be illustrated by the following example.

At a distance of 90 meters, one 4-car train produces B_{ptb} = 0.1 mG. At the same distance, assuming that the dipole loop current is caused by one 4-car train drawing 2.8 kA, solution of Eqn.3.9 shows that a dipole loop of width or height 14 cm will cause the same 0.1 mG.

Some currents, for instance riser currents, do not need to balance with others. All the currents going upward in the risers will equal all the currents going down through the cars. As long as riser resistances including contact resistances are reasonably the same and do not depart too far from their design value, riser currents will fall off ahead and behind a train fairly quickly, leading to acceptably sized current loops, as seen from a side view, ahead and behind the train. The current loops seen looking down the axis of the train have size determined by the distance from center of the track to tunnel wall, and that cannot change.

In large part, dealing with tolerances in parameters during North Link design and construction is going to be much different than dealing with tolerances during the design and manufacture of mass produced products. North Link designers will need the answer to the question of how tightly tolerances can be maintained without too great an

economic price being paid when given the opportunity to pre-check and individually select the components used for construction. This is a far different situation than designing table model radios so that they will work when constructed with resistors and capacitors with ten percent tolerances pulled from parts bins at random and plugged into circuits.

The approach the author proposes for dealing with the issue of tolerances and parameter variations for North Link is first to determine by modeling what tolerances are required, and then to establish control and selection procedures to guarantee that the requirements are met.

5.1 Effect of contact wire wear

The effect of contact wire wear is to decrease the conductivity of the contact wire. As contact wire conductivity decreases, contact wire current decreases and buried cable current increases. This pushes down the location of the centroid of positive current flow. If this location initially were right between the running rails, an effective long current carrying dipole loop, initially with zero height, would grow in height over time.

Using parameters very nearly the same as those of the presently proposed Hi-Lo system final design, namely

$$\frac{\text{Buried cable conductance}}{\text{Initial contact wire conductance}} = \frac{G_b}{G_{co}} = \frac{\text{Contact wire height}}{\text{Buried cable depth}} = \frac{h_c}{d_b} = 10 \tag{5.1}$$

and letting the contact wire wear so that

$$\text{Contact wire cond.} = G_c = [1 - (\text{wear fraction})]G_{co} \tag{5.2}$$

and using the following equation for the magnitude of effective dipole height, based on Eqn. 3.16

$$\left|h_d\right| = d_b \left| \frac{(G_c / G_b)[(h_c / d_b) - 1]}{(G_c / G_b) + 1} \right| \tag{5.3}$$

results in the graph shown in Figure 5.1 for the magnitude of the effective dipole loop height vs. wear fraction.

The graph shows nearly linear variation of effective dipole loop height with contact wire wear, with a consequent nearly linear buildup of magnetic field. For a wear fraction of 0.35 (35 percent wear), the dipole loop width reaches 14 cm, and the augmentation to propulsion B-field will be as great as B_{ptb} at distances of approximately 90 meters.

If the contact wire were initially over-sized in cross section or if the buried cable were under-sized by a factor of 15 percent, then the initial dipole height would be approx. 6 cm. As the contact wire wore, dipole loop height would decrease down to zero and then back up again, hitting 6 cm again at a wear fraction of approx. 0.3. This would keep the augmentation of B_{prop} due to contact wire wear to less than half the B_{ptb} level at a distance of approx. 90 meters, while allowing for overall 30 percent contact wire wear.

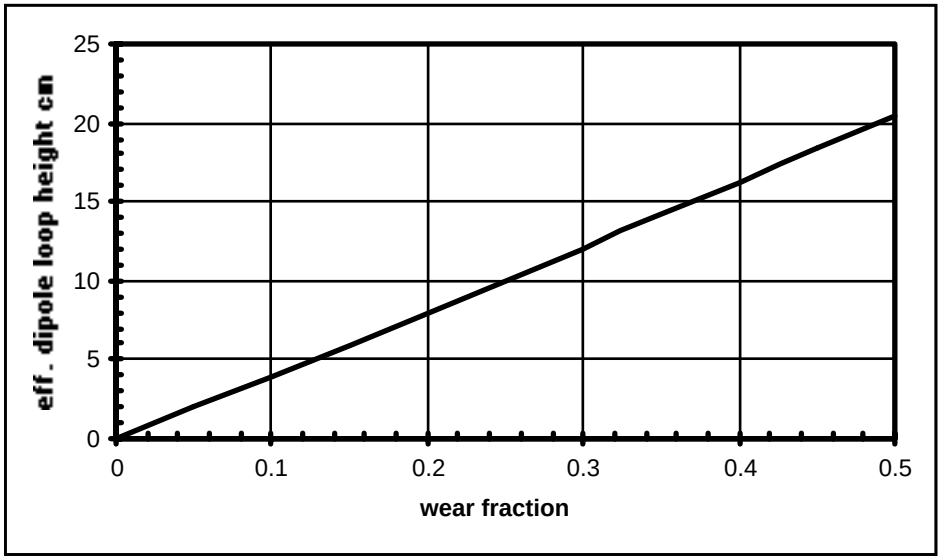

Figure 5.1 Effective height of current carrying dipole loop occurring due to contact wire wear.

The relation for the magnitude of B-field contributed by contact wire wear is

$$B_{cw} = \frac{2I\left|h_{dw}\right|}{r^2} = \frac{2 \bullet 2.8\left|h_{dw}\right|}{r^2} = \frac{5.6\left|h_{dw}\right|}{r^2} \text{ gauss} \qquad (5.4)$$

Equation 5.4 was not used to calculate the values of propulsion B-fields for the case of 30 percent contact wire wear included in Tables 2.1 and 3.3. Instead, the increased contact wire resistance values occurring due to wear were included in

calculations of circuit currents, and these new values of currents were used to calculate new values of B_{prop}. Actual calculated increases in B_{prop} due to contact wire wear tend to be slightly smaller than the B_{cw} values found from Eqn. 5.4. For instance, for Fluke Hall, Table 3.2 shows B_{prop} increasing from 0.025 mG to 0.083 mG, as wear goes from 0 to 30 percent, an increase of 0.058 mG, whereas Eqn. 5.4 gives a B_{cw} value of 0.061 mG. This comparison demonstrates that the above treatment of contact wire wear does give results slightly pessimistic but close to those of the more extensive modeling actually performed, and with much less effort.

5.2 Dimensional Construction Tolerances

Sound Transit and LTK civil engineers state that during construction the relative placement of running rails, conduit for buried cable and overhead contact wire support points can be made to an accuracy of ±0.25 in = ±0.625 cm in all directions. Such placement errors will contribute negligibly to the effective dipole width due to parameter variations, compared to, for instance the 14 cm variation in effective current carrying dipole loop width due to contact wire wear.

5.3 Contact Wire Stagger

In order to spread the wear caused by contact wires across the current pickup shoes on the car pantographs, the contact wires are installed in a staggered or zig-zag pattern, going from a maximum of 9 in (23 cm) toward one side of center to 9 in toward the other every 150 ft. Since the contact wire only will carry approx ten percent of total train current, the effect of the stagger would be at most a contribution to a lateral dipole loop width of 0.9 in (2.3 cm).

Variation of B_{prop} values due to varying lateral placement of the contact wire were calculated for one location at a slant distance from the track of 72 meters (236 ft) and the results shown in Figure 3.17. It is seen that as the contact wire varies position from 23 cm offset away from the lab to 23 cm toward the lab B_{prop} varies by at most 0.04 mG. The maximum effect of contact wire stagger was incorporated into the stray B-field values given in Tables 2.1 and 3.3 by performing all calculations for a slightly greater than worst-case contact wire lateral offset of 25 cm (9.8 in) away from the labs.

5.4 Cable Resistance Tolerances

Prior to installation wire and cable resistances can be checked while the wires and cables are still on their reels, to make sure that resistances are close enough to meet specifications. Additionally, tolerance specifications could be included in the lists of specifications for overhead contact wire and buried cable to assure that wire and cable met tolerance requirements when delivered.

Tolerance information has been received from one potential North Link supplier, but it related to the diameter of multi-conductor cable and not to cable resistivity. Since cable diameter is affected by sizes of areas of voids left when cables with original circular strands are swaged to decrease the diameter and achieve a more solid fill, resistance tolerance could not be inferred from the information provided. More tolerance information will be sought from this and other manufacturers.

If for whatever unforeseen reason the resistances of overhead contact wire and buried cable were to deviate from their nominal values by as much as 5 percent, the worst case would then occur if the overhead contact wire's resistance were 5 percent high and that of the buried cable were 5 percent low. When combined with a further increase in overhead contact wire resistance due to 30 percent reduction in initial cross section due to wear, total worst-case contact wire resistance would then be [1.05/(1-0.3)] = 1.5 times its nominal value.

As found from Eqn. 3.16 this increase, combined with the decrease in buried cable resistance to 0.95 times nominal value would yield a depression in elevation of the centroid of positive propulsion current equal to 17 cm (6.7 in), an additional 3 cm beyond the 14 cm depression due to the 30 percent overhead contact wire wear alone. The resulting small addition to propulsion B-fields would cause only very small increases in propulsion B-fields at critical lab locations, for instance by approx. 0.013 mG at Fluke Hall and EE-CS, and by lesser amounts at more distant labs.

Resistance tolerance of riser cable is a much less critical issue than that of buried cable and overhead contact wire. Whereas B-fields from the buried cable-running rail loops are expected to cancel those from the contact wire-running rail loops, the B-fields from riser loops are not expected to cancel the B-fields from other sources. Slight increases in riser cable resistance simply would lead to a slight decrease in resistance ratio ρ as given in Sec. 3.5 including Eqn. 3.22, which in turn would lead to a slight increase in the value of γ, the ratio of currents in adjacent risers ahead of or behind a train.

5.5 Contact Resistance Effects

5.5.1 Wheel-rail contact resistances

Unequal wheel-rail contact resistances will cause current imbalances between the rails. However, since in a Link light rail train any single wheel-axle set will be located adjacent to many additional wheel-axle sets, the imbalance current caused by a single high-resistance wheel-rail contact will largely be dissipated by nearby wheel-axle sets. This is because a wheel-axle set will serve as a low-resistance path between the rails for re-balancing all of the currents from the other wheel-axle sets except for its own.

Even in the case of a gross side-to-side imbalance of contact resistances for an entire train, the imbalance current flowing into one rail, defined as the excess over the current injected into the other rail, will divide between two paths. Assuming that the nearest substation is ahead of the train, a greater part of the imbalance current will flow through the rail into which it was injected directly back to the substation. A smaller portion will flow in the opposite direction, back to an impedance bond location where the rails are connected with a DC short-circuit, where it will flow across the short to the other rail, and then down that rail to the substation. If another impedance bond is located between train and substation, rail currents will be re-equalized at that location.

Figure 5.2 illustrates a circuit comprised of positive feed conductors, running rails, impedance bonds, substation, and a train fed by a single substation injecting imbalance current into a single rail. The total distance between the impedance bonds nearest the train is d meters. The distance from train to impedance bond in the direction toward the substation is a meters. Running rail has resistance R_r Ý/meter.

The division of injected imbalance current between the direct and back-and-around paths is related to the rail resistances of the paths. Rail currents I_1 and I_2 are

$$I_1 = \frac{(2d - a)}{2d} I_{imb} \quad \text{and} \quad I_2 = \frac{a}{2d} I_{imb} \tag{5.5}$$

The areas of the current-carrying loops formed by the rails is also related to the lengths of the paths. The areas of the loops are

$$A_1 = \frac{d_{rr}}{2} a \quad \text{and} \quad A_2 = \frac{d_{rr}}{2} (2d - a) \tag{5.6}$$

It is seen that the magnetic dipole moments of the two loops, given by their products of current times area, are equal. And since currents flow clockwise in one loop and counterclockwise in the other, dipole contributions to B-field will tend to cancel. In the vicinity of the circuit the cancellation will not be complete, but the partial cancellation will result in B-field levels smaller than those from a single loop.

As an example a circuit based on lab to track distances used in prior examples was modeled, namely 64 meters horizontal, 32 meters vertical and 72 meters (213 ft) slant distance. It was assumed that the lab was positioned midway between impedance bonds 200 meters apart, as shown in Fig. 5.2. Numerical results indicated that when the lumped train imbalance source was midway between the impedance bonds and adjacent to the lab, 0.28 kA of imbalance current representing ten percent of total train current would produce 0.025 mG of B-field at the lab due to the imbalance current. As train position moved toward either impedance bond, imbalance-produced B-field decreased toward zero.

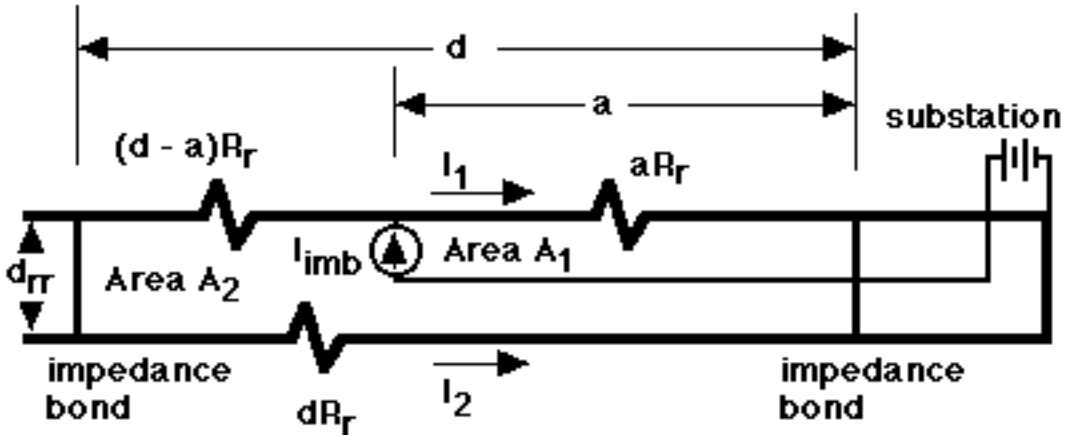

Figure 5.2. Magnetic dipole loops formed by imbalance current injected into running rails.

If all the current flowed in the smaller loop the resulting B-field at the lab would vary from 0 with the train at the impedance bond nearest the substation, to 0.056 mG with the train opposite the lab, to 0.112 mG with the train at the left-hand impedance bond. Thus the self-cancellation properties of the two loops formed are seen to reduce the imbalance-produced B-field by a factor a little greater than four.

This author believes that it is very unlikely that DC imbalance currents approaching ten percent of train current will ever occur. With continuously welded rail, a sheltered environment, and wheels kept round to minimize vibration, current imbalances should be very small.

There is the possibility of the sand dispensed to maintain traction going up the grades momentarily interfering with electrical contact between individual wheels and rails. However, the proximity of nearby wheel-axle sets making good contact should

provide current paths to rebalance the return current. Note that the requirement to use sand for sufficient traction is very unlikely in a tunnel.

If presence of either steady or intermittent imbalance currents in the running rails ever became suspect, clamp-on Hall Effect-type DC current probes could be temporarily installed in impedance bond leads to monitor imbalance currents.

5.5.2 Effects of other contact resistances

DC propulsion currents are conducted from the running rails to the substation return cables by means of impedance bonds, which are basically large center-tapped inductors. One end of an impedance bond makes contact with each running rail. In the case of North Link the center tap of the impedance bond nearest the TPSS will be connected to the substation return cable.

The transit industry is skilled in making good clean low-resistance ohmic contacts. Currents to each rail can be measured separately using portable easily used equipment, during initial operations and periodically thereafter, to assure that current imbalances due to unequal contact resistances are not too large. Contact resistance values can be checked in service using portable equipment.

Riser cable-to-contact wire resistance is a critical parameter since this resistance adds directly to that of riser resistance itself to yield the total resistance of each riser in the Hi-Lo mitigation circuit. If risers are to fulfill their mission of providing short current loops ahead and behind trains, then this contact resistance must be kept small compared to the riser resistance contributed by the riser cable proper, i.e., sufficiently smaller than the 0.326 mΩ value given in Table 3.1.

The best and most reliably documented information will be sought to serve as a guide for designing riser-to-contact wire clamping procedures. LTK has received preliminary information on clamp contact resistances that appears hopeful, but more information is required. Before procedures are implemented clamped contacts will be made up and contact resistances measured to assure that they fall within an allowable range. Micro-ohmmeters are the instruments used routinely to measure resistances such as wire-to-wire contact resistances and the resistances of transformer and motor windings.

Riser-to-contact wire resistances also could be checked in place when propulsion power is shut down, since the relatively high resistances of segments of overhead contact wire will tend to isolate the resistance of one contact wire-to-riser resistance from others during measurement.

Experience from Bielefeld appears to indicate that in general contact resistances are not a problem in a well maintained system.

5.6 Running Rail Resistance Tolerances

As with cables and contact wire, Sound Transit will coordinate with rail suppliers to assure tight resistance tolerances on rail selected for the Hi-Lo mitigation region. Rail resistances will be checked for acceptability before installation.

5.7 Temperature Variation of Buried Cable and Contact Wire

For critical locations near the UW campus all proposed rights-of-way are in tunnels. The slowly varying temperatures in tunnels should help assure that buried cables and contact wires stay near each other in temperature, so that their resistance shifts with temperature will track each other.

One possible cause of temperature difference between buried cable and contact wire might prove to be different rates of cooling after passage of a train. The specific heat of copper is 0.0912 gm-cal/gm-^{o}C = 0.381 joules/gm-^{o}C. Copper has a density of 8.92 gm/cm^{3}, which yields a weight of 10.85 kg per meter of length for 2400 kCM cable with 12.16 cm^{2} conducting cross section. With a resistance of 1.4 x 10^{-5} Ý/m, a 1-minute long pulse of 2.8 kA current such as might occur on one of the upgrades would produce 6,600 joules per meter length of electrical heating and raise the temperature of the cable by 1.6^{o}C. Given a temperature coefficient for copper of 0.0039/ ^{o}C, this would raise the resistance by 0.6 percent.

The rate of heating of overhead contact wire and buried cable will be the same. The contact wire will cool by convection. The buried cable will cool by a combination of conduction and convection. The question is, will the rates of cooling either be great enough or nearly equal enough so that over the course of a day their temperatures stay close enough to keep their current ratios within spec?

Since heat transfer from overhead contact wires and buried cables is a topic of general importance in the transit industry, data should be available to help answer this question. If it turns out that a propulsion power design using tracks fed from a single end results in too much cable heating the design might have to be modified to reduce heating. Increasing the cross section of buried cables while decreasing their depth is one option. Increasing the cross section of both buried cables and overhead contact wires is another. Providing cross-bonding between the running rails and cross-connecting the power feed cables at the end of the critical right-of-way section without substation, to provide additional current path, is another. Installing substations at both ends of the critical right-of-way section is a most expensive fourth.

The nature of heating and cooling cycles will depend specifically on the current vs. time characteristics at specific points on the rights-of-way.

During final design heat transfer data will be combined with information on expected North Link traffic patterns to determine likely changes in cable resistances due to temperature variation, and design changes will be made as required.

5.8 Predicted Propulsion B-Fields Due to Extreme Deviations in Parameter Values

If Hi-Lo mitigation can assure that North Link stray B-fields do not exceed the UW spec levels at Fluke Hall, it can provide such assurance for all other critical labs, with the exception of Wilcox, Roberts and the ME locations. Inspection of Tables 2.2 and 4.2 shows that for all the lab locations at which UW B-field spec levels are met, i.e., all labs except for Roberts and Wilcox Halls and the ME area, Fluke Hall has the smallest B_{prop} compliance factor CF. For this reason Fluke Hall was used as a test case to examine the effects of extreme parameter deviations on overall stray B-field levels. It was assumed that the following parameter deviations occurred simultaneously:

- Thirty percent overhead contact wire wear
- Overhead contact wire initial resistance 5 percent high
- Buried cable resistance 5 percent low
- Ten percent return current imbalance in the running rails (due to unequal rail resistances and/or unequal wheel-rail contact resistances)
- Riser-to-overhead contact wire contact resistance equal to 0.15 mΩ, approximately half the nominal riser resistance value
- Overhead contact wires offset 25 cm away from lab
- Risers located on tunnel walls toward lab

We believe that each of these parameter deviations are well beyond those that could be guaranteed by careful component selection during construction, coupled with proper maintenance.

Table 5.1 compares the results of the extreme case modeling for Fluke Hall to the prior results given in Tables 3.2, 3.3 and 4.1. Data for the first and second rows comes from those sources. NB and SB B_{prop} values for the last row required additional computation.

A comparison of the first two entries in Table 5.1 shows that as overhead contact wire wear increases from zero percent to 30 percent the B_{prop} compliance factor diminishes, but is still greater than 1 for the case of 30 percent wear.

Table 5.1 Example of extreme parameter deviations on stray B-fields at Fluke Hall. For all rows in this table risers are on the tunnel wall toward lab and overhead contact wire is offset 25 cm away from lab. CF = B_{prop} compliance factor.

Parameter deviations	B_{roos} + B_{som}	NB B_{ptb} mG	NB B_{prop} mG	NB B_{tot} mG	SB B_{ptb} mG	SB B_{prop} mG	SB B_{tot} mG	Overall B_{tot} mG	CF
No contact wire wear, no resistance deviations, no running rail current imbalance (NB data from Table 3.2, 0% wear, risers toward lab)	0.033	0.071	0.025	.096	0.054	.0195	0.054	0.184	4.4
30% contact wire wear, no resistance deviations, no running rail current imbalance (data from Table 3.3)	0.033	0.071	0.083	0.154	0.054	0.068	0.068	0.255	1.3
30% contact wire wear, 5% wire & cable resistance deviations, 0.15 mΩ riser-contact wire contact res., 10% running rail current imbalance	0.033	0.071	0.103	0.174	0.054	0.084	0.084	0.291	1.05

Note: Southbound B_{tot} = Max[(SB B_{ptb}), (SB B_{prop})], since SB B_{ptb} and B_{prop} peak at different times.

When the resistance deviations and running rail current imbalance noted above are added to the 30 percent overhead contact wire wear, the B_{prop} compliance factor diminishes to a value of 1.05, as the total stray B-field at Fluke Hall rises to 0.291 mG, still barely below the 0.3 mG spec limit.

A combination of still greater amounts of resistance deviations and running rail current imbalance would have to occur for B_{tot} levels to exceed UW spec levels at other critical labs with the exception of Wilcox, Roberts and the ME labs.

6 STRAY B-FIELDS FROM GEOMAGNETIC FIELD PERTURBATIONS

In the course of this program stray B-fields from geomagnetic field perturbations were measured from two sources in two locations. Measurements of perturbation B-fields due to nearby rail transit cars were measured near Portland, OR [Ref. 2]. And, measurements of perturbation B-fields due to nearby large transit buses were made on the UW campus [Ref. 3].

6.1 Perturbation B-fields Due To Rail Transit Cars

In the Seattle area the geomagnetic field B_{earth} has a strength of approx. 550 mG. Field lines point downward and north-northeastward, at an angle of 70^{o} with respect to the horizontal. Taking the x-direction to be west, y up and z north as was done for propulsion B-fields from trains on a north-south track, B_{earth} has x, y and z components approximately as shown in Table 6.1.

Table 6.1 Spatial components of the geomagnetic field in and near Seattle

Direction	B-component strength, mG
Transverse (west = +x)	-60
Vertical (up = +y)	-520
Longitudinal (north = +z)	+180
Magnitude	550

In the vicinity of iron and steel objects, such as steel bodied rail transit cars the otherwise parallel and undistorted magnetic flux lines of B_{earth} tend to bend and fringe toward the objects. With B_{earth} pointing nearly vertically, the concentration of magnetic flux lines tends to increase directly above and below the objects. And laterally from such objects, since magnetic flux lines are drawn toward the objects, magnetic flux concentration tends to decrease at one side or the other.

In June 2003 a series of measurements were made of the geomagnetic perturbations to B_{earth} caused by the passage of light rail cars of Portland's Tri-Met transit system. The measurements were made at Tri-Met in the greater Portland area. Portland is so close to Seattle that the characteristics of the geomagnetic field are practically identical at both locations.

The cars had weight, construction and dimensions very close to the specifications for Link light rail cars. A track was chosen running practically due north-south with a slight downgrade from south to north. One-, two- and four-car trains were coasted down the track and the perturbations to B_{earth} were measured vs. time at distances of 10, 20 and 50 meters from the track. The car current collection arms were down, and the cars drew zero current from the contact wire. Data collection at 100 meters distance was attempted, but data could not be distinguished from the random background fluctuations.

Figure 6.1 shows the components of geomagnetic field perturbation B_{ptb} vs. time for a four car train at a distance of 20 meters from the track center line.

Analysis of perturbation B-field data for 4-car trains shows that the magnitude of peak B_{ptb} occurring at a lab when a train passes is very accurately represented by the empirical relation, where slant distance r from lab to track is given in meters,

$$B_{ptb,max} = \frac{2000}{r^{2.2}} \text{ mG} \qquad (6.1)$$

The data underlying Eqn. 6.1 was taken with magnetometers located vertically approximately at train level. The question arises as to the behavior of B_{ptb} vs. r along lines that are slanting upward or downward at an angle away from the train. Provided a train's B_{ptb} field can be modeled near the train as a 2-dimensional dipole field arising from magnetization by the vector sum of vertical and transverse geomagnetic field, $|B_{ptb}|$ can be expected to decrease approximately as $1/r^2$ as r increases along any slanting line independent of its angle of elevation. The magnitudes of B_{ptb} components arising due to the axial component of geomagnetic field can be expected to be independent of angle of elevation relative to the train. Parts of the train comprised of highly concentrated ferrous mass can be expected to give rise to B_{ptb} components behaving like 3-dimensional magnetic dipoles that fall off as $1/r^3$ but have twice the magnitude in directions along geomagnetic field lines as in directions perpendicular to those lines. For these reasons it is presumed that Eqn. 6.1 will give results accurate enough for the scope of this project, while keeping in mind that the final design of the North Link B-field mitigation system must contain a margin to accommodate some levels of uncertainty such as these.

B_{ptb} levels for the critical UW labs calculated using Eqn. 6.1 have been included in Tables 2.1 and 3.3.

Figure 6.2 compares the variation with distance of the levels of unmitigated propulsion B-field from a very long contact wire-running rail loop 4.3 meters high conducting the2.8 kA current of a single train, the perturbation B-field from a 4-car North Link train passing by, the Hi-Lo mitigated propulsion B-field from a 4-car train, and the overall sum of Hi-Lo mitigated propulsion and perturbation fields. Comparison of the

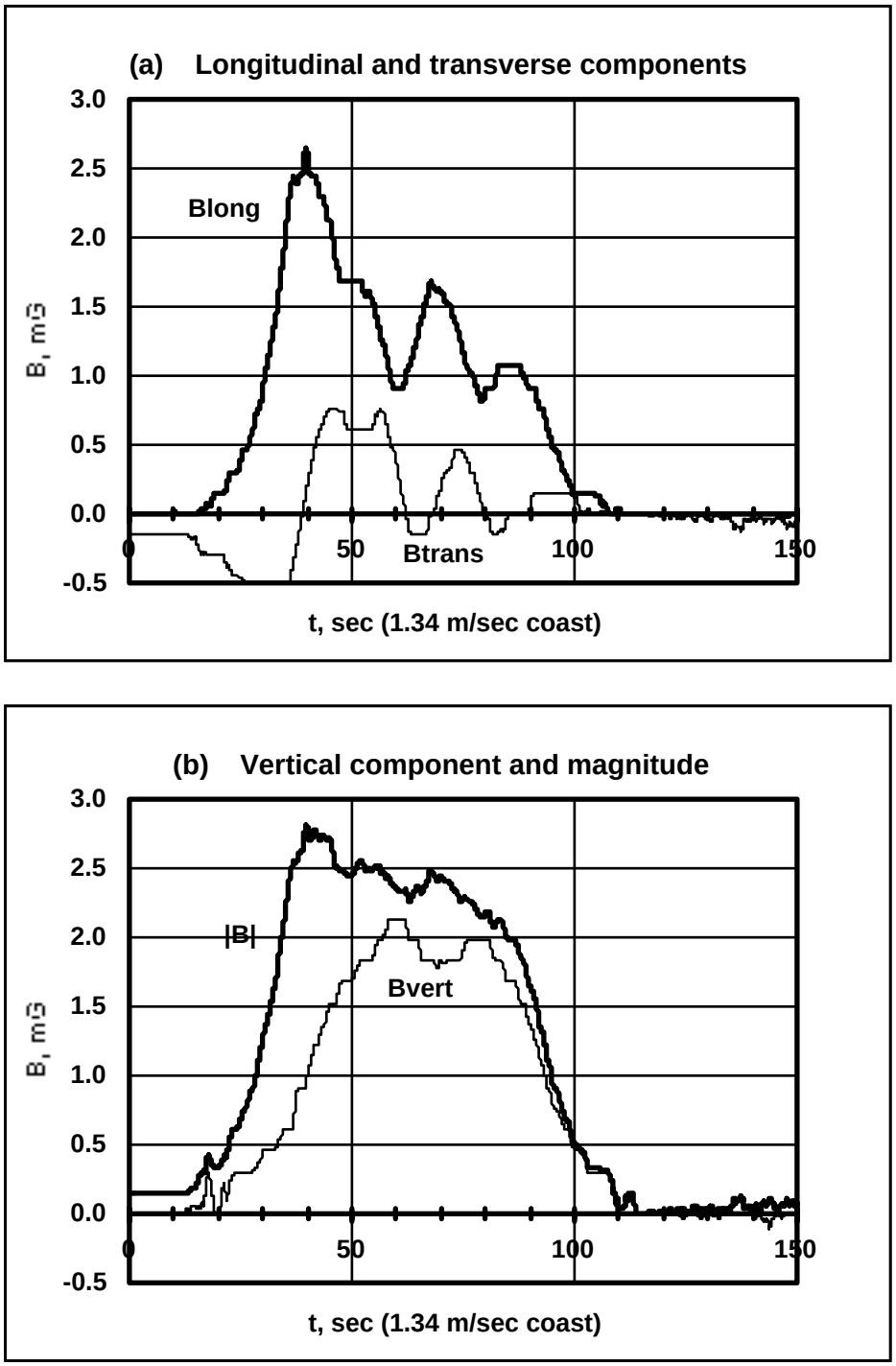

Figure 6.1 Geomagnetic perturbation B-field from a 4-car train passing at 20 meters distance**.**

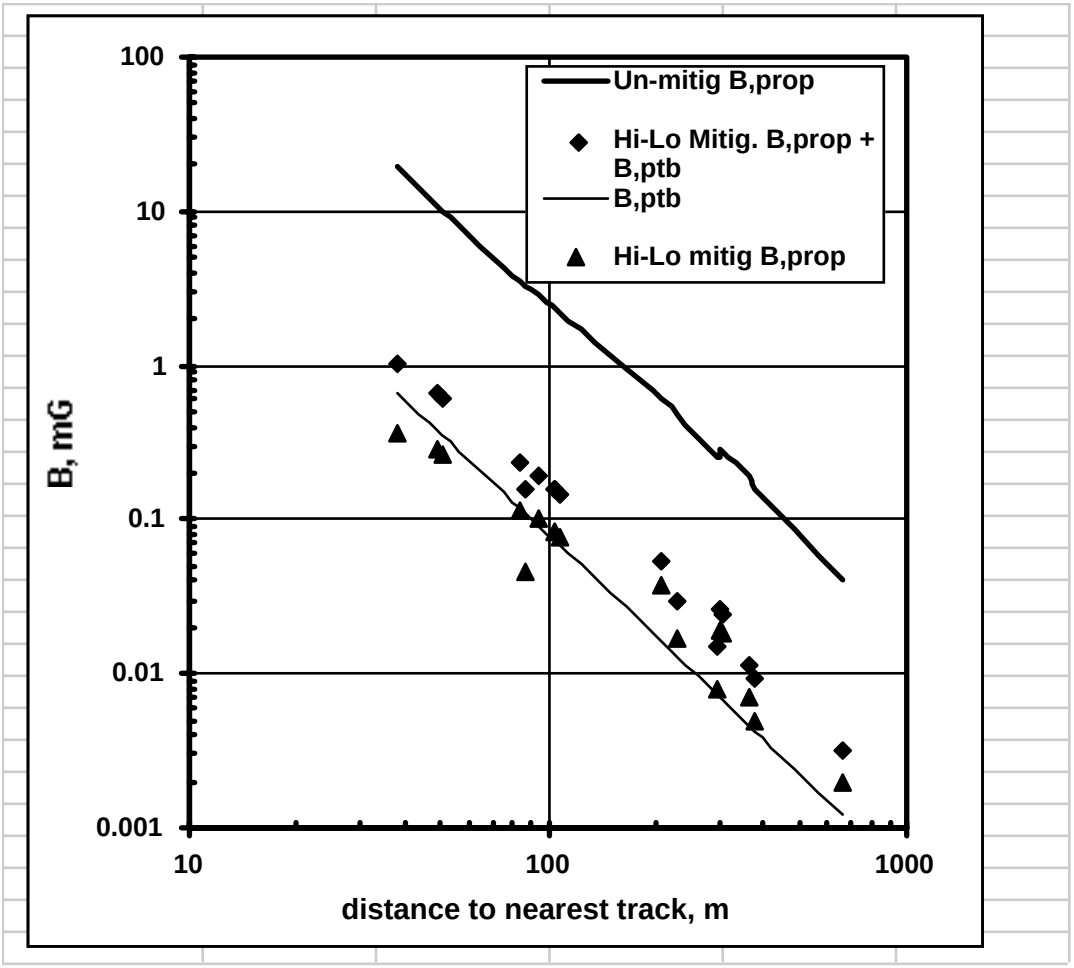

Figure 6.2 Comparison of un-mitigated B_{prop}, B_{ptb} and Hi-Lo mitigated B_{prop} field levels arising from passage of a train vs. distance to track.

magnitudes of the peak B-field levels vs. distance leads to the conclusion that overall stray B-field levels can only be mitigated down to the level of the perturbation B-fields.

Examination of Figures 3.15 and 6.1 show complex behavior for both Hi-Lo mitigated Bprop fields and Bptb fields as a function of train location. To be sure of not underestimating the vector sums of the two types of fields, it is prudent to directly add the magnitudes of the two fields to obtain a working estimate of the peak magnitude of their vector sum.

To achieve a maximum level of B_{ptb} equal to the 0.1 mG level requested by the UW at the most sensitive laboratories, Eqn. 6.1 indicates that a distance of 90 meters is needed. The slightly greater distance of 105 meters is needed to get the sum of B_{ptb} plus Hi-Lo mitigated B_{prop} down to the 0.1 mG level under the most ideal circuit conditions. The required distance will increase further when the effects of contact wire are factored in.

6.2 Perturbation B-fields Due to Large Transit Buses and Other Vehicles on the UW Campus

In November 2003 B-field measurements were made on the UW campus to assess the existing magnetic field environment at locations near sensitive laboratories. [Ref. 3] During the course of these measurements special attention was given to quantifying the perturbation B-field levels arising from large articulated diesel powered transit buses. These vehicles have a length of approx. 60 ft (18 meters) and are the most frequently encountered large vehicles on the main roads through the campus. It could generally be inferred that other very large vehicles such as large delivery trucks and large garbage trucks would produce stray B-field levels comparable to those caused by the buses.

Measurements of the B_{ptb} due to the large articulated buses were made at sufficiently many distances to allow determination of a general empirical formula for the maximum B_{ptb} to be expected during the passage of a bus nearby.

Figure 6.3 shows a graph of $B_{ptb}(t)$ recorded during the passage of a large articulated bus at a distance of 7.7 meters (25 ft). $|B_{ptb}|$ reaches a peak value of 5.81 mG. Table 6.2 summarizes peak magnitudes of the $B_{ptb}(t)$ pulses observed due to large articulated buses passing at a number of distances.

Table 6.2 Summary of peak perturbation B-field data for articulated diesel buses. Data is from Reference 3.

r meters	|B,ptb| mG	data record & time
7.7	5.81	uw3-ME-Stevens - ADB SB 14:32:10
13.5	1.60	uw3a - ME-Stevens - ADB NB 14:19:53
16.5	0.89	uw3a - ME-Stevens - ADB SB 14:17:10
22	0.48	uw3 - ME-Stevens - ADB SB 14:47:30
25	0.25	uw3 - ME-Stevens - ADB NB 14:50:27
38	0.10	uw7 - Benson-Herb Garden - ADB NB 21:13:54

A graph of peak $|B_{ptb}|$ vs. distance is shown in Fig. 6.4. The graph shows that data fit reasonably well to two empirically determined straight lines on the log-vs.-log plot, one with magnitude varying as $1/r^2$ for r < 18 meters (60 ft), and the other with magnitude varying as $1/r^3$ for r > 18 meters. With distances measured in meters and B-field stated in mG, the empirical relation for B_{ptb} vs. r is

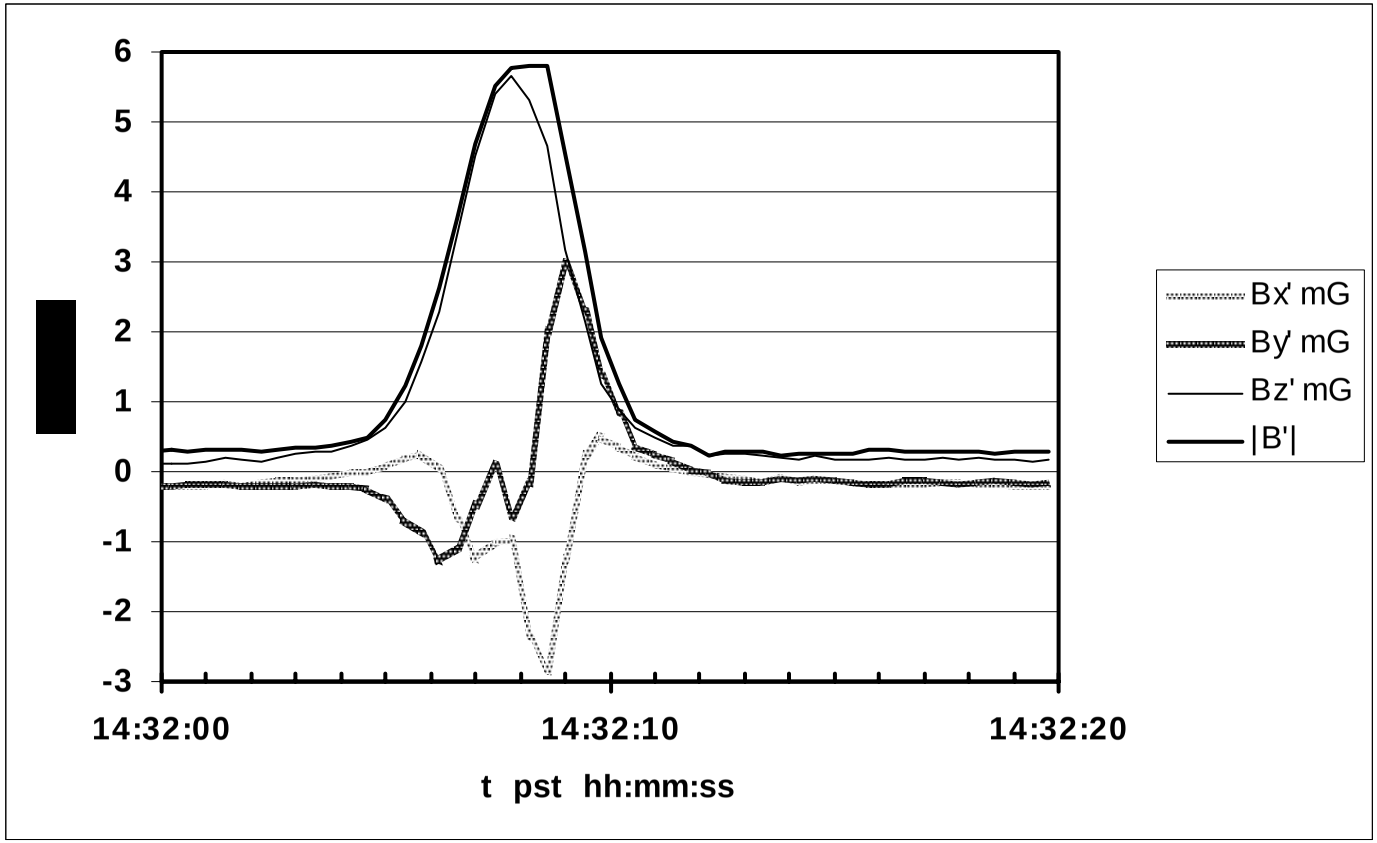

Figure 6.3 Perturbation B-field recorded on the UW campus near the ME Bldg. and Stevens Way due to the passage of a large articulated transit bus at a distance of 7.7 meters (25 ft). Directions for this graph: X-north, Y-west, Z-up.

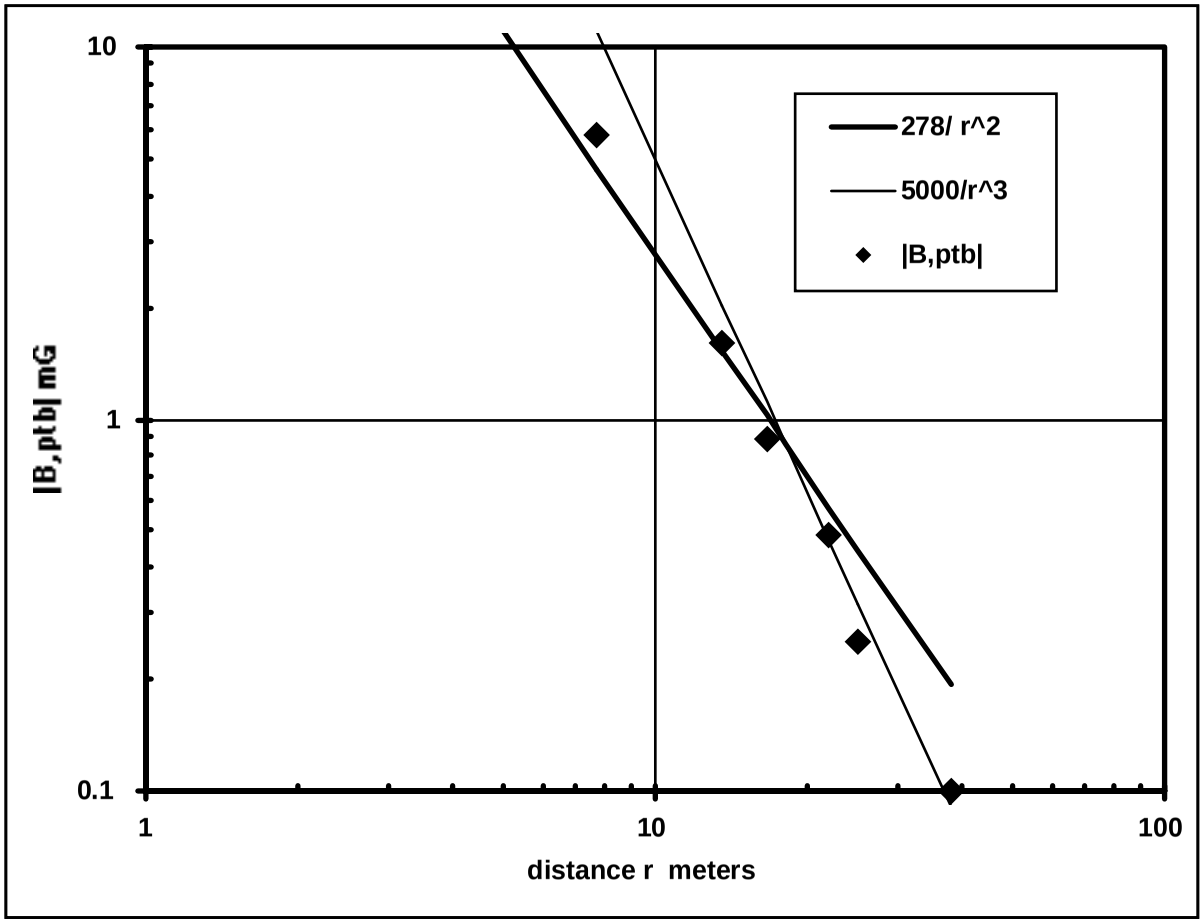

Figure 6.4 Peak magnitude of perturbation B-fields vs. distance due to passage of large articulated transit buses. Measurements were made on the UW campus in Seattle. [Ref. 3]

$$B_{ptb}(r) = \frac{278}{r^2} \quad \text{for} \quad r < 18 \text{ meters}$$
$$= \frac{5000}{r^3} \quad \text{for} \quad r > 18 \text{ meters} \qquad (6.2)$$

Observations of time varying B_{ptb} field levels due to cars, light trucks and vans passing nearby in parking lots adjacent to sensitive labs were also made, but more informally. It was noticed that when magnetometers were set up in the parking lot between Roberts and Wilcox Halls and near at the SE corner of Fluke Hall right next to the driveway, sizeable perturbation B -field pulses were recorded from the passage of passenger sized vehicles. One such B-field pulse recorded by the passage of such a vehicle at a 2 to 3 meter distance in the Wilcox-Roberts parking lot is seen in Figure 6.5.

The implications of the results from B-field measurements on the UW campus are as follows: Application of Eqn. 6.2 shows that in order to avoid unacceptably large perturbation B-fields from large articulated buses or vehicles of similar size, a lab must be located far enough away from the traffic lanes used by the buses. Specifically, Table 6.3 gives the minimum distances required to meet the various UW B-field spec levels.

Table 6.4 lists the distance from the critical UW labs to the nearest streets or roads, the UW stray B-field spec levels for the labs. The Table 6.3 data are then used to calculate the predicted distance of penetration of stray B-fields above UW spec levels from large buses and trucks into the labs. It is seen that such penetration is predicted for the Physics and Astronomy Bldg. near 15th Ave. NE, the ME Bldg. near Stevens Way, Roberts and Wilcox Halls near Mason Road, CHDD near Columbia Road, and slightly for the UWMC Surgery Pavilion near Montlake Blvd. In at least one instance, that of the Physics and Astronomy Bldg, such penetration of stray B-fields was anticipated, and sensitive apparatus have been located over 25 meters from the traffic. [Ref. 4] Monitoring of existing B-fields at these locations will be conducted during system start-up to establish a threshold for monitoring.

Large buses and similarly sized trucks on roads are not the only consideration. At many UW campus locations parking lots butt up right against buildings with present or future severe stray B-field requirements, or are even located directly underneath as in the case of the UWMC Surgery Pavilion. In addition small but frequently used access roads run closer to critical buildings than the roads listed above. Automobiles, pickup trucks and vans using these smaller roads and parking lots could cause additional stray B-field levels greater than UW specs inside buildings.

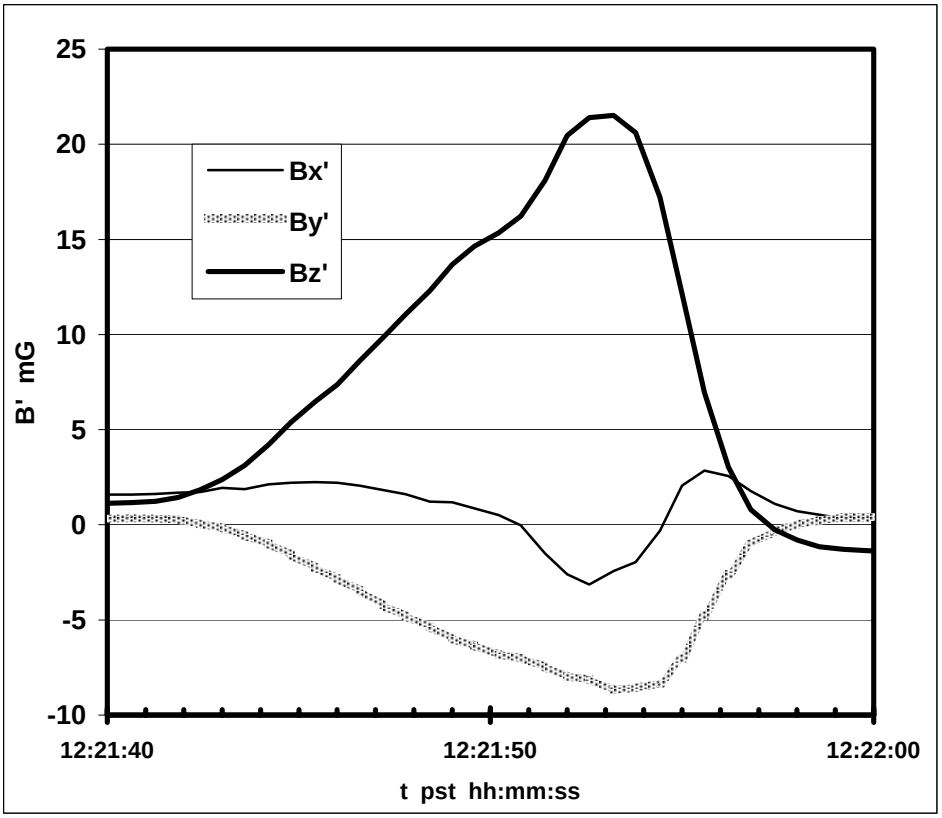

Figure 6.5 B_{ptb} pulse observed from passing passenger size vehicle at 2-3 meters distance in the Wilcox-Roberts parking lot on the UW campus. Directions for this graph: X-north, Y-west, Z-up. [Ref. 3]

Table 6.3 Distances from large articulated transit buses required to meet various UW B-field spec levels

UW B-field spec level, mG	Required distance, m
0.1	37
0.2	29
0.3	26
0.5	22
1.0	17
5.0	10

Table 6.4 Stray B-field penetration distances into critical UW labs due to large buses or trucks on nearby streets and roads.

UW Building	nearest street or road	distance, m	UW B-field spec level, mG	min. dist. from large buses to meet spec, m	B-field penetration distance above spec, m
Bagley Hall	Stevens Way	75	0.1	37	-
Chem Bldg.	Stevens Way	48	0.1	37	-
EE-CS	Stevens Way	12	5.0	10	-
Physics-Astron.	15th Ave. NE	10	0.5	22	12
Johnson Hall	Stevens Way	71	5.0	10	-
Fluke Hall	Montlake Blvd.	47	0.3	26	-
"	Mason Road	17	0.3	26	9
ME Bldg.	Stevens Way	14	0.2	29	15
ME Annex	Stevens Way	47	0.2	29	-
Roberts Hall	Mason Road	17	0.1	37	20
"	Stevens Way	64	0.1	37	-
Wilcox Hall	Mason Road	7	0.1	37	30
"	Pacific Place	44	0.1	37	-
Henderson Hall	40th Ave NE & NE Pacific	3	Note	Note	Note
CHDD	Columbia Rd.	17	0.3	26	9
Diagn. Imaging	Columbia Rd.	27	5.0	10	-
Surgery Pav.	Montlake Blvd.	15	1.0	17	2
Fisheries Ctr.	Columbia Rd.	44	0.1	37	-
Marine Science	Columbia Rd.	48	1.0	17	-

Notes: Henderson Hall is so close to the adjacent streets that large rapidly passing buses and trucks probably cause Henderson Hall's stray B-field limit given by the relation $|dB/dt| < 0.2$ mG/sec to be exceeded..

7 EFFECTS OF GROUND LEAKAGE CURRENTS AND SNEAK PATH CURRENTS

7.1 Ground Leakage Currents

The Hi-Lo propulsion B-field mitigation system depends specifically on the B-fields due to propulsion currents in the running rails canceling the B-fields due to currents in the overhead contact wire and buried cable. This balance can only occur if running rail current equals the sum of the contact wire plus buried cable currents. If part of the running rail current leaks into the ground and takes a circuitous path back to the substation, the balance will be upset and unacceptably large levels of propulsion B-field, falling off very slowly with distance away from the track, can result.

North Link will incorporate rubber insulating pads placed between running rails and ties to provide electrical insulation. Given the specifications for mounting pad resistance, ground leakage currents are predicted to be well below the levels that would cause a problem.

LTK Engineering Services, Sound Transit's engineering consultant for North Link, has developed a system for monitoring the health of rail-to-ground insulation. Examination of insulation levels over time will provide an accurate indication of the overall condition of the insulation between running rails and ground, so that maintenance can be performed as needed.

The track isolation monitoring system will provide for the measurement of rail-to-ground isolation by controlling and measuring the voltages across spans of rails and rail-to-ground voltages. The system will contain a power supply to induce a dc current source into the rail at selected locations near traction power substations. The equipment will be located in pits and/or enclosures at trackway level.

Remote monitoring will be accessible at traction power substations via LAN from the remote monitored trackside locations. Internet accessibility can be provided if required.

A great deal of experience exists in the transit and power industries for dealing with the causes and effects of ground leakage currents. Methods exist for interrupting current flows in buried pipes and conductors. The prime approach to be taken for North Link will be to avoid having North Link propulsion currents enter the ground in the first place.

The Sound Transit corrosion control design criteria requires that measures be taken to ensure that any stray currents that do leave the running rails be contained in the tunnel structures. These measures include:

- Welding of longitudinal tap splices in the top layer of first-pour reinforcing steel. Test facilities will be installed at each end of station structures and at every collector bar.
- In underground trackway structure inverts, a continuous bare steel cable will be run in the concrete for monitoring track-to-earth resistance values and dc current values.

7.1.1 Ground Leakage Current Theory

Assume we have two rails in parallel yielding series track resistance R_{tk} ohms/m, and we have rail pads with net leakage conductance to ground for the two rails of G_L S/m, as pictured in Fig. 7.1.

Current I_{tk} flows from left to right in the rails. A very small fraction of this current leaks off to the ground through the insulating pads, giving rise to ground leakage current $I_{gnd}(x)$. End-to-end circuit length is D meters.
For $-D/2 < x < +D/2$, leakage current to ground in an incremental length dx is

$$dI_{gnd} = V(x)\, G_L\, dx \qquad (7.1)$$

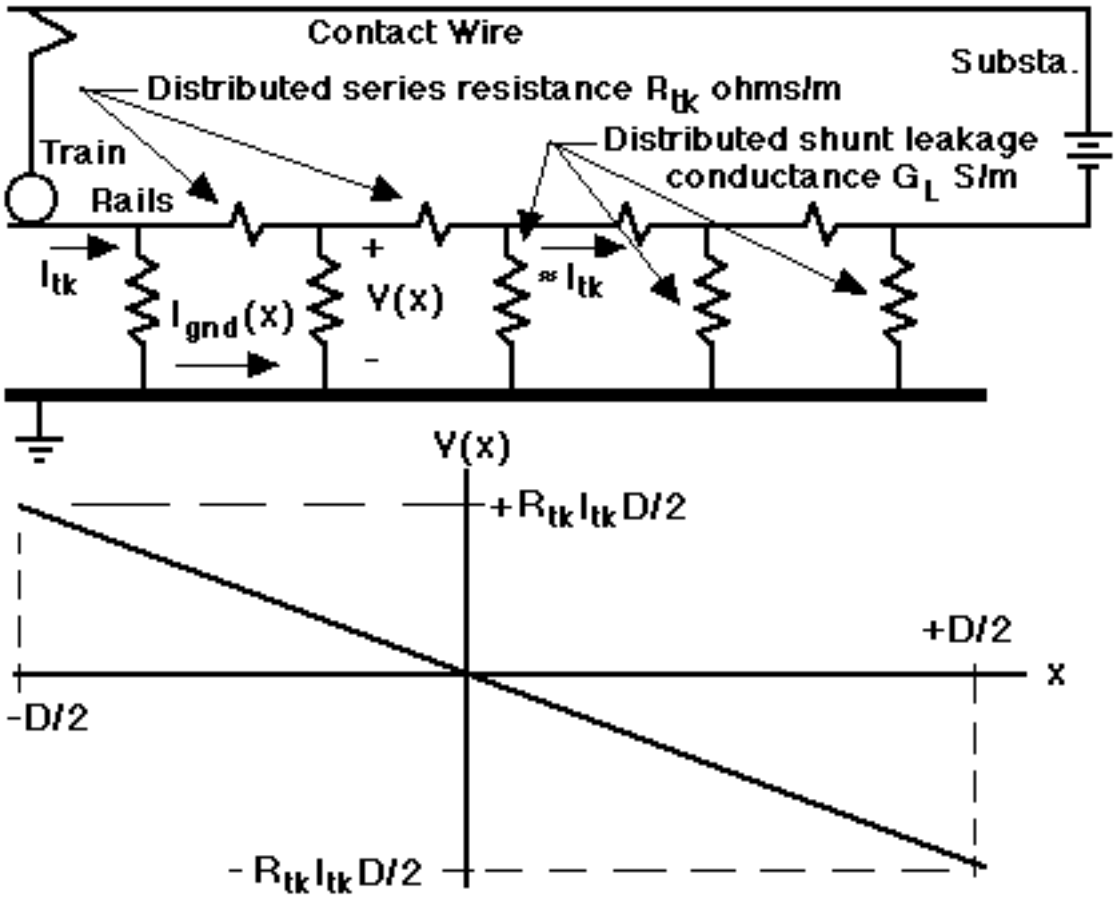

Figure 7.1 The rail-to-ground leakage current circuit.

Since I_{gnd} is very small, track current in the rails is approx. constant at value I_{tk}, independent of x. Therefore, V(x) is given by the relation

$$V(x) = -R_{tk} I_{tk} x \qquad (7.2)$$

Putting this relation for V(x) into the one above for dI_{gnd} and integrating from x = -D/2 to 0, yields the value of peak leakage current I_L, defined as the ground current at the midpoint of the circuit:

$$I_L = I_{gnd}(x=0) = I_{tk} R_{tk} G_L D^2/8 \qquad (7.3)$$

Using values D = 1600 meters (1 mile), I_{tk} = 2.8 kA, $R_{tk} = 1.56 \times 10^{-5}$ Ý/m, and $G_L = 6.56 \times 10^{-6}$ S/m the peak leakage current is 0.092 amperes.

The relation for B-field in the vicinity of a single long straight conductor (with I in amperes and B in gauss) is

$$B=0.002\ I/r \qquad (7.4)$$

As close as r=18 meters 0.092 A of unbalanced current would only produce additional B-field of 0.01 mG. At the approx. 72 meter distance of the nearest critical laboratory, the level would be 0.0026 mG. This level is well below that deemed critical by any of the UW researchers, and represents a very small increase in stray B-fields when added to those predicted from other sources.

7.1.2 Assurance of Ground Leakage Current Performance over Time

The above analysis indicates that if the insulating pads are doing their job up to spec, the resulting leakage currents will be acceptable. Examination of the relations shows that there is a fair amount of leeway in the value of pad resistance before leakage currents will rise to the level of being a problem. It will be part of the continuing diagnosis and maintenance program for the Link light rail system to keep leakage currents to an acceptable level.

Concern has been voiced that ozone produced in the subway tunnel due to ionization of air by the electrical system could cause rapid degradation of rail pad resistance. Ionization of the air is generally caused by electrical arcing.

Electrical arcing often is observed between the current pickup shoes and third rail in heavy rail rapid transit systems, and is caused by pickup shoe bounce. However, in a light rail system with overhead contact wire the pantograph typically has a relatively smooth ride under the contact wire, and contact bounce leading to arcing typically is not seen to occur. Isolated arcing incidents probably will occur when the front axles of transit cars cross insulated joints at breaks in the propulsion power system, but these events will be relatively small in number.

The traction motors for North Link will be brushless 3-phase AC induction motors, unlike the DC motors with commutator brushes that can cause arcing, used in rail transit systems in the past. These should not contribute to ozone production. Sharp points on high-voltage conductors could be sources of corona discharge and ozone production. The extent of such a problem could be investigated by making ozone concentration measurements in TriMet tunnels in Portland.

Information has been obtained on one type of rail mounting pad whose construction provides electrical insulation as well as acoustic isolation. Sound Transit's acoustics specialist has recommended this type of pad for possible use. This type of pad, called the "Cologne egg", has a documented history of use in rail transit service in a number of cities. Operational information will be obtained from the involved transit authorities to serve as a guide in planning the maintenance program required to deal with in-service electrical degradation of such pads due to ozone or dirt.

7.2 Sneak Path Currents

To maintain current balances between the running rails of each track and that track's overhead contact wire and buried cable, it is important to avoid inadvertent and unwanted current paths in the propulsion feed circuit, referred to as sneak paths, that can result from cars bridging the insulated joints and contact wire gaps at the ends of the campus portion of the North Link system.

The basic configuration of traction power substations and tracks envisioned for North Link in the UW area is shown in Fig. 7.2. To avoid sneak paths special design procedures will be followed. The cross-bonding of running rails in one track with the rails of the other track, normally done to provide net lower resistance for DC return currents, will not be used in the Montlake to NE 45th St. region. Two dedicated rectification substations, one for the northbound track and one for the southbound track, will be used to power trains operating under the campus from Montlake to NE 45th St. Insulated joints and contact wire gaps will be incorporated in each track at each end to eliminate the possibility of unwanted unbalanced currents flowing into the campus portion of North Link. The locations of the insulated joints and contact wire gaps are noted as locations A, B, C and D in Fig. 7.2. (The buried cable has been omitted from Fig. 7.2.)

Figure 7.2 pictures an event that must not be allowed to occur, namely the simultaneous bridging by rail cars of the insulated joints at points A, B, C and D. Focusing on the train near corner C, it is seen to bridge the rail gap there while drawing its pantograph current from the Roosevelt TPSS. Likewise, trains near the other corners bridge their rail gaps. Train C's return current will follow two paths back to the Roosevelt TPSS. Part of the return current will flow northward directly through the southbound running rails, while the remainder will flow southward to Corner A, through the bridging car, through the cross bonding or return circuit of the Rt. 520 TPSS,

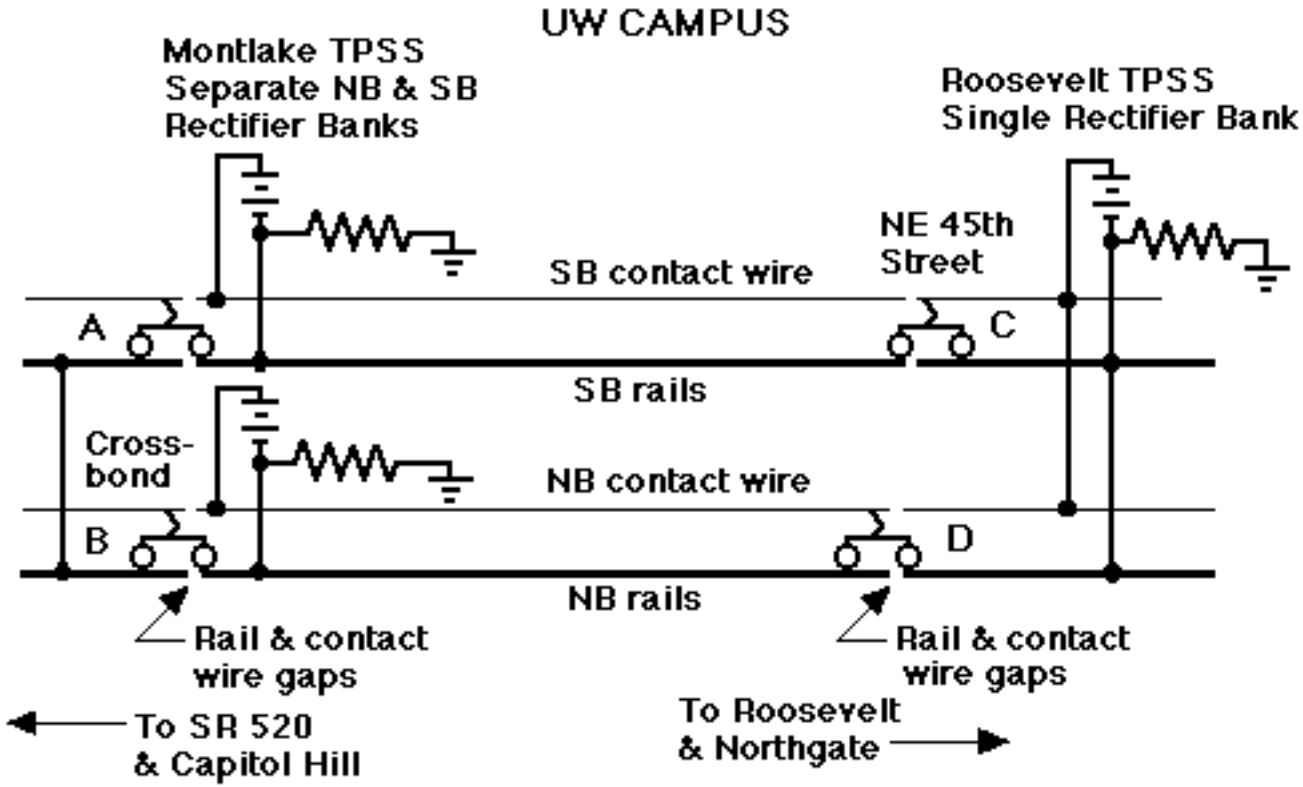

Figure 7.2 A North Link propulsion circuit encompassing the UW campus with potential sneak paths.

through the bridging car at Corner B, northward in the northbound rails, through the bridging car at Corner D, and then back to the Roosevelt TPSS. The southbound and northbound rail currents through the UW campus would not be balanced by currents in overhead contact wire and buried cable. These currents would flow in a 12-meter (39 ft) wide loop extending through the entire campus, giving rise to unacceptable B-field levels. Propulsion currents for the rail cars at Corners A, B and D would behave similarly.

It can be seen from the circuit diagram in Fig. 7.2 that the above sneak path problem can be solved by removing the bridging rail car at any one of the four corners. Therefore, one solution would be to not allow trains to simultaneously transit the rail gaps at all four corners. This restriction could be built into the automatic train control system.

An alternative solution would be to incorporate a dead zone, or non-bridging zone, in the running rails and overhead contact wire at any one of the four corners, as shown in Fig. 7.3. In this scheme two sets of insulated joints are placed in the running rails at a separation a little greater than the distance between the end axles of a rail car. A dead section of overhead contact wire is positioned in the middle of the dead zone. This section of dead contact wire must have sufficient length to assure that a train's pantograph cannot make contact with live contact wire while its wheels are all in the dead zone. Single cars would coast through the dead zone. Cars in multi-car trains would be pushed or pulled through. Battery power would keep a car's vital electrical systems running during the brief transits of the dead zone.

The above solution incorporating a dead zone with a length a little greater than that of a single car is made possible by the present plans to have the 1.5 kV propulsion circuits and ground circuits of separate cars in each train electrically isolated from each other. Signals will flow between cars, but not propulsion currents.

If the propulsion power and ground circuits of separate cars were connected together a dead section of track could still be positioned at one of the four corners shown in Fig. 7.2 to break the sneak path loop. However, in that case the dead section would have to be long enough to accommodate an entire train. Such a long dead section would probably be impractical. In such a situation, an alternative plan would be to have a "switched" section of track, with circuit breakers used to electrically connect the contact wires and running rails of the switched section to the circuits at either end, with the switching taking place when the train was completely in the switched section.

To maintain electrical isolation of the northbound and southbound tracks when trains are using the crossover to be located near University of Washington Station, a dead section of track as shown in Fig. 7.3 could be positioned in each cross track.

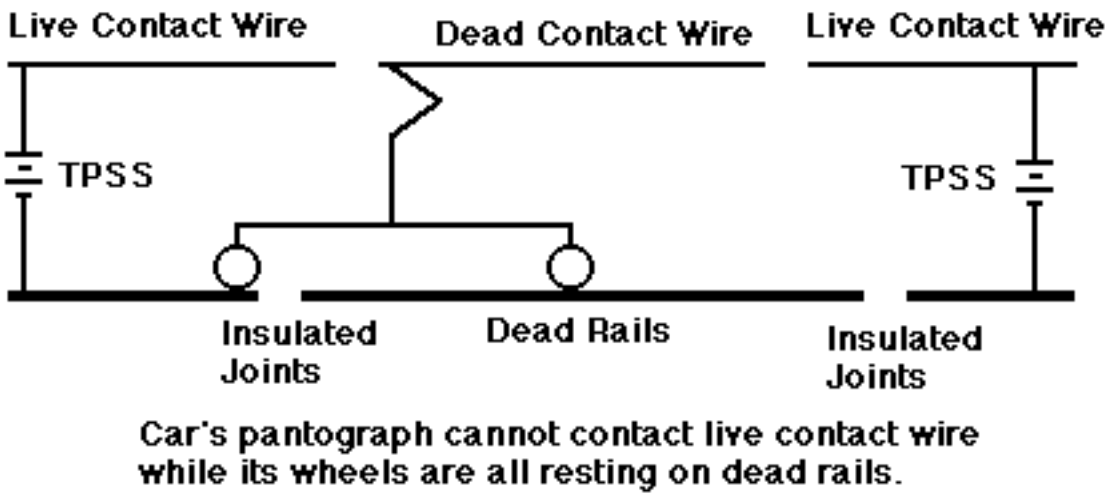

Figure 7.3 Single rail car transiting a dead zone. The "dead contact wire" is always dead. The "dead rails" cease to be dead when a pair of insulated joints at either end is bridged by a car's wheels.

Note the high-resistance paths from TPSS negatives to ground shown in Fig. 7.2. The author believes that some conducting path of non-infinite resistance will be needed from the negative node of each TPSS to ground to assure that the running rails are caused, in a deterministic way, to be very nearly at ground potential. The existence of these resistive paths to ground would result in the flow of sneak-path ground currents, driven by the voltage drops along the running rails resulting from the flow of DC return currents in those rails.

The author believes that the resistances employed can be sufficiently large to keep the sneak path ground currents sufficiently small, and still maintain rail voltages sufficiently close to ground potential. Determination of the optimum value of these resistances will be made during final design.

8 MONITORING OF B-FIELD LEVELS ON THE UW CAMPUS

Little direct history exists to serve as a guide in developing the system to monitor North Link stray B-fields during eventual operation. As discussed in Sec. 9 below, one other rail transit system, in Bielefeld, Germany, has been operating a B-field mitigation system similar in design to North Link's Hi-Lo mitigation system for a number of years. Another such system in St. Louis will enter service in 2006. Examination of B-field monitoring practices in Bielefeld, and of the development and trial of monitoring practices in St. Louis, should provide information useful in the development of North Link's B-field monitoring system.

The receipt of operational data from Bielefeld presently being sought, and from St. Louis, will allow planning of the B-field monitoring system required to economically diagnose North Link's long term B-field performance to become more specific. An analysis is presented below of likely B-field monitoring requirements and procedures, based on information available at present. To provide both economy and effectiveness, the establishment and evolution of North Link's B-field monitoring program will have to be based on developing experience at North Link and elsewhere. Additionally, the precise nature of the B-field monitoring program will have to take into account the final established B-field requirements of critical laboratories, which may differ from those presently stated.

Monitoring can be carried out using a combination of magnetometers installed at permanent sites, tied to specialized instrumentation control computers based on PCs and portable magnetometers tied to laptop computers capable of gathering B-field data at other locations on campus.

A UW committee has prepared a report giving suggested guidelines for B-field monitoring on the UW campus. The information therein has been considered.

8.1 Monitoring Situations

Three situations exist under which B-field levels on the UW campus arising from North Link operations should be monitored: during final construction prior to system startup; during pre-revenue and early revenue operation; and on a long-term basis during normal operation.

During the final phases of construction baseline ambient B-field data can be gathered at critical points on the UW campus to provide an indication of the magnitude and time variation of B-fields existing in the absolute absence of North Link traction currents.

During the final construction phase it also will be prudent to use dummy loads in place of rail transit cars and measure B-fields arising from the flow of currents in the Hi-Lo mitigation circuitry. For transit applications a dummy load is generally a resistor of large physical size that can conduct current approximating that of one to several transit cars for brief moments during testing. A bank of dynamic brake resistor grids from transit cars is one possibility. Testing could be performed at progressively higher current levels to verify performance of the Hi-Lo B-field mitigation design and to assure that B-fields will not be created that would interfere with UW laboratory operations. Similar testing was carried out in Bielefeld as described in Appendix A. In addition to measuring B-field levels, currents in the conductors could be measured to assure that they have the proper predicted relative levels.

It may also be advantageous during this period to perform at least some testing at night during times when human-caused and geomagnetic ambient fluctuations are smaller. Trains could be operated in a max current-coast-max current-coast mode to provide B-field signatures that would more clearly delineate B-fields from trains as opposed to those from other sources. Once again, data from multiple runs, timed using a portable timer provided to the operators, could be averaged to make train-caused B-fields stand out from the background.

During early operation of rail transit cars, in the test period before the start of revenue operation, and continuing into early revenue service, final checks can be made of the performance of the Hi-Lo mitigation design, and baseline performance data can be gathered for future reference during long term operations. The monitoring performed during this period should be repeated after future major system modifications or upgrades.

The third B-field monitoring situation is monitoring as part of the North Link long term preventive maintenance program. At intervals to be determined between three and twelve months B-field data could be analyzed to determine if levels are staying at or near baseline values.

Data could be correlated with train movements to determine if observed B-fields were actually caused by train activity. Provided trains all have nearly similar profiles of current vs. time and speed and distance vs. time, B-fields from multiple runs could be averaged or otherwise processed to separate out the effects of variable ambient conditions. Information on train motion would be accessible from the automatic train control system.

8.2 B-Field Monitoring Equipment and Software

The equipment required for B-field monitoring should be based on that used for the 2003 B-field testing in Portland, Baltimore and the UW campus [Ref's 2 & 3]. The key pieces of portable equipment are three-axis flux-gate magnetometers capable of portable battery powered operation, interfaced to portable computers for analyzing the data and processing and transmitting results. Magnetometers should have a resolution at least as fine as 0.01 mG (1 nT) with a dynamic range of 1 G (0.1 mT). A direct cable interface to computers should be provided. Two U.S. manufacturers of magnetometers appearing to meet these characteristics are Walker Scientific, Inc. of Worcester, MA (www.walkerscientific.com) and MEDA, Inc. of Dulles, VA (www.meda.com).

8.3 Magnetometer Arrays

Experience shows that when gathering data for B-fields generated by a specific object there is great advantage in using an array of sensors positioned at various distances from the object. For the Portland Tri-Met B-field tests magnetometers were placed at distances of 10, 25, 50, 75, and 100 meters from the track, with all magnetometers tied to a single controller. [Ref. 2] For the B-field measurements on the UW campus in November 2003 two separate magnetometers and controllers were used. [Ref. 3]

The technical advantage of simultaneously gathering B-field data from multiple sensors is that the geomagnetic field variations can be expected to be the same at all sensor sites, at least if the sensors are outdoors well away from metal objects. The logistical advantage is that data can be taken much more rapidly.

8.4 Mobile vs. Permanently Installed Monitoring Systems

For pre-operational monitoring and monitoring during car testing, monitoring could be performed using portable equipment. For long-term monitoring, both permanently installed and portable apparatus have advantages and disadvantages.

The advantage of portable equipment is that it can be taken anywhere and set up to record B-fields in a very flexible manner. However, the advantage of portability is offset by the fact that the person performing the testing has to have the necessary skills and practice to re-charge batteries, set up the equipment, and operate it in the field.

The advantage of permanently installed equipment is that it can be set up once and then run for several years. The equipment could be interfaced to the internet to allow easy access to data practically anywhere, by persons familiar with using the data

but not necessarily familiar with operating the equipment. Periodically maintenance personnel could scan the data to observe any deviations from nominal behavior.

The disadvantage of permanently installed equipment is that it only would measure B-fields in one location; the question that then looms is where.

Of the envisioned causes of degradation to the Hi-Lo B-field mitigation system, one believed by this author to be most likely is increases in riser-to-overhead contact wire contact resistances. If the contact resistances increase sufficiently for a number of adjacent risers, stray B-field levels could increase as trains passed that location and the affected risers were asked to conduct current. Such an occurrence would be a local event. The affected labs would be those nearest to the location in question. When performing B-field monitoring to assess the potential B-field exposure of a particular lab due to North Link operations the monitoring may have to be done near that lab, possibly midway between that lab and the North Link right-of-way. That means that one permanent B-field monitoring location possibly could only help protect a limited number of labs.

Perhaps the use of one or two permanent B-field monitoring arrays in the main campus and one in the medical area, together with a portable array system would be the optimum plan.

8.5 B-Field Monitoring Site Requirements

Magnetometer sites should be located away from main roads so that the observation of North Link B-fields can be made without continual interference from surface vehicular traffic. Back basement corners of buildings well away from Stevens Way might be suitable for arrays in the north end of campus, to intercept B-fields on their way to Bagley and Chem, with similar locations near CHDD to protect the Fisheries Center and other nearby buildings. The monitoring stations would have to be in controlled environments with restrictions placed on proximity to metal objects or persons. Absent suitable sites in buildings, installation locations would have to be constructed.

Monitoring sites should be located closer to the ROW than nearby sensitive labs for ease in detecting the buildup of problem B-fields. The closer to the ROW, the more North Link B-fields will predominate over other local B-field sources. However, a certain minimum distance from the ROW needs to exist for B-field levels to depend on the overall integrated effect of the Hi-Lo mitigation system as opposed to currents in the closest conductors.

9 OTHER B-FIELD MITIGATION SYSTEMS SIMILAR TO NORTH LINK

Two other propulsion B-field mitigation systems similar to North Link's Hi-Lo mitigation system presently exist. One in Bielefeld, Germany, operated by operating agency moBiel, has been in operation on a tram line running by the University of Bielefeld for several years. Another is in planning for the Cross County Extension of the St. Louis MetroLink, that will run by research labs at the main campus of Washington University.

9.1 Bielefeld

Appendix A provides detailed information from Bielefeld. Persons associated with the tram line in Bielefeld have provided answers to many of our questions concerning their B-field mitigation activities. Additional information comes from a number of their reports and published papers. As documented in Appendix A, Dipl.-Ing. Ulrich Bette of the Technische Akademie Wuppertal provided a great deal of information on the design of the Bielefeld B-field mitigation system.

Additional information directly related to Bielefeld B-field mitigation is contained in a paper by Prof's .W. Schepper and C.R. Rabl of the University of Bielefeld [Ref. 5]. This paper is presented as Appendix D.

Information specifically related to B-field mitigation at Bielefeld and more generally as well is contained in a paper by W. Braun, R. Meisel, E. Schneider & M. Zachmeier [Ref. 6]. This paper is presented as Appendix E.

The Bielefeld tram line draws peak currents per train of 3.2 kA compared to the Link 2.8 kA. However, one key difference is that the Bielefeld line is on flat ground going by the critical labs, so that peak currents do not have to be drawn while passing the labs. In Seattle with the 4 percent grade through the center of campus, peak current has to be drawn by northbound trains clear through campus.

Distances from track to critical labs are much greater at Bielefeld. They had the option of several routes to build on, and they chose a route that is 180 meters from the critical labs instead of one 70 meters away.

In Bielefeld, the transit operator moBiel must meet a 0.5 mG stray B-field spec at a distance of 180 meters. At a distance of 180 meters our Hi-Lo B-field mitigation techniques are expected to produce B-fields in the 0.05 mG range. The Bielefeld system of buried cables, risers, no cross-bonding of running rails in the mitigated area, dedicated substation for the mitigated area, insulated joints at the ends of the mitigated area, are very similar to plans for North Link.

Measurements have been made at Bielefeld to see if their "Hi-Lo" mitigation provides the expected B-field mitigation. Results show that it does. These were not fully operational tests, because some additional work was required on electrical isolation of the tracks. This work was performed in early 2005.

The biggest potential problem at Bielefeld is ground leakage currents. To minimize ground leakage currents a system of specialized rail supports is used there. Each running rail rests on a concrete pier approx. 16 inches (40 cm) wide by 16 inches deep that runs longitudinally the length of the line. Each pier contains steel reinforcing rods that are welded together end-to-end to form a continuously conducting metallic path from one end to the other.

The purpose of these continuous conducting paths is to intercept leakage currents from the rails so that they do not leak into the ground. In practice, when propulsion currents in the rails raise the voltage at one end of the rail section and lower the voltage of the other end, current that has leaked out of the running rail and into the re-bar at the high-voltage end will flow down the length of the re-bar and back into the running rail at the other end, thus constraining such leakage currents to take a well-defined path in close proximity to the running rail.

At periodic intervals the re-bar conducting paths are broken and leads are brought up to terminal points at the upper surfaces of the piers. Normally these terminal points are jumpered together. When it is desired to measure the leakage current flowing in the re-bar, the jumpers are replaced by ammeters.

Periodically the rail to re-bar resistance is measured to verify the resistance of the rubber insulating pads between the rails and supporting piers.

A series of fully operational tests of the performance of the Bielefeld B-field mitigation system was performed in May 2005. Sound Transit sent representatives to observe those tests. The report of the observations of this testing is provided in Appendix F.

The researchers at the University of Bielefeld report that the tram line does not interfere with their operations.

9.2 St. Louis

Appendix B provides detailed information from St. Louis. Technical requirements for B-field mitigation in St. Louis are more similar to Seattle's than are Bielefeld's. The St. Louis target is 0.5 mG at a 62.5 meter (205 ft) slant distance. Based on the results of this report, they should have no trouble meeting that, providing they do not have too much ground leakage current. The separate substation plus electrical isolation will help keep ground currents down.

The St. Louis system will employ a separate dedicated substation in the "Hi-Lo" mitigated area, insulated joints in running rails and breaks in catenary at the ends of the mitigated area, and buried cables and risers. Their risers will be spaced 80 ft (24 meters) apart in the most critical areas, widening out to 160 ft and then 320 ft toward the ends of mitigated area.

We do not yet know what the trackway grade is in the vicinity of the critical Washington University labs. Midway in their mitigated region, the tracks go from at-grade into a tunnel. In the at-grade portion, it appears that the rails will rest on ties on ballast. In the tunnel rails on rubber cushions on ties on a slab apparently will be used.

In the tunnel (a single wide tunnel for both tracks), the risers will go up the tunnel walls. In the at-grade region they will have central poles down the middle of the ROW and the risers will go up the poles.

St. Louis, like Bielefeld, will use a deeper buried cable than Seattle. This probably will produce greater increases in B-field level with contact wire wear than will occur in Seattle. We have not been provided with information to show that either Bielefeld or St. Louis has considered this.

The St. Louis transit line is presently in construction, with non-revenue service testing scheduled for July 2006 and initial operation scheduled for October 2006.

Representatives of Sound Transit visited St. Louis in February 2005 to collect further details on the design and implementation of their B-field mitigation system.

REFERENCES

1. S. Ramo, J.R. Whinnery & T. Van Duzer, Fields and Waves in Communication Electronics, Second Ed., Wiley, 1984, ISBN 0-471-87130-3, pp. 70-72.

2. F.R. Holmstrom, "Field Observations of Rail Transit Stray Magnetic Fields in Portland and Baltimore", September 2003, prepared for Sound Transit and LTK Engineering.

3. F.R. Holmstrom, "Stray Magnetic Fields from Transit Buses on the University of Washington Seattle Campus", December 2003, prepared for Sound Transit and LTK Engineering.

4. Private communication, Prof. Robert Van Dyck, Dept. of Physics, University of Washington, Seattle, WA.

5. W. Schepper and C.R. Rabl, "Electromagnetic Field Emissions of Electrical Railways", an English translation of the original German paper entitled, "Emissionen elektromagnetischer Felder von elektrischen Bahnen", published in the Proceedings of the .Computer Theoretikum und Praktikum fuer Physiker, XI. Computerworkshop Halle, 1996, Seiten 85-105, ISSN 0179-2792. (See Appendix D of this report.)

6. W. Braun, R. Meisel, E. Schneider & M. Zachmeier, "Electric and MagneticFields of Railway Installations", an English translation of the original German paper entitled, "Elektrische und magnetische Felder in der Bahnstromversorgung", published in Elektrische Bahnen, Vol. 96 (1998). (See Appendix E of this report.)

Appendix A

Information from
Bielefeld, Germany

APPENDIX A

INFORMATION FROM BIELEFELD, GERMANY

A.1 Email from Dr. Willi Schepper, August 2004

The information below was provided by Dr. Willi Schepper of the University of Bielefeld Physics Dept. via email in August 2004.

Dr. Schepper's address

Dr. Willi Schepper
University of Bielefeld
Department of Physics
Universitätsstraße 25
33501 Bielefeld
GERMANY
Email: schepper@physik.uni-bielefeld.de

U. Bielefeld Physics Dept. English-language web site

www.physik.uni-**bielefeld**.de/index-eng.html

Question 1. Of the three routes A, B and C described in your paper, was Route A the one that finally was built?

> **Answer** Route A with the larger distance to the laboratories has been built in Bielefeld.

Question 2. Have B-field measurements ever been made near your Bielefeld tram line to correlate predicted and actually resulting B-fields? And if so, what was the correlation?

> **Answer** B-field measurements have been made, the results agree with our calculations.

Question 3. In your paper you noted that riser cable contact resistances in the milli-ohm range could make B-field levels worse. Do you have actual data for the contact resistances in question? In Seattle, if necessary, welded cable contacts will be used to minimize contact resistances.

> **Answer** The contact problem has been investigated by an expert for corrosion Prof. Heitz. He has found, that the contact resistances show good values still after 15 years. After that it seems not necessary to use welded contacts.

Question 4. Is there anyone in addition to you that we might contact for further information about the Bielefeld B-field reduction efforts, perhaps at Siemens AG or the Bielefeld transit agency?

> **Answer** You can contact Dipl.-Ing. D. Vahrson, Gadderbaumer Str. 2, 33602 Bielefeld from the Bielefeld transit agency. He can arrange a contact to the German engineers of Siemens. I sent my translated article in Nov. 2003 also to Thomas Uwe Schmid, who has contacted me as representative of Siemens for the Seattle tram project. Here is his email adress:
>
> thomas_uwe.schmid@siemens.com

Question 5. Are there any other important questions that we have failed to ask? I am not asking about imbalances due to ground leakage currents, since near the UW the running rails will be insulated from the ground.

> **Answer** An excellent insulation of the rails is very important. Otherwise leakage currents will disturb the magnetic field reduction efficiency. I have shown the influence in Fig. 7 of my article.

Comment We will be most grateful for any information you could provide that would be useful in designing the Seattle tram line for successful operation near the UW.

> **Reply** I would be pleased to be helpful for you and transfer my experience to the new Seattle tram line. Don't hesitate to contact me. I still have all the expert's opinions instructed for the Bielefeld tram line and also my programs for designing the Bielefeld tram line and can offer you to simulate critical tram sections near the laboratories in Seattle.

A.2 Email from Thomas Schmid of Siemens AG, 4 October 2004

The following information was provided by:

Thomas Schmid
Siemens AG, TS EL SI 1
Mozartstraße 33b
D-91052 Erlangen
GERMANY
Telephone: +49-9131-7-23918
Cell Phone: +49-160-530 40 64
FAX: +49-9131-828-23918
email: thomas_uwe.schmid@siemens.com
website: http://vt3.ts.siemens.de/cfm/einheiten/i

Answers to your questions from Mr. Egid Schneider, our senior expert for DC traction power supply:

Question 1 Can Siemens, Bielefeld let us know who the designer was?

Answer The Technical Akademy Wuppertal, Mr. Bette designed the conductor arrangement with compensating conductors below the running rails. This includes the calculation of the magnetic fields with and without compensation. The reason for the effort were complaints of the University of Bielefed because of the expected magnetic fields. Siemens TS EL Engineering department verified the calculations and made the assessment how to ensure long-term stability of the proposed measures. Siemens installed the catenary systems including the compensation conductors.

Question 2 Has anyone made measurements to verify designs?

Answer Mr. Bette measured the magnetic fields during operation of the new line.

Question 3 Can you provide me with a Siemens contact in Bielefeld - preferably English speaking?

Answer Mr. Bette, Technical Academy Wuppertal

Phone: +49-404-7495-637
Email: u.bette@taw.de
He speaks english.

Question 4 We would like to know who the Bielefeld owner project manager is/was.

Answer Mr. Heidenreich, Head ot technical department Stadtwerke Bielefeld. We haven't reached him yet to instruct him and we don't know if he speaks english.

Question 5 Who is the Bielefeld owner equivalent person to Ahmad Fazel?

Answer From the picture I got, Mr. Heidenreich would be the adequate contact for Ahmad Fazel. For first contact to the Bielefeld project I recommend a Phone call or an E-Mail to Mr. Bette. I gave him the information about the open questions. Additionally I attach the tranlation of a publication about our proceeding in system design concerning electrical an magnetic fields. There is also an example about specific compensation method for magnetic fields of 3rd rail systems. The same procedure applies to the compensation procedure for overhead contact lines.

A.3 Email from Thomas Schmid of Siemens AG, dated 21 October 2004

The following information regarding technical contacts at moBiel, the transit operating agency in Bielefeld, was provided in an email from Thomas Schmid dated 21 October 2004.

Mr. Heidenreich prefers to communicate via email, because reading/writing english is much easier for him, than speaking.

Siemens AG offered him to do the translation work if that may be required.

Contact:

Mr. Heidenreich, Technischer Head
ralf-michael.heidenreich@mobiel.de
tel. +49-521-514287

Mr. Henning, responsible for technical aspects of the University Line
tel. +49 521 514314

A.4 Email from Ulrich Bette dated 14 November 2004

The following information was provided 14 November 2004 by:

Dipl.-Ing. Ulrich Bette
Technische Akademie Wuppertal e. V.
Laboratory for Cathodic Protection and Interference
Hubertusallee 18
D-42117 Wuppertal
Germany

email address: ulrich.bette@www.taw.de

Telephone No.: 49-202-7495-632

Web page:

www.taw.de/taw/taw_cms.nsf/index/CMS96C657939AC7E93EC1256C4E00597488

While paraphrasing slightly and providing dimensions in feet and inches not included in the original, the following text presents all the information contained in a long email graciously sent by Mr. Bette.

In Bielefeld the tram line passes the Institute of Physics at a distance of 150 m (492 ft).

The calculations made during the preliminary planning showed that without B-field mitigation, three trains, each with a current input 1.4 kA, for a total current of 4.2 kA, would cause stray propulsion B-fields of approx. 190 nT [1.9 mG] at the Institute of Physics, due to currents in the 5 meter high catenary and overhead contact wire and in the running rails. Working in units of kA and gauss,

$$B = (2\ I\ h) / r^2 = 2 \bullet 4.2 \bullet 5/150^2 = 0.0019 \text{ gauss} = 1.9 \text{ mG}$$

Moreover, it had to be assumed that there would be additional changes in the DC B-field if the line was extended because the operation in the adjacent line sections would lead to stray currents in the ground. The interrelations are explained below:

According to measurements the operation on the line sections into town produces rail potentials of up to 25 V due to the IR voltage drops caused by return current in the running rails.

When the tram line is extended beyond the university, this rail potential also will be present at the running rails of the line extension, so that current will escape into the earth via the running rails (stray ground current).

The magnitude of stray ground current depends on the insulation between the running rails and earth. At the time at which the calculations were made for planning purposes (in 1995) it was known that the university line was to be extended by about 600 m beyond the university. As it was not known at that time what kind of track would be used, it was assumed that the rails would be laid in a closed ballast.

At that time as per European draft standard EN 50122-2 (and IEC 62128-2), a conductance per unit length of 2.5 S per km per track was assumed for that kind of track. For a double-track, 600 m long line this conductance per unit length means a ground resistance of 0.33 ohm:

$$1 / [(2 \text{ tracks}) \bullet (2.5 \text{ S/track-km}) \bullet (0.6 \text{ km})] = 0.33 \text{ ohms}$$

Thus, the rail potential of 25 V would lead to a stray current of 75 A, which would flow through the running rails in front of the university to the running rails of the line extension and which would also result in a change in the DC B-field. At a distance of 150 m this current would make up a change in DC B-field of 100 nT [1.0 mG].

The university itself had required that the changes in the DC B-field caused by the tram operation should not exceed 50 nT [0.5 mG].

Due to this requirement many measures were taken, as noted below:

To avoid changes in the DC B-field due to stray current, the two tracks in front of the university were separated electrically from the continuing rail sections and

from one another by way of insulated rail joints. Therefore, it was necessary to set up separate traction power supplies for the two tracks of the University line section. The sectioning points were fitted so far away from the university that the passing of the sectioning points (spark chopping) would not lead to radio frequency disturbance.

If a single sectioning point is considered, the insulated rail joints of a track were staggered, and the disconnector of the overhead contact line was fitted exactly in the middle between the insulated rail joints. As a result of these measures, which merely prevent changes in the DC B-field due to stray current, the line section in front of the university was about 630 m long.

To avoid stray current, more severe requirements were made for the insulation of the two tracks against earth within the line section in front of the university. Here the conductance per unit length should not exceed 0.25 S per km per track.

If the contact line-running rails-train system is considered, the further calculations showed that a single train drawing 1.4 kA passing on a track would still lead to changes in the DC field of 62 nT [0.62 mG] and thus be higher than the limit value required by the university:

$$B = (2\ I\ h) / r^2 = 2 \bullet 1.4 \bullet 5/150^2 = 0.00062 \text{ gauss} = 0.62 \text{ mG}$$

Therefore, two copper cables each with a cross section of 240 mm^2 [473 kCmil] were laid in the middle under each track at a depth of 1 m under the rail center and connected with the contact line Ri100 at regular distances via equalizing conductors of 4x95 mm^2 Cu. [4x95 mm^2 = 380 mm^2 = 750 kCmil] The overhead contact line system itself was designed as a high catenary [messenger wire], but the messenger wires were not used for current conduction; i.e. the support cables connecting messenger wire to contact wire were insulated. Due to this measure the major part of the traction power flows via the compensating leads under the tracks and thus near the running rails so that the generated fields compensate themselves mutually for the most part.

The change in the DC B-field is lowest at big distances from the route if the product of the contact line height h_F multiplied with the cross section of the contact line A_F is the same as the product from the laying depth of the compensating leads t_K multiplied with the cross section of the compensating leads A_K. This condition for compensation is indicated in the enclosed figure.

The schematic arrangement of the overhead contact lines and the compensating leads under the running rails also appears from the enclosed figure.

Comment: A similar circuit is being planned for a tunnel section in Bonn.

Special considerations have to be made for the arrangement of the equalizing conductors, i.e. the locations at which the compensating leads and the contact

line are interconnected. The locations of the equalizing conductors have not be defined for Bonn yet, but in Bielefeld equalizing conductors were fitted at the beginning and the end of the line section and in the zones directly before the stations. The traction current flowing from the compensating cables to the contact wire via the equalizing conductors also generates a magnetic field, which is partly recompensated by the current flowing through the vehicle.

Although the tram line in Bielefeld has been operated for about two years, the final examinations have not been made yet because there is a footbridge from the station at the university to the main entrance of the university, into which an insulating joint has been fitted to separate the university potential from the station potential. In that way there are no compensating currents. However, this joint is still ineffective so that the electrical separation still has to be made at another place.

Only when these measures have been finished can the final EMI measurements be made.

However, before the line was commissioned, we made check measurements to prove the efficiency of the compensating circuit. For that purpose a current of 400 A was fed from the substation via series resistors, and the changes in the magnetic field caused for that reason were measured at distances of 5, 10, 20 and 25 m at right angles to the track. The measured changes in the DC B-field corresponded to the field pattern calculated beforehand. From these measurements it could be derived that the circuit functions properly.

After the commissioning of the line the DC B-field was measured directly at the university for a period of 30 minutes on a random basis. Simultaneously, the current flowing in the running rails was measured. The objective was to use correlation calculations to determine the correlation between the changes in the DC B-field and the current flowing in the running rails and thus to determine the changes in the DC B-field caused by train operation.

However, the changes in the B field caused by train operation were lower than the interference level that existed anyway. Therefore, these measurements could not show the correlation.

The theoretical calculations showed a value of 7.8 nT [0.078 mG] as the maximum change in the DC B-field caused by a vehicle.

As mentioned above, the insulating joint in the footbridge is to be completed this year. Therefore, it has been planned to make the relevant final measurements at the beginning of next year. However, Bielefeld University has informed us that the tram cars have not produced interference to date.

A.5 Translation by Thomas Heilig, TriMet, Portland, OR of Email from Dr. Willi Schepper, U. of Bielefeld, dated 12 January 2005

From: Heilig, Thomas [mailto:HeiligT@trimet.org]

Sent: Wed 1/12/2005 12:13 PM

To: Gustafson, John

Subject: FW: Magnetfeldbegrenzung der Strassenbahn

John:

Here's the answer from Dr. Schepper from Bielefeld, with my quick & dirty translation:

1) A visit in Bielefeld can be arranged anytime. Should you be thinking of meeting with me, let me tell you to dates when I will be at conferences in Nagoya/Japan (March 30 - April 22) and Budapest/Hungary (May 30 - June 15).

2) The field compensation arrengement described in the article was constructed for the first time in Bielefeld on line A (shown in Figure 1 in the article), and it has proven to be successful. [NOTE: The article is included as Appendix D of this report.]

The critical portion of the line (720 m) in fornt of the Institutes of Physics (Building D) and Chemistry (Buildings E and F) was divided into for compensation segments (section between two parallel feeders). The shortest segment is 100 m, the longest is 278 m. The field values at a point with a given distance from the line decrease for shorter compensation segments. There are five parallel feed connections between the underground cable and the contact wire. The parallel feed connections consist of 3 cables with a cross section of 95 mm^2. The underground parallel feeder consists of 2 cables with a cross section of 240 mm^2. The underground feeder is in HDPE conduit 1 meter below the rail.

Attached is a picture showing a traction power pole with parallel feed connections. At the bottom is the case where the connections between underground cable and parallel feed connections are made.

The article also shows that compensation becomes ineffective through rail-to-earth insulation faults (Figures 4 and 7). The rails are therefore mounted on concrete ties with insulating fasteners.

Photo: A traction power pole with parallel feed connections on the University tram line in Bielefeld near the University.

3) Comparative tests were performed by the Technical Academy of Wuppertal (Dipl. Ing. Bette) with the following result: The field values measured with a simple method (Hall sensor) at a distance of 20 m corresponded to the predicted values for a given traction current.

4) If you are interested in optimizing the critical segments (determination of position and distance between the parallel feed connections), I can perform the filed calculations for you.

-----Original Message-----
From: schepper@Physik.Uni-Bielefeld.DE [mailto:schepper@Physik.Uni-Bielefeld.DE]

Sent: Wednesday, January 12, 2005 8:28 AM

To: Heilig, Thomas

Subject: Re: Magnetfeldbegrenzung der Strassenbahn

Sehr geehrter Herr Heilig,

ich will kurz auf Ihre Fragen antworten:

1) Ein Besuch in Bielefeld kann jederzeit gerne arrangiert werden. Wenn Sie dabei an ein Treffen auch mit mir denken, nenne ich Ihnen 2 Termine, an denen ich auf Tagungen in Nagoya/Japan (30.3.05-22.4.05) bzw. Budapest/Ungarn (30.5.05- 15.6.05) bin.

2) Die im Artikel beschriebene Kompensationsschaltung wurde in Bielefeld zum ersten Mal realisiert und zwar auf der Trasse A (in Bild 1 des Artikels markiert) und sie hat sich sehr gut bewährt.

Die kritische Strecke (720m) vor den Instituten für Physik (Hochhaus D) und Chemie (Hochhäuser E/F) wurde in 4 Kompensationsabschnitte (Strecke zwischen 2 Parallelkabeln) aufgeteilt, von denen der kürzeste 100m, der längste 278m lang ist. Die Feldwerte in einem Aufpunkt mit einem vorgegebenen Abstand von der Trasse sind ja umso kleiner je kürzer der Kompensationsabschnitt vor dem Aufpunkt ist. Es gibt also an 5 Stellen auf der Strecke Verbindungen über ein Parallelkabel (3*95 mm^2) zwischen Erdkabel (2*240 mm^2) und Fahrdraht. Das Erdkabel wurde in HDPE-Rohren in 1m Tiefe unter den Schienen verlegt.

Ich habe Ihnen im Anhang ein Bild geschickt, auf dem Sie einen Mast mit dem Parallelkabel zwischen Erdkabel und Fahrdraht erkennen. Unten sehen Sie den Schaltkasten für die Verbindung des Parallelkabels an das Erdkabel.

In dem Artikel wird ja auch gezeigt, dass die Kompensation durch eine fehlerhafte Schienen-Isolierung obsolet wird (Bilder 4 und 7). Deshalb sind die Schienen auf Betonplatten unter Verwendung isolierender Dübel befestigt.

3) Vergleichsmessungen wurden durchgeführt von der Technischen Akademie Wuppertal (Dipl-Ing Bette) mit folgendem Ergebnis. Die mit einfacher Methode (Hallsonde) im Abstand von 20m gemessenen Feldwerte entsprachen der numerischen Vorhersage unter Berücksichtigung des gemessenen Fahrstroms.

4) Wenn Sie Interesse haben an der Optimierung der kritischen Streckenabschnitte (Festlegung der Position und Abstände der Masten für die Parallelverbindung), kann ich gerne Feld-Berechnungen dazu vorlegen.

Mit freundlichen Gruessen

Willi Schepper

Dr. Willi Schepper

University of Bielefeld

Department of Physics

Universitätsstraße 25

33501 Bielefeld

Email: schepper@physik.uni-bielefeld.de

A.6 Information from Ulrich Bette Provided by Email 17 January 2005 in Response to Questions Posed 21 December 2004

The following questions were emailed to Ulrich Bette on 21 December 2004, and his answers were received via email on 17 January 2005:

Question 1 CABLE CONTACT RESISTANCE VALUES AND RANGES: Since unlike most transit applications, very small values of contact resistance are required if current is to divide between different current paths made up of short lengths of conductor with large cross section, we would like to know if cable contact resistances were measured during development or installation of the B-field mitigation circuits near the University. If resistances were measured, could we get the values for various types of contacts (cable-to-cable, cable to overhead contact wire, etc.)?

Answer We had measured the transfer resistance of the feeding terminals beforehand to be able to assess whether this resistance had to be considered. The measured resistance lied between 11 micro-Ohm and 37 micro-Ohm. The average value amounted to 26 micro-Ohm. Merely in one case a value of 294 micro-Ohm was measured; this value was an outlier.

The compensating conductors fitted under a track have been connected with the contact line via three 95 mm2 Cu cables. Such a cable is about 8 m long so that the longitudinal resistance of a cable amounts to approx. 1.5 milli-Ohm. The transfer resistance of the feeding terminals only increases the total resistance by 1.7 %.

If it is also considered that the compensating conductors and the contact line have only been connected at four positions and that the shortest distance between two connections is 170 m, the longitudinal resistance of the contact line is calculated to approx. 30 milli-Ohm on this line and that of the compensating conductors to approx. 6.3 milli-Ohm. The resistance of three connecting cables switched in parallel, inclusive of the transfer resistance, is calculated to 0.51 milli-Ohm and thus of less importance as regards the current distribution. Even if it is assumed that the transfer resistance is as high-resistance as the measured “outlier”, the total resistance of the connecting cables is only increased by 30 micro-Ohm to 0.54 milli-Ohm and would not change the current distribution much. However, this statement only applies to the Bielefeld case. If the distances between the connecting cables are shorter than 170 m, the resistance of the compensating conductors and the contact lines is lower, too, so that the resistance of the connecting cables is felt more. Perhaps more than three cables would then have to be switched in parallel.

The transfer resistance from the contact line to the current collector of a train was not considered in detail; it is in series with the resistance of a vehicle and did not influence the current distribution in our case.

However, it has to be considered that a passing train can lead to high-frequency disturbances. More information is given in IEC 62236-2: „Railway applications - Electromagnetic compatibility – Part 2: Emission of the whole railway system to the outside world“. As regards tunnel structures it has to be said that the reinforcement of tunnels of reinforced concrete is interconnected in an electrically conductive way in Germany to e.g. reduce stray current. The interconnected reinforcement screens high-frequency disturbances to the outside.

Question 2 CURRENT DISTRIBUTIONS IN THE VARIOUS CONDUCTORS: For the tests that were performed at reduced current levels, are data available on the measured currents in each branch of the B-field mitigation circuit, and how the measured results compare with the theoretical predictions? If this data is available, could we get it? If currents in the branches were calculated while neglecting contact resistances, and the measured currents agreed with calculated currents, that would indicate that contact resistances are so small that they do not matter.

Answer The current in the single branches was not measured within the scope of the measurements with reduced current.

Question 3 MAGNETIC FIELDS ARISING FROM CURRENT DISTRIBUTIONS: Is data available that allows comparison of the B-fields arising from the test currents flowing in the B-field mitigation circuit, and the B-fields calculated using the Biot-Savart law? If so, could we get this data?

Answer We have measured the current flowing over the resistor and then calculated the current distribution that resulted from the planning. The magnetic changes in the DC field were calculated in accordance with the law of Biot-Savart on the basis of the calculated current and the arrangement of the single conductors. The measured values corresponded to the calculated values, see Diagrams 1 and 2 [shown below]

A.7 Web Sites and Travel Information for Bielefeld moBiel and University of Bielefeld

The University of Bielefeld English-language website is:

www.uni-bielefeld.de/international

The Physics Dept. website (mostly only in German) is:

www2.physik.uni-bielefeld.de/index.html?&L=1

The moBiel transit operator website is:

www.mobiel.de

The light rail (tram, streetcar, S-bahn) line running by the University is called the University Line.

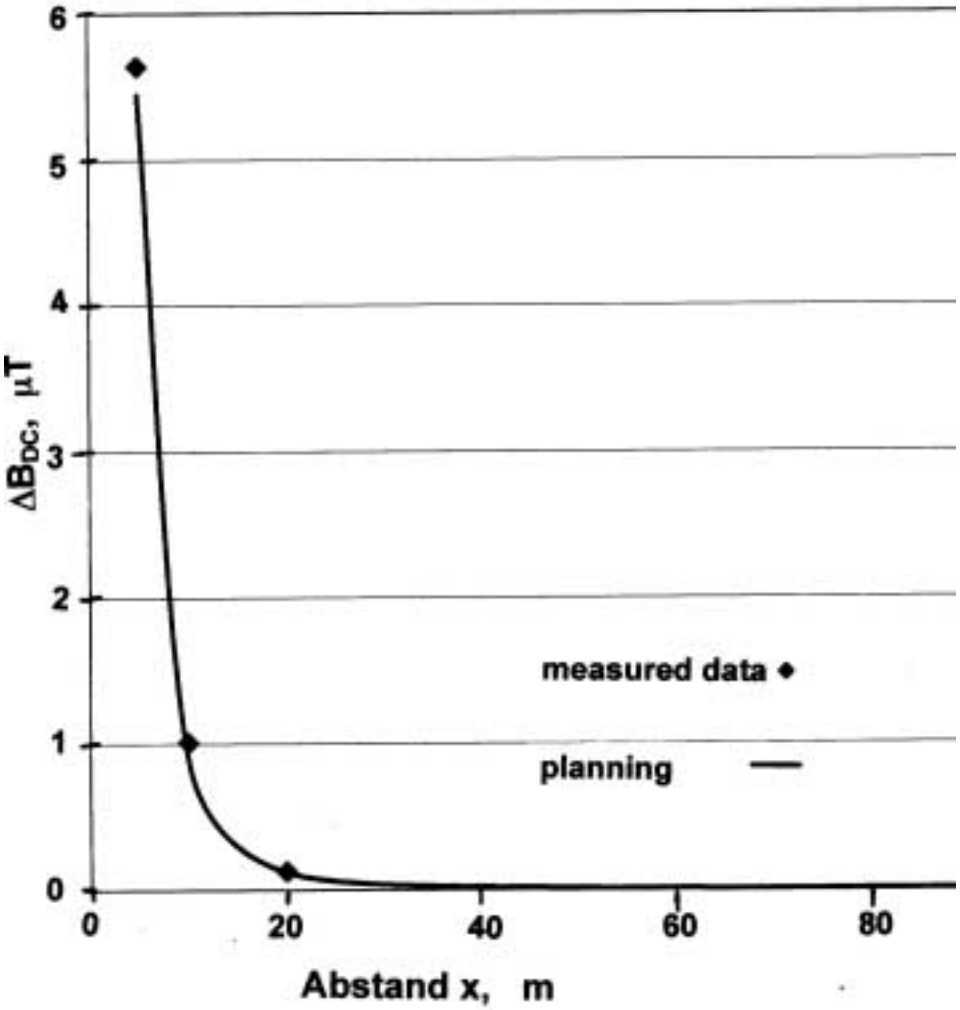

Diagram 1: Magnetic field alterations, University Bielefeld, Train at point 2 - Track 71, 03.07.2001

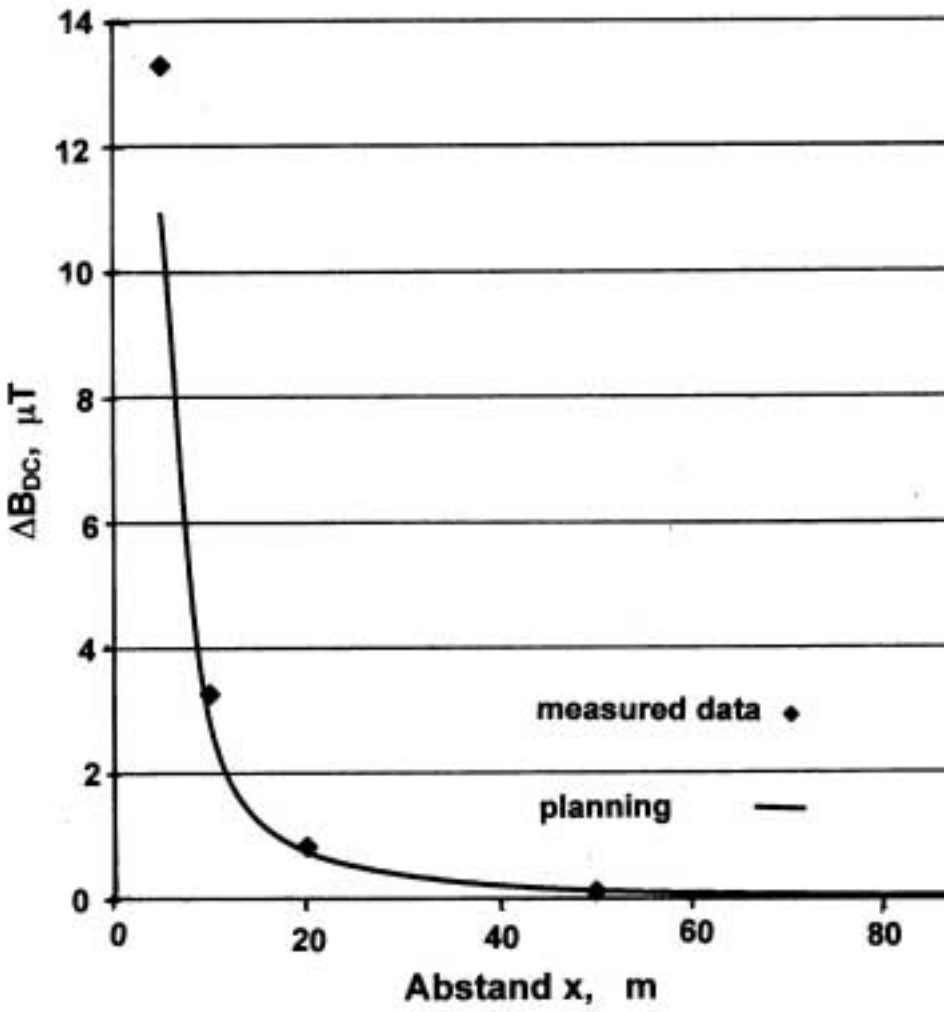

Diagram 2: Magnetic field alterations, University Bielefeld, Train 40 m behind point 3 - Track 71, 03.07.2001

The city of Bielefeld English-language website is:

www.bielefeld.de/en/index.html

This website has buttons to click for travel, etc. The website map is hard to use; but if you click enough buttons you can bring up the map shown below.

For a general map and driving directions websiite go to

www.multimap.com

and enter Germany, Bieiefeld and Universitatstrasse in the upper left corner. This website behaves approximately the same as maps.yahoo.com.

Bielefeld is in the state of Westphalia in northwestern Germany.

The regional airport nearest Bielefeld is Airport Paderborn-Lippstadt (airport code PAD), 45 km south of Bielefeld. PAD is served by connecting flights to and from Frankfurt (four flights/day each way) by a Lufthansa affiliate, and by flights to and from Munich.

To reach Bielefeld from Seattle one can fly Lufthansa Seattle-Copenhagen-Munich-PAD. From Boston one can fly Lufthansa Boston-Frankfurt-PAD.

A.8 Papers about the Bielefeld light rail line B-field mitigation efforts in English translation

Appendix D of this report, a paper entitled, "Electromagnetic Field Emissions of Electrical Railways" is an English translation of an article in the original German entitled, "Emissionen elektromagnetischer Felder von elektrischen Bahnen" by.W. Schepper and C.R. Rabl, published in the proceedings of the .Computer Theoretikum und Praktikum fuer Physiker, XI. Computerworkshop Halle, 1996, Seiten 85-105, ISSN 0179-2792.

Appendix E of this report entitled "Electric and MagneticFields of Railway Installations" is an English translation of an article in the original German entitled, " Elektrische und magnetische Felder in der Bahnstromversorgung" by W. Braun, R. Meisel, E. Schneider & M. Zachmeier, published in Elektrische Bahnen, Vol. 96 (1998).

Map: University of Bielefeld district in the northwestern part of Bielefeld. Scale 1 km x 1 km, copied from the www.bielefeld.de website. University tram line follows the No. 10 route at top of map.

Appendix B

Information from
St. Louis

APPENDIX B

INFORMATION FROM St. LOUIS

The following information was provided by the St. Louis MetroLink transit authority:

* * *

Washington University
EMF Mitigation Design Measures

Following is a description of the measures included in the MetroLink design to reduce magnetic fields associated with the MetroLink traction electrification system that could affect the stability of the ambient static magnetic field, and therefore the measurement baseline of specific scientific instruments located on the Washington University Hilltop Campus.

1. The typical MetroLink traction electrification system consists of:
   - An Overhead Contact System (OCS) over each track. The OCS consists of a messenger (or catenary) wire and a contact wire suspended from the messenger wire by hangers. The OCS carries positive supply current from the traction power substation to a Light Rail Vehicle (LRV).
   - Two steel running rails for each track. The running rails carry negative return current from the LRV back to the traction power substation.

   The contact and messenger wires are electrically connected and both supply positive current to the train. The running rails under the train complete the Direct Current (DC) electrical circuit by returning negative return current to the substation. The flow of current in the OCS and in the running rails generates a magnetic field that perturbs the earth's geomagnetic field. These magnetic field perturbations, while weak, will create a disturbance to the earth's magnetic field that may affect scientific experiments being performed on the Washington University Hilltop Campus using NMR spectrometers.

2. The traction electrification system adjacent to the Hilltop Campus includes features designed to reduce the static magnetic field from the MetroLink system at selected campus locations. The design area extends from project stationing 3408+60 (approximately 100 ft east of the east end of the Skinker station platform) to project stationing 3440+80 (adjacent to the

Washington University Millbrook parking facility). The traction electrification system in the design zone consists of:

- An Overhead Contact System (OCS) over each track. The contact wires in the design zone are located 15 ft above the top of the corresponding running rails. The messenger wires in the design zone are electrically isolated from the contact wires above each track and from the messenger wires outside of the design zone by electrical insulators at project stationing 3408+70 and 3440+70 (approximately 10 ft inside the design zone at the east and west ends of the zone).
- Two steel running rails for each track.
- A parallel electrical feeder cable in a 4" fiberglass reinforced epoxy (FRE) conduit under each track. Each feeder cable consists of 1-250 and 2-750 kcmil copper cables. The feeder cable conduits are centered between and 32 inches below the top of the corresponding MetroLink running rails.
- 26 riser cables per track. The riser cables connect the under-track parallel feeder cable to the OCS. The riser cables at each end of the design zone connect the OCS messenger wire to the parallel feeder cable. The end risers consist of 2-750 kcmil copper cables. The 24 intermediate riser cables (between the end riser cables) connect the OCS contact wire to the parallel feeder cable. The intermediate risers consist of 1-350 kcmil copper cable.
- The two parallel electrical feeder cables (one cable under each track) are cross-connected through normally-closed tie-breaker switches at each end of the design zone. The four running rails (two rails for each track) are cross-connected at each end of the design zone. The cross-connects allow the supply and return currents to be balanced across the two OCS and four running rails, respectively. The tie-breaker switches allow isolation of the parallel electrical feeders during contingency outages.

3. With the typical traction electrification system, the OCS and running rails form a magnetic dipole source. The traction electrification system in the design zone adjacent to the Hilltop Campus creates two opposite dipole sources, the first formed by the running rails and the OCS and the second formed by the running rails and the parallel feeder cable installed (buried) below the running rails. The two dipole sources combine with opposite polarity, and tend to cancel each other out, thus reducing the magnetic

field from the traction system. The height of the design zone contact wire above top of rail, the insulators in the design zone messenger wire (which reduce the electrical current that flows into the OCS within the design zone from the OCS outside of the design zone), the size and depth below top of rail of the design zone supply cable, and the size and number of feeder cables have been selected through engineering analysis summarized in the Enertech report dated May 29, 2002 and Zaffanella email of August 24, 2002 to significantly reduce magnetic fields from the traction system.

* * *

Additional information has been received from MetroLink in the form of prints and drawings that essentially document the information above.

Appendix C

Propulsion B-Field Computation

APPENDIX C

PROPULSION B-FIELD COMPUTATION

C.1 THE PHYSICAL CIRCUIT

To illustrate the steps involved in computing B-fields from propulsion currents in circuits employing Hi-Lo B-field mitigation, a simplified example has been prepared. The physical layout of the circuit is shown in Fig. C.1. The actual Hi-Lo B-field mitigation circuits for 4-car trains contained over 30 risers. Initial analysis showed that the significant riser and cable currents could be determined by solving equivalent circuits with twelve risers. The simplified circuit of this example contains only one car and two risers, but it suffices to show examples of each type of conductor in the circuit and the separate segments of risers and pantographs that carry current in different directions. For instance, each riser cable has a lower segment running parallel to the x-axis, then the longest segment running upward parallel to the y-axis, then another x-direction segment, and a final y-segment running down to the contact wire in its offset position.

The pantograph has a segment running in the x-direction from the offset contact wire position to the center of the car, and the main y-direction car segment running down through the current source to a point directly between the running rails. From this point stubs run in the +x and -x directions to divide the car current between the running rails. The running rails, buried cable and overhead contact wire run in the z-direction. Each of these has a stub connecting it to the common node at the origin of the coordinate system.

In reality the buried cable and overhead contact wire would be connected to the cable carrying positive propulsion current from the TPSS and the running rails would be similarly connected to the negative substation return. In Fig. C.1 the TPSS voltage source is shown near the origin of the coordinate system. In a circuit theoretic twist, it will be seen that since the car current source is in series with all conductors carrying positive current from the substation, substation voltage has no part in determining currents in the circuit and therefore the substation voltage source can be omitted from the electrical circuit model used to find the currents.

C.2 THE ELECTRICAL CIRCUIT

The system with the physical layout shown in Fig. C.1 has the electrical circuit shown in Fig. C.2. Each node in this circuit is numbered, with the ground or common node denoted by No. 0. Directions of positive current through the five resistive branches is indicated. These directions are determined by the

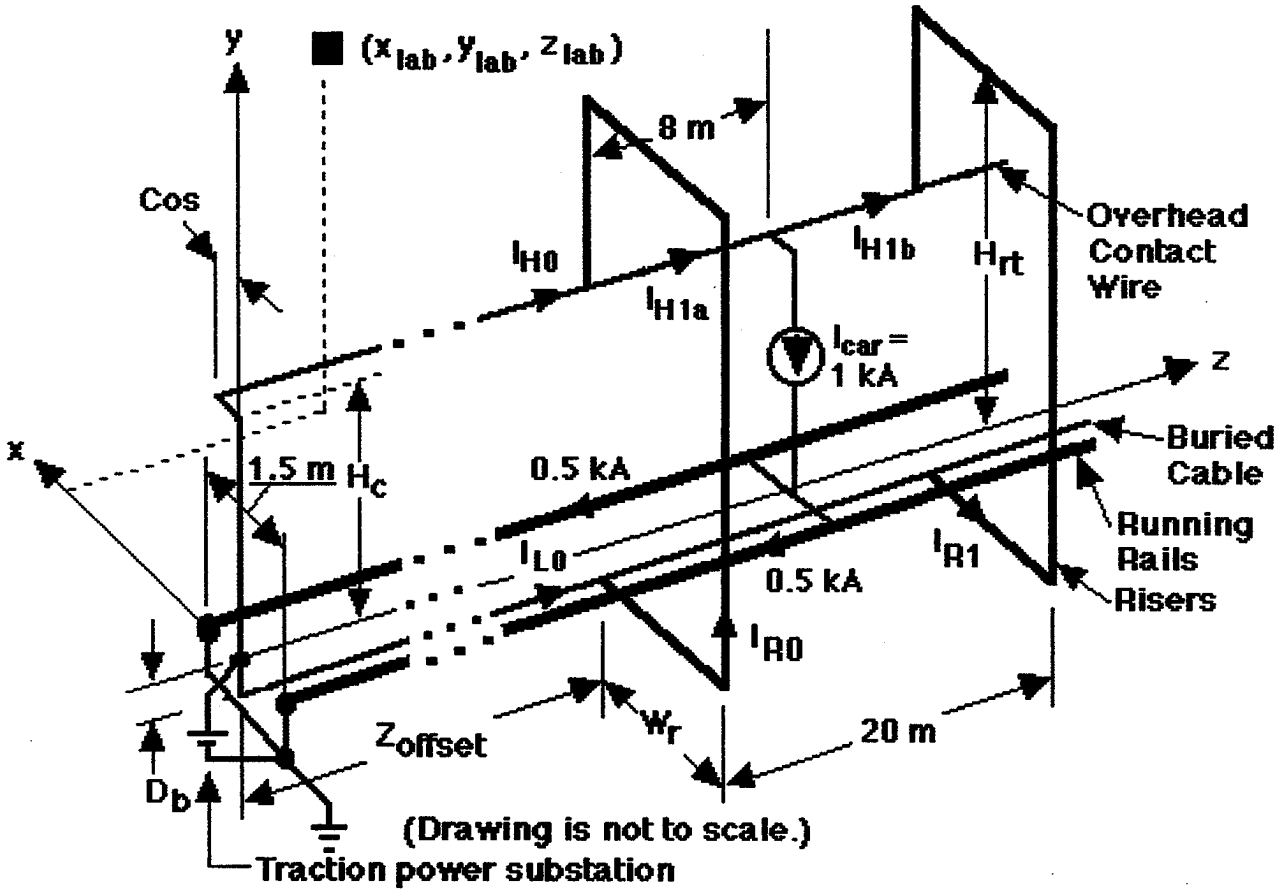

Figure C.1 Physical layout of simplified Hi-Lo propulsion B-field mitigation circuit containing two risers and a single car drawing 1 kA. Since currents in the buried cable, overhead contact wire, risers and car leads are all determined by the 1 kA car current, running rail resistances and substation DC voltage may be neglected when calculating riser, buried cable and overhead contact wire currents.

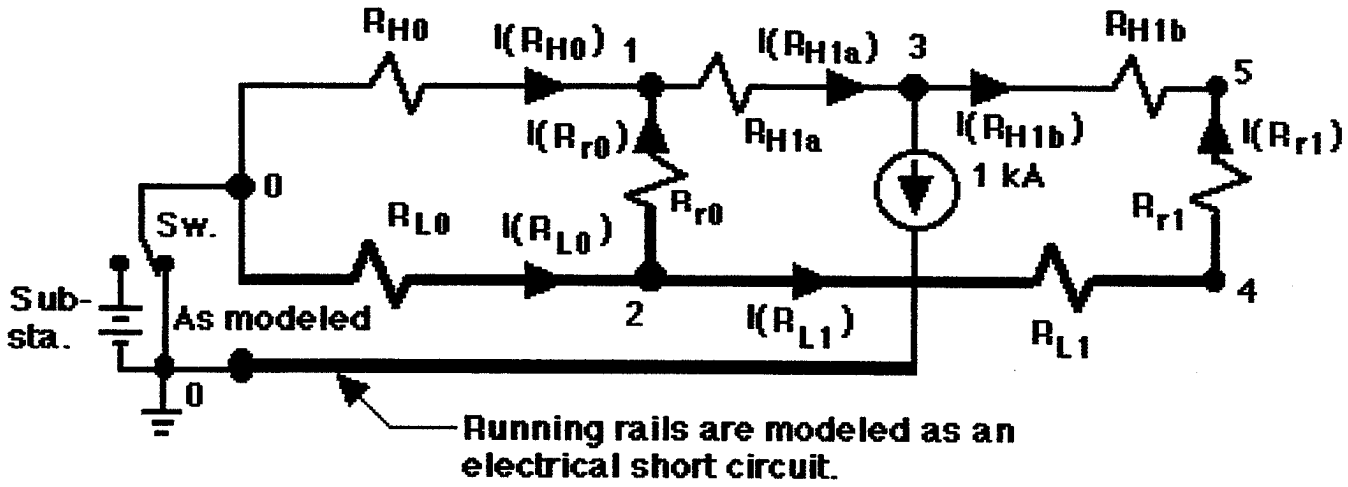

Figure C.2 Electrical circuit resulting from Hi-Lo B-field mitigation circuit containing two risers and one car drawing 1 kA. Running rails are modeled as an electrical short circuit. Division of 1 kA propulsion current between the rails is specified on the spreadsheet used for B-field computation. Nodes 0 - 5 are shown. Directions of currents through resistors are shown.

ordering of the nodes listed for each resistor in the SPICE input file that will be discussed shortly.

In the sample circuit, as in the actual circuits, car current flows down and through the running rails back to the common node. And, as in the actual circuits, running rail resistance can be neglected when solving for currents in the risers segments of buried cable and overhead contact wire. Therefore, the running rails are simply considered part of the common node when solving for the currents in risers and segments of buried cable and overhead contact wire.

In specifying the resistance values in the circuit resistances were normalized to the value of buried cable resistance between two risers, which was taken as one unit of resistance. By comparison the resistance of each riser was 0.973 units, and the overhead contact wire riser-to-riser resistance was 9.88 units. All currents are stated in units of kA.

C.3 ELECTRICAL CIRCUIT ANALYSIS

The computer program PSpice, a product of the OrCAD division of Cadence Design, was used for electrical circuit analysis. A copy of the demo-student-evaluation version of this program to run on Windows-based PCs can be obtained by going to the www.orcad.com web site, clicking on PSpice A/D, then clicking on OrCAD Demo CD. If you have broadband access to the Internet, at the www.orcad.com page you can click on Downloads and then click on OrCAD 10.0 Demo Software. You will have to fill out an on-line form and submit it to receive authorization to make the download.

The demo-student-evaluation version has all the functionality of the full commercial product but is limited to circuits of no more than 64 nodes or 10 semiconductor devices. This capacity is sufficient for any of the circuit analysis required in the Hi-Lo B-field mitigation program to date.

OrCAD PSpice is a proprietary version of SPICE (Simulation Program with Integrated Circuit Emphasis), developed by Lawrence Nagle at UC-Berkeley in the mid-1970's. Numerous manuals, texts and reference works exist for SPICE and PSpice, the author's favorite being SPICE for Circuits and Electronics Using PSpice, Second Ed., by Muhammad H. Rashid, published by Prentice-Hall, Englewood Cliffs, NJ, 1995, ISBN 0-13-124652-6, paperback.

Below, the PSpice input file describing the circuit in Fig. C.2 and specifying the computation to be performed is followed by the data output file:

PSpice Input File

```
HiLo-demo.cir  -  Demo SPICE model of catenary feed ckt with
*  high continuous catenary 4.308 meters up and buried feed cable
```

```
*  45.7 cm down.  1-car train current = 1.0 kA/car.
*  PANTOGRAPH IS 8 METERS PAST RISER.
*  0 PERCENT CONTACT WIRE WEAR! (Increase RH for wear.)
********************
*     Parameters
********************
.param wearfact = 0.0  ;  0.0 < wearfact < 1.0
.param RH = {9.88/(1-wearfact)}   ;  R(4/0 HD Cu) = 1.655e-4 ohms/m
.param RL = 1.0  ;  reference level for 2000 kCM SA Cu
*                   R(2000 kCM SA Cu) = 1.675e-5 ohms/m
.param Rr = 0.973 ;  9.73 meters of 1000 kCM riser
*                   R(1000 kCM SA Cu) = 3.35e-5 ohms/m
.param Icar = 1.0 ; ALSO SET THIS VALUE IN THE .DC SWEEP STATEMENT!
.param Zoffset = 8 ; Zoffset expressed in units of 20-m long
*                    riser-spacings.  This statement is absent from
*                    SPICE files for actual Hi-Lo circuits containing
*                    more than three 20-m long riser sections with
*                    risers between train and substation.
********************
*     The circuit
********************
RH0   0  1  {RH*Zoffset}
RL0   0  2  {RL*Zoffset}
Rr0   2  1  {Rr}
*
RH1a  1  3  {RH*0.4}
RH1b  3  5  {Rh*0.6}
RL1   2  4  {RL}
Rr1   4  5  {Rr}
*
********************
*   Source
********************
I1  3 0 dc {Icar}
.op
.dc I1  1.0  1.0    1 ;  REMEMBER TO MAKE CURRENT MATCH Icar VALUE!
.print dc i(RH0) i(RH1a) i(RH1b) i(RL0 ) i(RL1) i(Rr0)  i(Rr1)
.end
```

PSpice Data Output File (edited to remove redundancies)

```
**** 12/14/04 14:08:10 **** Evaluation PSpice (Nov 1999) ****

I1          I(RH0)      I(RH1a)     I(RH1b)     I(RL0)      I(RL1)
1.000E+00   9.779E-02   6.234E-01  -3.766E-01   9.022E-01   3.766E-01

I(Rr0)      I(Rr1)
5.256E-01   3.766E-01
```

C.4 B-FIELD COMPUTATION

The resistor currents from the circuit analysis are next entered into the spreadsheet programmed for B-field computation. The expressions for the

spatial components of B-fields occurring at laboratory locations due to currents flowing in circuit segments oriented parallel to the x-axis are those given in Eqn's 3.6 and 3.7, with similar relations found by cyclic permutation of the subscripts used to find fields from the y- and z-direction segments.

Microsoft Excel spreadsheets were used for the computations for this project primarily because at the outset they were at hand, were sufficient for the job, the author did not have to master any other software to use them, and Excel lent itself to ease of preparing graphs and tables.

The spreadsheet for computing B-fields due to currents in the circuit shown in Fig's C.1 and C.2 is shown as Table C.1. If you have a Microsoft Word electronic copy of this report you can probably click several times on the first page of the table to launch Microsoft Excel, save the spreadsheet as a .XLS file, and see how it works.

C.5 VERIFICATION OFACCURACY OF SPREADSHEET CALCULATION OF B-FIELDS

To verify that the B-field calculation spreadsheets actually gave valid answers B -fields arising from a number of standard simple conductor arrangements were calculated. One example of this is the calculation of B_X, B_Y and B_Z at various points in space resulting from a square loop conducting 1 kA with successive corners at the locations

(x = 100, y = 200, z = 300),

(x = 104, y = 200, z = 300),

(x = 104, y = 204, z = 300),

(x = 100, y = 204, z = 300)

This loop has an area of 16 m^2. At a point 100 m in the z-direction from the center of the loop the theory of B-fields arising from very small loops predicts that $B_X = B_Y = 0$ and $B_Z = 2IA/r^3 = 2 \cdot 1 \cdot 16/100^3 = 3.2 \times 10^{-5}$ G. The spreadsheet answer, calculated for an actual finite-size loop, is $B_X = B_Y = 0$ and $B_Z = 3.197... \times 10^{-5}$ G. At a point in the z-direction 200 m from the center of the loop, small-loop theory predicts $B_X = B_Y = 0$ and $B_Z = 2IA/r^3 = 2 \cdot 1 \cdot 16/200^3 = 4 \times 10^{-6}$ G. The spreadsheet yields $B_X = B_Y = 0$ and $B_Z = 3.999... \times 10^{-6}$ G.

Table C.1 Sample Excel spreadsheet used for B-field Computations for Hi-Lo mitigation circuits.

CATFDSE-094-DEMO.xls - 1car - end pantograph 8 meters past riser No. 4

This sheet is designed for easy entry of new currents. Inputs from SPICE are initial contact wire current & riser currents

In this example with car current fixed at 1.0 kA, the IH0 and IR0 vlues from SPICE determine all other currents.

Coordinates: X-west, Y-up, Z-north

Currents (input data is in bold)

IH0 =	**0.0978**	(Note:
IL0 =	0.9022	IL0=1.0000-I1H)
IR0 =	**0.5256**	
IH1a =	0.6234	
I1L =	0.3766	
I1R =	0.3766	
IH1b =	-0.3766	

Input parameters

Contact wire height, m	**Hc =**	**4.3**
Buried cable depth, m	**Db =**	**0.457**
Contact wire offset, m	**Cos =**	**-0.25**
Riser side (+1 west, -1 east)	**RS =**	**-1**
Riser loop eq width, m	**Wr =**	**2.31**
Riser X-position, m	**Xr =**	**-2.31**
Riser top elev, m	**Hrt =**	**4.8**

Lab Position		**Lab B-fields, G**	**Bx**	**By**	**Bz**	**|B|**
Xlab =	**100.0**	**Z-conductors**	-1.932E-04	6.035E-04	0	*
Ylab =	**38.4**	**X-conductors**	0	1.608E-06	-1.180E-05	*
Zlab =	**200**	**Y-conductors**	-8.811E-07	0	1.677E-05	*
Train Z-offset		**Totals**	-1.941E-04	6.051E-04	4.965E-06	6.354E-04
Zoff =	**180**	**|B| =**	**0.6354**	**mG**		
	180.00					

Z-Conductors (z1 = z1' + Zoff, z2 = z2' + Zoff)

conductor	**z1'**	**z2'**	**x1**	**y1**	**z1**	**z2**	**I**	**Bx**	**By**	**Bz**	**dsq**	**d1**	**d2**	**brackets**
TkL0	*	*	0.75	0.00	180	0	0.50	1.184E-03	-3.059E-03	0	11325.1	108.28	226.55	0.69810
TkR0	*	*	-0.75	0.00	180	0	0.50	1.153E-03	-3.024E-03	0	11625.1	109.66	227.21	0.69785
TkL1	**8**	0	0.75	0.00	188	180	0.50	1.232E-04	-3.183E-04	0	11325.1	107.09	108.28	0.07265
TkR1	**8**	0	-0.75	0.00	188	180	0.50	1.185E-04	-3.110E-04	0	11625.1	108.49	109.66	0.07177
H0	*	*	-0.25	4.3	0	180	0.0978	-2.077E-04	6.105E-04	0	11212.9	226.30	107.76	-0.69818
L0	*	*	0	-0.457	0	180	0.9022	-2.126E-03	5.471E-03	0	11509.9	226.96	109.13	-0.69796
H1a	0	8	-0.25	4.3	180	188	0.3766	-8.359E-05	2.458E-04	0	11212.9	107.76	106.57	-0.07299
H1b	8	20	0	-0.457	188	200	0.3766	-1.413E-04	3.637E-04	0	11509.9	107.95	107.28	-0.11116
L1	0	20	-0.25	4.3	180	200	0.3766	-2.126E-04	6.249E-04	0	11212.9	107.76	105.89	-0.18559
Z-Conductor Total fields								**-1.932E-04**	**6.035E-04**	**0**				
								Bxtotz	**Bytotz**	**Bztotz**				

Table C.1, cont'd

X-Conductors (z1 = z'1 + Zoff)														
conductor	z1'	*	x1	x2	y1	z1	I	Bx	By	Bz	dsq	d1	d2	brackets
LrailRet	*	*	0.75	0	0	0	0.5	0	6.436E-06	-1.236E-06	41474.6	226.55	226.88	0.00267
RrailRet	*	*	-0.75	0	0	0	0.5	0	-6.408E-06	1.230E-06	41474.6	227.21	226.88	-0.00266
ContWfeed	*	*	0	-0.25	4.3	0	0.0978	0	4.222E-07	-7.199E-08	41162.8	226.19	226.30	0.00089
Car1Lrail	8	*	0	0.75	0	188	0.5	0	-3.628E-06	1.161E-05	1618.6	107.79	107.09	-0.00098
Car1Rrail	8	*	0	-0.75	0	188	0.5	0	3.559E-06	-1.139E-05	1618.6	107.79	108.49	0.00096
Riser0Lo	0	*	0	-2.31	-0.457	180	0.5256	0	1.815E-05	-3.527E-05	1909.9	109.13	111.25	0.00330
Riser0Hi	0	*	-2.31	-0.25	4.8	180	0.5256	0	-1.693E-05	2.843E-05	1529.0	109.53	107.61	-0.00246
Riser1Lo	20	*	0	-2.31	-0.457	200	0.3766	0	0.000E+00	-2.657E-05	1509.9	107.28	109.44	0.00274
Riser1Hi	20	*	-2.31	-0.25	4.8	200	0.3766	0	0.000E+00	2.146E-05	1129.0	107.69	105.73	-0.00191
X-Conductor Total Fields								0	1.608E-06	-1.180E-05				
								Bxtotx	Bytotx	Bztotx				
Y-Conductors (z1 = z'1 + Zoff)														
conductor	z1'	*	x1	y1	y2	z1	I	Bx	By	Bz	dsq	d1	d2	brackets
ContWfeed	0	*	0	0	4.3	0	0.0978	7.235E-06	0	-3.618E-06	50000.0	226.88	226.19	-0.01850
BurCabFeed	0	*	0	0	-0.457	0	0.3766	-2.946E-06	0	1.473E-06	50000.0	226.88	226.96	0.00196
Car1	8	*	0	4.3	0	188	1	-4.207E-05	0	3.506E-04	10144.0	106.33	107.79	0.03556
Riser0up	0	*	-2.31	-0.457	4.8	180	0.5256	4.111E-05	0	-2.103E-04	10867.3	111.25	109.53	-0.04250
Riser0dn	0	*	-0.25	4.8	4.3	180	0.5256	-4.209E-06	0	2.110E-05	10450.1	107.61	107.76	0.00418
Riser1up	20	*	-2.31	-0.457	4.8	200	0.3766	0.000E+00	0	-1.584E-04	10467.3	109.44	107.69	-0.04303
Risr1dn	20	*	-0.25	4.8	4.3	200	0.3766	0.000E+00	0	1.593E-05	10050.1	105.73	105.89	0.00424
Y-Conductor Total Fields								-8.811E-07	0	1.677E-05				
								Bxtoty	Bytoty	Bztoty				

One direct demonstration of the efficacy of the spreadsheet-based computational method was the computation of the B-field at a Point 3 in Fig. 6.1 located at an axial distance of 400 meters from the end of a semi-infinite loop (modeled as 5000 m long) 4.3 meters high. The author calculated the B-field at the point just taking into account the contribution from the short vertical conducting segment, and obtained an answer exactly twice as large as the spreadsheet provided. After an hour of more careful pencil and paper analysis and checking, involving use of approximate relations for the cosine of angles very close to 180^{o}, an answer was found that took into account B-fields from the short vertical segment as well as the semi-infinite straight conductors pointed almost but not quite directly away from the observation point.

In conclusion, the spreadsheet technique for calculating B-fields gives answers as reliable as the data fed in.

C.6 APPROXIMATE PROPULSION B-FIELD ANALYSIS AT BAGLEY AND JOHNSON HALLS AND THE CHEMISTRY BLDG. TO ACCOUNT FOR CURVED TRACK

As can be seem from Fig. 2.1, Bagley and Johnson Halls and the Chemistry Building are near the center of the northwestward going curve of the right-of-way. To calculate propulsion B-fields a spreadsheet was programmed with relations derived from Eqn's 3.4 and 3.5 allowing calculation of B-fields from straight conducting segments arbitrarily positioned in 3-dimensional space.

A model circuit was constructed consisting of two conductors vertically spaced by 15 cm, the effective height of the dipole current loop occurring from 30 percent overhead contact wire wear. The circuit followed 8 straight-line segments from the south end of the Montlake station to the south end of the Brookline Ave. station. The top conductor carried 2.8 kA northward, with the current returning in the bottom conductor.

The loop height was chosen as 15 cm since a straight infinitely long loop of this height conducting 2.8 kA produced estimated B-fields at Bagley Hall equal to those calculated by the more generally used methods described above.

It was found the effect of the curvature of the circuit was to increase the B-fields calculated at Bagley and Johnson Halls and the Chemistry Bldg. by approximately 30 percent.

Similar calculations of the curvature effect were performed for EE-CS and Fluke Hall. At EE-CS calculated B-field magnitude due to the straight 2-conductor 2.8 kA loop located at northbound rail location was 0.059 mG, while B-field due to curved loop was 0.066 mg; yielding a difference due to curvature of 3.8 percent of the 0.184 mG total B-field level given for EE-CS in Table 3.2.

For Fluke hall, located on the outside of the curve, the corresponding numbers were 0.076 mG due to the straight loop, 0.061 mG due to the curved loop, a reduction of 0.015 mG due to loop curvature, a reduction of 6.7 percent of the 0.223 mG total B-field level given for Fluke Hall in Table 3.2.

Other critical labs are either well removed from regions of curvature of the tracks; are closer to the tracks, causing proximity to count more and curvature less in determining B-fields; or at such great distance from the tracks that B-field levels are well below UW spec levels.

Because of the special sensitivity of Bagley Hall and the Chemistry Bldg. the effects of track curvature were included in their reported B-field values, and for Johnson Hall since it lies so close to the other two. The effects of track curvature were not included in the reported B-field values for EE-CS, Fluke Hall or other labs.

Appendix D

Electromagnetic Field Emissions
of
Electrical Railways

Electromagnetic Field Emissions of Electrical Railways* [1]

W. Schepper and C.R. Rabl
University of Bielefeld, Faculties of Physics and Chemistry

Synopsis

Electrical railways generate electromagnetic fields that can interfere significantly with physical experiments. *1. Steady fields:* The limit value determined for magnetic induction 50 nT = $10^{-3} B_E$ in Bielefeld was based on the normal daily variation of the earth's magnetic field (B_E = 53 µT). According to the Biot-Savart law, the magnetic field of the contact wire (height = 5 m) of the tramway is $B_Ð^1 = \mu_0 I/(2Ùr_0)$ = 9.1 µT for I = 3200 A and r_0 = 70 m. When the return current -I through the rails is taken into account, the field decreases to that of the conductor loop ($B_Ð$ = h $BÐ^1 /r_0$ = 652 nT). This field can be reduced by an earth cable with a five-fold cross-section laid 1 m below the rails and connected to the contact wire by cable links. The field contributions of the two conductor loops above ground (contact wire-rail) and below ground (rail-earth cable) then compensate each other approximately. - *2. High-frequency fields:* In wet and frosty weather, sparking on the contact wire generates pulses with an interference range of as much as 100 MHz. In the traditional measuring method, frequency response measurements obtained with a selective test receiver on a tramway section are compared with lab values. However, this comparison is in urgent need of interpretation, as FFT calculations show. The reason is the difference in the provenance of the signals recorded by the measuring receiver: much interference of a small magnitude in the laboratory, but few high-magnitude pulses on the tramway.

1 Historical background

The opposition of physicists to tramway routes goes back quite a way. There is a hand-written letter by Hermann von Helmholtz, President of the Physikalisch Technische Reichsanstalt in Berlin dated 16. 6. 1893. It deals with the routing of the tramway in front of the Institute of Physics in Breslau. With the tramway line at a distance of 50 m, he predicts *substantial adverse effects on physical research.* He refers to an earlier expert report, in which he had already mentioned *noticeable interference* (Halle, distance 400m). After his move from Würzburg to the southern wing of the new university building in Munich's Ludwigstrasse, Röntgen complained about *magnetic interference due to the tramways, which makes certain forms of physical research impossible.* In 1897, Prof. Petersen in Frankfurt opposes the Hauptwache-Jahnstrasse line unless it is converted to *accumulator operation, as the planned operating mode will severely harm the two institutes of physics in the vicinity.*

2 Problems elsewhere

During the discussion in Bielefeld, we became aware of problems in other localities as well. In Heidelberg, in the Neuenheimer Feld, a tramway was to be laid at 20 m from the Institute of Physics and Chemistry and the Institute of Mineralogy and Petrography; the route was rejected by the institutes in question and by the university management. In Halle, severe interference is being experienced on the scanning transmission electron microscopes, probably because the tramway power supply cable runs too close to the Institute of Physics. Interference on the

*Computer Theoretikum und Praktikum für Physiker, XI. Computerworkshop Halle, 1996, Pages 85-105, ISSN 0179-2792.

[1] Bahn generally refers to railways (Eisenbahn); in this text, tramways (Strassenbahn) are implied – tr. note.

electron microscopes is also being reported by the local MPI[2] for Microstructure Physics. In Vienna, interference on the electron microscopes is also complained about. An attempt to shield the low-frequency supply (16 2/3 Hz) at high cost by means of copper screens failed.

3 Tramway lines in front of the Bielefeld University

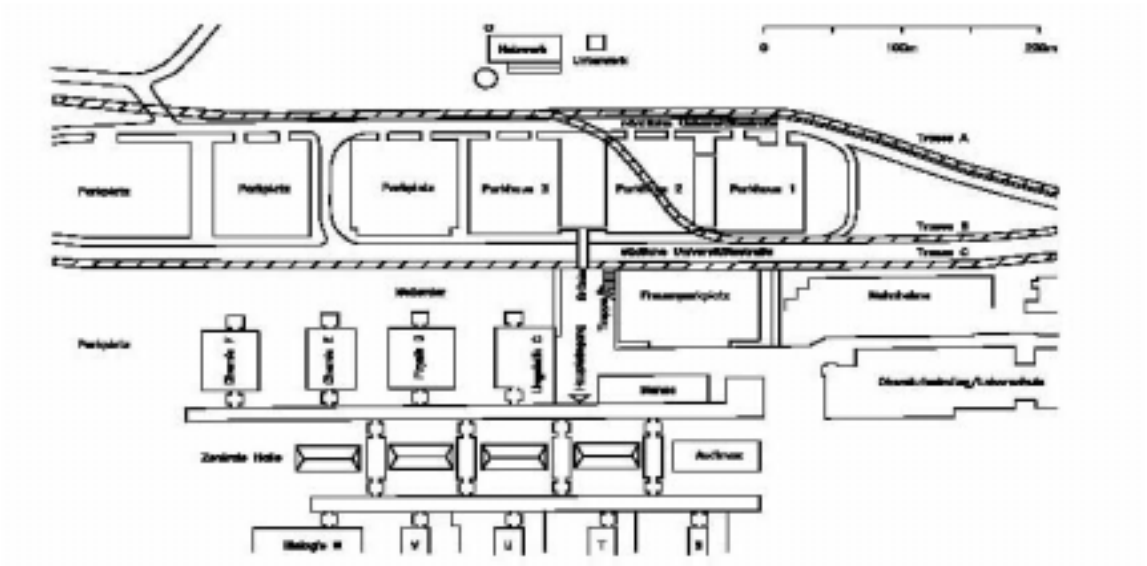

Heizwerk: Heating plant; Unterwerk: Substation
Nördliche / südliche Universitätsstrasse: Northern / Southern university road; Trasse: Tramway line; Parkplatz: Parking area; Parkhaus: Parking garage
Brücke: Bridge; Treppe: Stairs; Frauenparkplatz: Ladies' parking area; Wohnheime: Residences
Chemie: Chemistry; Physik: Physics; Linguistik: Linguistics; Haupteingang: Main entrance; Oberstufenkolleg/Laborschule: Upper-grade lecture rooms/Lab school
Zentrale Halle: Central hall; Auditorium; Biologie = Biology

Fig. 1: Tramlines at the university: line A (180 m), line C (55 m), line B through parking garage 2

Fig. 1 shows that there are three tramway sections at issue in Bielefeld. The university, in conjunction with the faculties of chemistry and physics, decided in favour of line A on the far university road; the students initially preferred line C (55m) and subsequently a line that enters on the near University Road (line B, 70m) and then turns away at parking garage 2 to join the line on the far university road.

4 Limit values

As Fig. 13 shows, the field values of magnetic induction that occur in everyday life vary over a range of several powers of ten. At the upper end, there is the NMR spectrometer, widely used for chemical analysis (14T) as well as the nuclear spin tomograph used for medical diagnoses (1.5 T). In all motors, generators and transformers, the typical fields lie around 0.8 T (residual field of dynamo sheet). The absolute limit for people with pacemakers is three powers of ten lower, at 0.5 mT. For such people, the voltages that are induced in the supply wires to the heart when moving through the fields are dangerous. One power of ten lower down, we find the absolute value of the terrestrial magnetic field (B_E = 53 µT). Three powers lower lie the normal daily variations of the

[2] Max Planck Institute – tr. note.

earth's magnetic field (< 30 nT), on which the limit value 50 nT is based. But at the indicated end of the scale (1 nT), the detection limit of magnetic fields has not yet been reached, however; with SQUID (Superconducting Quantum Interference Device) equipment, components are now available with which field values down to 1 fT = 10^{-6} nT can be measured. This makes it possible to use the fields of cardiac currents (MCG, 10 pT), brain currents (MEG, 1 pT) and muscle currents (100 fT) for diagnostic purposes [1]. Fig. 13 also shows the typical measuring probes for the measuring ranges [2].

NMR spectrometers have automatic field regulation that makes adequate correction for the variations in the earth's magnetic field (deuterium lock), but cannot completely compensate for the significantly more rapid variations produced by a passing tram. In many experimental physics laboratories, the earth's magnetic field is compensated by Helmholtz coils. This is necessary, for example, in order to transport charged particles over greater drift distances (2 m) for energy analysis. To this end, the current in the power supply coils is adjusted in such a way that the field generated will counteract the terrestrial magnetic field. Unfortunately, this compensation is effective only in a small volume, and with the control electronics to only $10^{-3}B_E$. Compensation of external fields by means of an active regulating circuit presents problems, as low-noise triaxial measurement of the small field values is difficult. Moreover, the fields of neighbouring coil arrays may influence each other and grow into periodic control oscillations.

5 Magnetic fields

Magnetic field calculations in conductor arrangements are based on the Biot-Savart law in equation 1:

$$H = \int_{Leiter} \frac{I\ sin\alpha\ ds}{4\pi r^2};\ B = \mu_0 H \qquad \text{(Leiter = conductor)} \qquad (1)$$

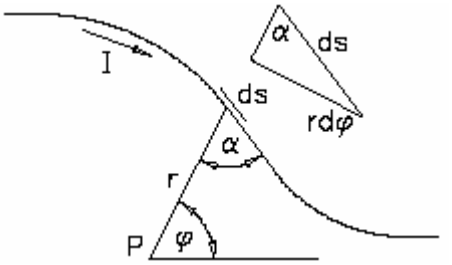

where Ā = angle between the direction of the line element ds and the radius vector $\vec{r}$ at the test point P where the field strength H is to be calculated. The vector H is perpendicular on the vectors $d\vec{s}$ and $\vec{r}$; H can be decomposed into its constituents by projection. r and , are the co-ordinates in the fixed-point polar co-ordinate system on the test point P. With a simple trigonometric relation between the variables (Ā; , , r; dr; ds), equation 1 is simplified as follows:

The integration must extend over the full length of the conductor. In the special case of a straight conductor of infinite length

$$sin\alpha = \frac{rd\varphi}{ds};\rightarrow B = \frac{\mu_0 I}{4\pi}\int_{\varphi_u}^{\varphi_o}\frac{d\varphi}{r(\varphi)}$$

$$sin\varphi = \frac{r_0}{r};\rightarrow B = \frac{\mu_0 I}{4\pi r_0}\int_{\pi}^{O} sin\varphi d\,\varphi = -\frac{\mu_0 I}{4\pi r_0}cos\varphi\Big|_{\pi}^{O} = -\frac{\mu_0 I}{2\pi r_O} = B_{\infty}^{(1)}$$

the familiar textbook formula for $B_Ð^{(1)}$ is obtained. The field contribution $B_Ð^{(1)}$ of the contact wire alone at a distance r_0 = 70 m is 9.1 µT. The field decreases linearly with the distance r_0. Taking into account the return current –I through the rails, the field contributions of the two conductors must be added vectorially. $\vec{B}$ is perpendicular on the plane defined by the test point P and the conductor. The components B_x and B_y result from the projection of the B vector:

$$B(x_A, y_A) = -\frac{\mu_0 I}{2\pi r_0}\vec{p};\ \vec{p} = \frac{1}{r_0}\begin{bmatrix} y_F - y_A \\ x_A \pm x_O \\ 0 \end{bmatrix};\ \begin{array}{|l|c|c|}\hline & y_F & x_O \\ \hline Fahrdraht & h & 0 \\ Schienen & 0 & x_s \\ \hline \end{array} \qquad (2)$$

contact wire
rails

$$r_0 = \sqrt{(x_A \pm x_s)^2 + (y_A - h)^2} \qquad (2)$$

In equation 2, different values for the conductor height, rail offset x_0 and direction of the current must be considered. The first expert report compiled on the route [4] was restricted to the evaluation of equation 2 for the 3-conductor configuration (contact wire, 2 rails). The field contributions of the contact wire and rail compensate each other approximately. At large distances from the rails r_0, the field is at its maximum for a test point height $y_A = \frac{h}{2}$. For the largest remaining field component B_x, the evaluation of equation 2 for large distances produces approximately

$$y_A, h << r_0 \rightarrow B_\infty \approx \frac{\mu_0 I}{2\pi}\frac{h}{r_0^2}$$

$B_Ð$ is the field of a conductor loop of infinite length at a height h and at a distance of r_0 from the test point. A local dependency ~ r_0^{-2} exists for the twin-conductor configuration. Compared with the contact wire alone, the field already shrinks to the proportion $\frac{h}{r_0} = \frac{5}{70} = \frac{1}{14}$ at 652 nT. The field decreases linearly with the height of the contact wire. $B_Ð$ can be calculated exactly with equation 2.

However, it is also possible to perform the integration for a conductor of infinite length analytically:

$$\vec{B} = \frac{\mu_0 I}{4\pi r_0}(cos\varphi_u - cos\varphi_o)\ \vec{p};\ cos\varphi_u = \frac{z_u}{r} = \frac{z_u}{\sqrt{z_u^2 + r_0^2}} \qquad (3)$$

In the calculation of the cos function, the z- (z_u; z_o) and x-distance from the test point (r_0) as well as the projection vector $\vec{p}$ for the constituent decomposition B_x and B_y from equation 2 is used. Equation 3 was also used for the integration over conductors in the x- and y-directions; then the co-ordinates must be transposed cyclically. In the conductors (cable links, tramway line) a component B_z also occurs. The fields of all straight tramway sections were calculated in this way.

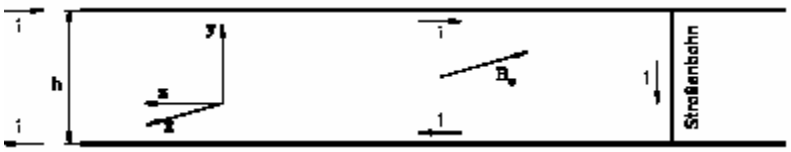

Contact wire

Tramway

Rails

Fig. 2: Conductor loop of a conventional tramway showing power feed at left, increase of the conductor loop as the tram travels from left to right, and the xyz co-ordinate system on which the calculations are based

Fig. 3 and 4 both show the plot of $|B|(z)$ for the straight tramway sections A and C for two different distances as calculated with equation 3; the power feed is located at far left in the figure, as in Fig

2. For the selected current (I =3200 A), the meeting of 2 trams with twin traction at point z was considered. As the tram travels from left to right, Fig 2 shows that the conductor loop and therefore the strength of the field keeps increasing; with extensive conductor lengths, the field reaches the limit value B_D of a conductor loop of infinite length. The current through the tram produces a rise in the plot of the field which is very distinct in the nearby section C. In the field plot in Fig. 4, a stray current of 2% has been incorporated. Such scatter currents readily occur when the rail bed is inadequately insulated; this allows part of the current to leak into the ground, where it continues to flow. The disturbed compensation between the contact wire and the rails causes an increase in the field, which also increases with the increase of the conductor loop. According to [4], stray currents of up to 5% certainly occur.

If the conductors do not form a straight line, all three field components of the vector $\vec{B}$ occur.

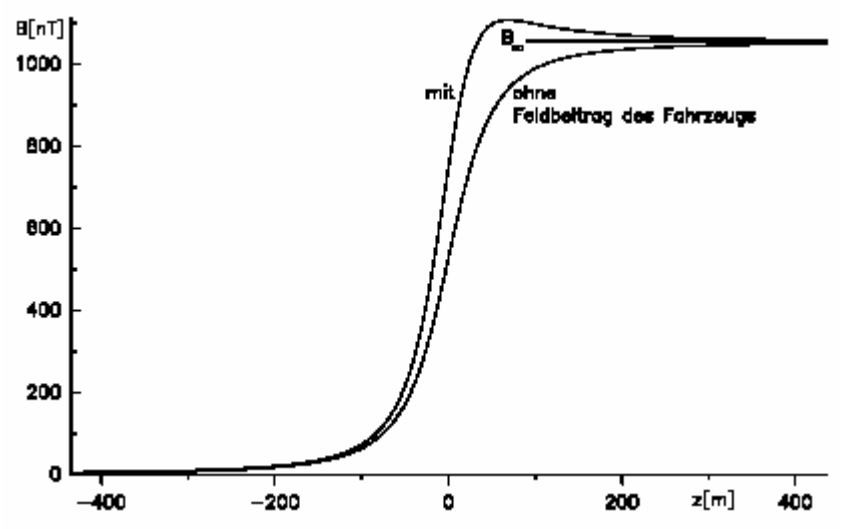

with / without field contribution of tram

Fig. 3: Field strength $|B|(z)$ for tram passing on section C (distance 55 m), with and without field contribution by the tram, with B_D as reference

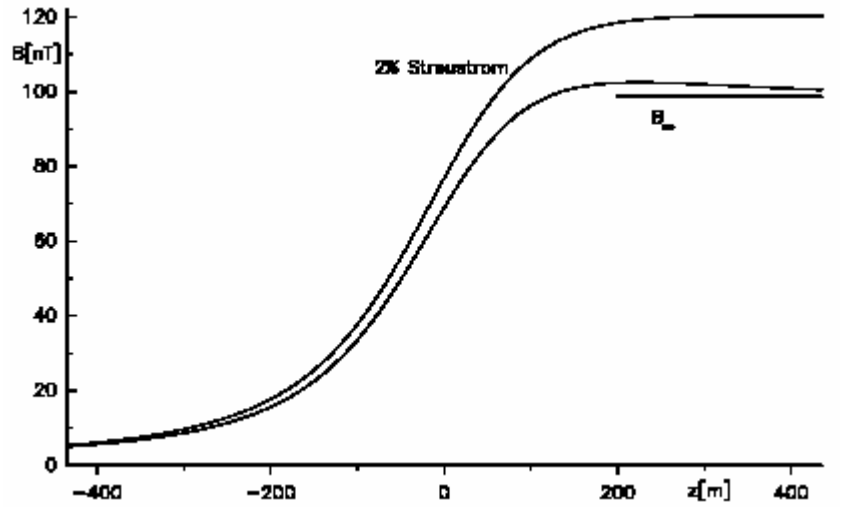

With 2% stray current

Fig. 4: Field strength $|B|(z)$ for tram passing on section A (distance 180 m), with field contribution by the tram, second curve with 2% stray current, with B_D as reference

They are obtained automatically by the following integration:

$$\vec{B} = \frac{\mu_0 I}{4\pi} \int_{Leiter} \frac{\vec{r} \times \vec{ds}}{r^3};\ \vec{r} \times d\vec{s} = \vec{r} \times \vec{s}\, dz = \begin{bmatrix} r_y s_z - r_z s_y \\ r_z s_x - r_x s_z \\ r_x s_y - r_y s_x \end{bmatrix} dz \qquad (4)$$

Conductor (4)

$$\vec{r} = \begin{bmatrix} x(z) \\ r_y \\ z \end{bmatrix};\ r_y = \begin{bmatrix} h - y_A \\ -y_A \\ t - y_A \end{bmatrix} \begin{matrix} Fahrdraht \\ Schienen \\ Erdkabel \end{matrix};\ Bahnkurve:\ \vec{ds} = \vec{s}\, dz = \begin{bmatrix} m \\ 0 \\ 1 \end{bmatrix} dz$$

Contact wire
Rails; track: curve
Earth cable

Equation 4 follows directly from equation 1 for a conductor with a finite z component. The vector representation has the major advantage that for $d\vec{s}$ and $\vec{r}$ only the components that are easy to indicate need to be inserted. The cross product ensures that once again $\vec{B}$ is perpendicular on the two vectors $d\vec{s}$ and $\vec{r}$. The vector product was decomposed into the 3 components. $\vec{r}$ is the radius vector from the test point (height y_A) to the section of the conductor for which the field contribution is being calculated. The x component r_x to be calculated from the rail curve x(z) is constant for segments of the tramway section (70 m and 180 m respectively). The y components r_y must be substituted for the individual conductors in accordance with equation 4; the z component r_z = z corresponds to the conductor position.

For straight segments of the tramway section, only the z component (m = 0) exists for $d\vec{s}$ in equation 4; but for the straight intermediate section there are 2 components as well as a curve x(z) with the gradient m =dx/dz. The conductors of the cable links possess either only y components or only x-components.

$$y - Leiter:\ \vec{ds} = \vec{s}\, dy = \begin{bmatrix} 0 \\ 1 \\ 0 \end{bmatrix} dy;\ x - Leiter:\ \vec{ds} = \vec{s}\, dx = \begin{bmatrix} 1 \\ 0 \\ 0 \end{bmatrix} dx$$

Conductor

The integration of equation 4 is done along the conductor sections via z for the contact wire, earth cable and rail, via y for the y components of the cable links and the current through the vehicle, via x for the contact wire and earth cable supply of the cable links. For the integration, the 5-point Gauss formula with increment control was used. The integration programme according to equation 4 was checked by comparison of the field calculation on a straight section according to equation 3; |*B*| displayed the required invariance in a rotation of the xz co-ordinate axes.

5.1 Parameterisation of the section over 2 segments of a circle and a straight section, power supply to the tramway segments

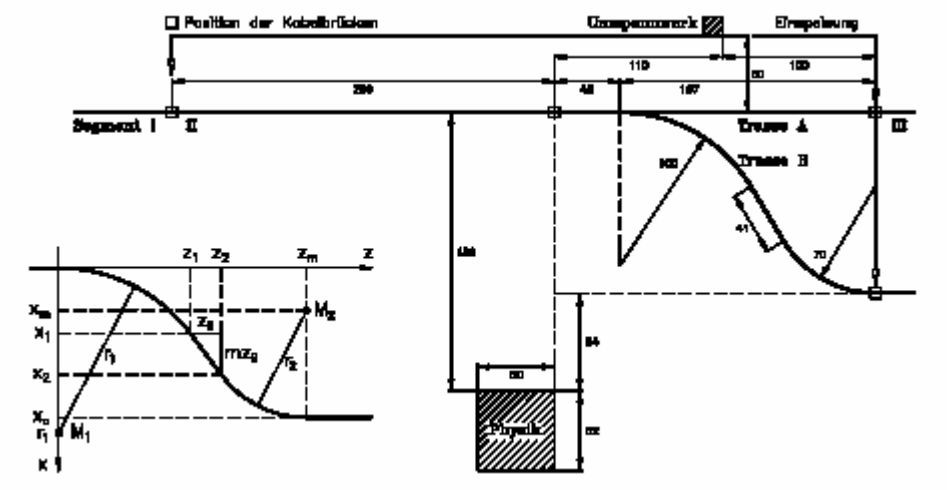

Fig. 5: Right: Plan sketch of the power supply to the A and B sections; left: parameterisation of the B section

The tramway section will comprise 3 segments, of which the two end segments (I, III) will be wired conventionally (without earth cable) and the middle segment will have a compensation circuit. From the distribution station, the power is supplied electrically separated to the middle (II) and right-hand (III) segments by a 4-core cable; the left-hand segment (I) will have another cable. There are insulated rail joints between the segments. Consequently segments I and II are supplied with power from the right and segment III from the left. The track curve x(z) consists of two circle equations (r =100 and 70m), the straight intermediate section and the straight sections of the adjacent track segments.

The tramway section is described by the following equations:

x(z) and gradient at an intermediate point *z*1 **for the first circle:**

$$(z - z_{m1})^2 + (x - r_1)^2 = r_1^2;\ x = r_1 - \sqrt{r_1^2 - (z - z_{m1})^2};\ z_{m1} = 0 \tag{5}$$

$$2(z - z_{m1}) + 2(x - r_1)x' = 0;\ x' = m(z) = -\frac{z - z_{m1}}{x - r_1} = \frac{z}{\sqrt{r_1^2 - z^2}} \tag{6}$$

x(z) for the intermediate section:

$$x - x_1 = m_G(z - z_1);\ m_G = m(z_1);\ x_2 = x_1 + m_G(z_2 - z_1) \tag{7}$$

x(z) for the second circle:

$$(z - z_{m2})^2 + (x - x_m)^2 = r_2^2;\ x = x_m + \sqrt{r_2^2 - (z - z_{m2})^2}$$

Determination of the parameters *xm*; *zm*

From the uniformity of the gradient at the transition between straight and curved (*x'* = *mG*), the parameters must be determined:

$$2(z - z_{m2}) + 2(x - x_m)m_G = 0;\ x_m = x_2 + \frac{z_2 - z_{m2}}{m_G} = x_2 - \frac{r_k}{m_G};\ x_o = x_m + r_2$$

$$(z - z_{m2})^2(1 + \frac{1}{m_G^2}) = r_2^2;\ z_{m2} = z_2 + r_k;\ r_k = \frac{r_2}{\sqrt{1 + 1/m_G^2}}$$

For the determination of a field contribution according to equation 4, the integration programme specifies the co-ordinate z. The position x(z) and the gradient dx/dz = m(z) are calculated by means of equations 5, 6 and 7 (with different parameters z_{mi}, r_i for the two circles); z_1, z_2, zm_2, r_k are determined beforehand as auxiliary variables. In the left and the right-hand sections, x is constant and m =0.

6 Compensation conductor

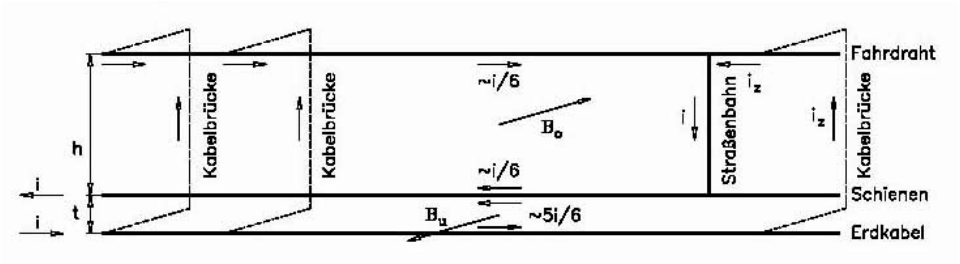

With an additional conductor (earth cable), it is possible to compensate the maximum field value $B_Ð$ in the compensation mode. This circuit was the result of a discussion on the reduction of the field values of the A section to less than 50 nT. Its operation, which was first demonstrated by means of an analogous resistance model (according to the lab diary, on 30. 10. 1992) can be readily explained in the sketch. The current to the tramway is supplied via the parallel circuit of earth cable and contact wire. As the conductor cross-section is five times that of the contact wire, the currents in the contact wire and earth cable are å i/6 and å 5i/6. The field emanating from all conductors can be divided into 2 subfields for the upper (B_o) and lower (B_u) conductor loops. In the upper conductor loop, only 1/5 of the current is flowing, but with five times the flow area. Therefore the two subfields (B_o and B_u) are equally large, but oriented in opposite directions and compensate each other when the tram is far removed from the test point or near a cable link. On the other hand, if the tram is travelling exactly between the cable links, the field passes through a maximum. The compensation is then disturbed, as the travelling current i_z in the last conductor segment changes its magnitude and sign (i/6.-5i/6).

7 Equivalent circuit

Current equations:	Mesh equations:
$i_1 + i_2 - i_3 - i_4 = 0$	$i_1R_{P1} + i_1R_{F1} - i_2(R_{E1} + R_{P2}) + i_4R_{P2} = 0$
$i_3 + i_4 - i_5 - i_6 = 0$	$i_2R_{P2} + i_3R_{F2} - i_4(R_{E2} + R_{P2} + R_{P3}) + i_6R_{P3} = 0$
$i_5 + i_6 - i_7 - i_8 = i$	$i_4R_{P3} + i_5R_{F3} - i6(R_{E3} + R_{P3} + R_{P4}) + i_8R_{P4} = i(1 - \varrho)R_{F3}$
$i_7 + i_8 - i_9 - i_{10} = 0$	$i_6R_{P4} + i_7R_{F4} - i_8(R_{E4} + R_{P4} + R_{P5}) + i_{10}R_{P5} = 0$
$i_9 + i_{10} = 0$	$i_8R_{P5} + i_9R_{F5} - i_{10}(R_{E5} + R_{P5} + R_{P6}) = 0$

According to the circuit in Fig. 6, 5 current and 5 mesh equations follow for the 10 unknown currents. The law according to which the equations are structured is clearly discernible, with the first and last equations being treated separately.

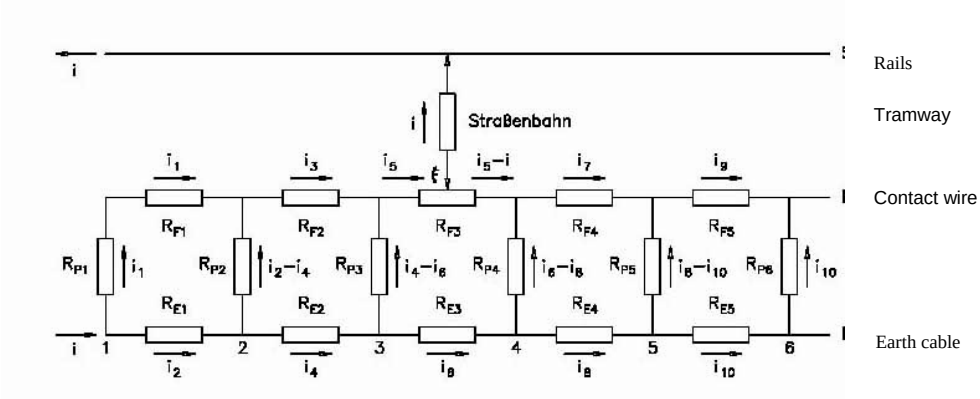

Fig. 6: Compensation circuit, resistance network

The coefficient matrix can therefore be programmed generally for a given number of meshes, so that the number of nodes can be entered as a parameter. The right-hand side of the equations is 0 up to 2 (the third equations in this case), which are determined by the position of the tram (in the third mesh, in this case). The sum of the current for nodes 2 – 5 are[3] already fulfilled by the approach itself. The sum of the current for the nodes 1 ($i = i_1+i_2$) is contained in the equations, as appears when all current equations are added up. To solve the equation system, the subprogramme *gaussj* from [3] was used. According to the equation system, the resistances R_Fi, R_{Ei} and the tap (pick-up) ϱ as a function of the tram position zF are included in the division of the current. Both variables result from line integrals over the section conductors, as the conductor lengths, besides the constant specific resistance ϱ̄ and the conductor cross-section A, are also included in the resistances.

$$R_{Fi} = \frac{\rho}{A}\int_{z_i}^{z_{i+1}} \sqrt{1+m^2(z)}\,dz;\ \xi = \frac{\rho}{A\,R_{Fi}}\int_{z_i}^{z_F} \sqrt{1+m^2(z)}\,dz$$

Fig. 7 shows the plot |B|(z), calculated according to equation 4, for the curved section in Fig 5. Fig 5 shows that this section consists of 3 segments with electrically separate power supply, the two end sections being constructed in the conventional way. In the middle segment, the most important one for the fields (-250 m< z < 210 m), with a compensation circuit, the power is supplied on the right-hand side in the figure at z = 210 m. The section is laid at a minimum distance of 180 m from the corner of the Physics building (z =0). A comparison of Fig 4 and 7 shows the effect of the compensation circuit. However, the compensation is already severely disturbed by a stray current of 1%, as the upper curve shows. Furthermore, small transition resistances in the mΩ range between the cable links and the contact wire can also materially disturb the current distribution between the contact wire and the earth cable, and thereby the compensation effect. For these reasons, an additional planned C section with a compensation circuit (20 cable links, 40 m apart) was scrapped. Because of the vectorial superposition of the components, the field no longer decreases to the minimum exactly at the right-hand cable link in Fig 7. When the tram turns into the uncompensated adjacent section on the left, there is a sudden change in the field, as the middle section then no longer carries a current. Upon the transition to the section on the right, the curve dips only slightly, as the change in the field is not as sudden.

[3] The source sentence is defective, and the meaning is not clear. Translated literally – tr. note

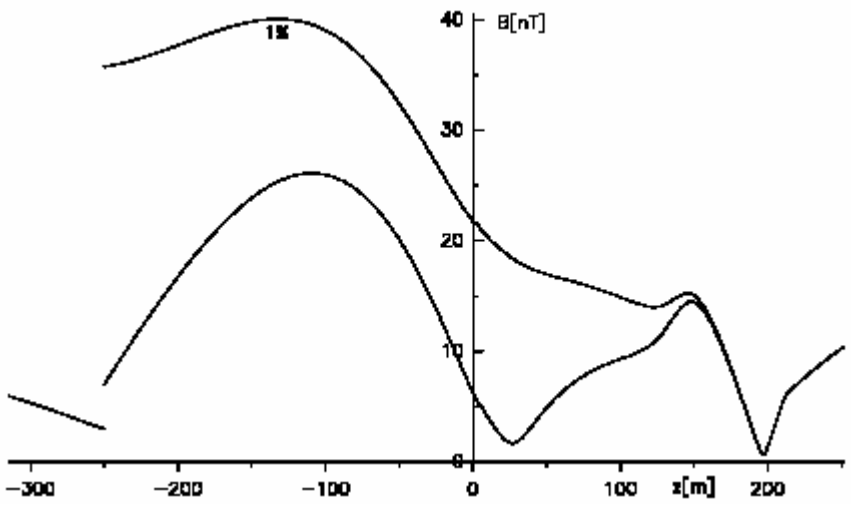

Fig. 7: Field strengths |B|(z) for passage of the tram on the B section according to Fig. 5

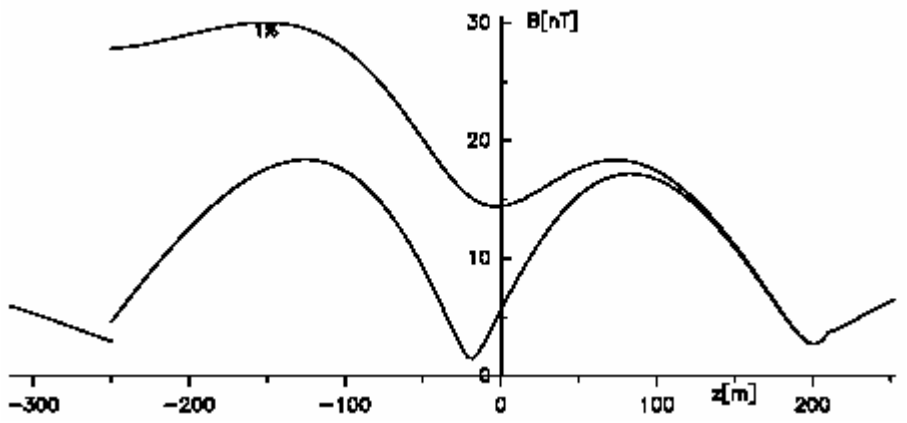

Fig. 8: Field strengths |B|(z) for passage of the tram on the A section according to Fig. 5

Fig. 8 shows the plot |B|(z) for section A according to Fig. 5, calculated with equation 3. The position of the middle cable link was moved to the left by 30 m. Compared with section B, the field values are 42% better if the stray current is not taken into account.

8 High-frequency pulse fields

Especially in frosty winter weather, but on wet spring and autumn days, arcing on the contact wire causes high-frequency interference pulses, as probably everybody has seen at some time or other. Via the extremely high-resistance particle detectors connected to electron multipliers (Channeltron/Channelplate, typical multiplication factors > 106), these pulse fields affect the electronic measuring systems (amplifiers, counters, discriminators etc.). In physical experiments, the measuring apparatus and the experiment itself are susceptible to interference even if the individual electronic measuring devices comply with the interference immunity provisions of the EMV Act. Such interference is not limited to physical measurements. Last winter, the indicator panels on the A40 highway broke down completely because of the spark discharges of a tram.

8.1 Shielding

Naturally, shielding precautions are taken on all equipment to protect against in-house interference. Despite all shielding precautions, however, substantial openings remain in the apparatus, with considerable penetration by electromagnetic interference fields. Such openings are inevitable for connecting lasers, for high-voltage and measuring operations, manipulators and more. Links are also created by the connection of the equipment to the mains supply and the cooling system. Further shielding would make the set-up and execution of many experiments so unwieldy that they it would no longer be practicable.

8.2 Measuring with a frequency-selective receiver

In the expert report [4], frequency-selective interference level measurements to VDE 847 were performed on a reference section of the Dortmund city tramway and in the Physics and Chemistry Laboratories in Bielefeld. An ESH2 measuring receiver with an HFH2-Z2 active frame aerial by Rhode & Schwarz was used with which the middle frequency can be varied between 9 kHz and 30 MHz; the bandwidth was set at ǂf = 10 kHz. The receiver has a sample & hold circuit after the rectifier that records the maximum intensities registered in the measuring period of 1 s by means of a plotter. The results are shown in Fig. 9. At first glance, the comparison suggests that interference is not to be expected, as the in-house level is only just reached even in frosty weather. However, the measurements are in urgent need of interpretation, as shown in the FFT calculations.

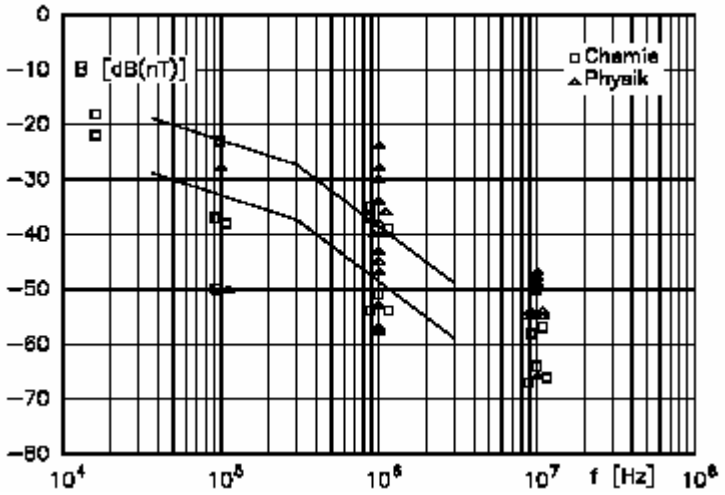

Fig. 9: Comparison of laboratory measurements (points) and tramway measurements (2 lines, 3 frequencies) in frosty weather; top line: 55 m, bottom line: 180 m

8.3 FFT simulation

The customary frequency response measurements to DIN/VDE detect high-frequency pulse interference only very incompletely, because for the counting electronics used in physics devices only the time behaviour of the pulses (parameters: peak values, rise and decay times) is decisive. The inadequacy of the frequency response measurements can be demonstrated by FFT calculations, amongst others. In addition, experimental investigations with a pulse testing generator to DIN VDE 0841 produced interference that lies far higher than would be expected on the basis of the comparison with the in-house interference level. The reason is that the in-house noise level is due to numerous incoherent interference events with a low pulse height, but also by many periodic signals (computer switching power supplies etc.).

8.4 Pulse function

To simulate the in-house interference level, the pulse function f(t)

$$f(t) = \begin{cases} \hat{c}e^{-a(t-t_o)}(1-e^{-b(t-t_o)}) & t > t_o \\ 0 & t \le t_o \end{cases};\ F(s) = \frac{b\hat{c}}{(a+s)(a+b+s)}$$

with the Fourier transform F(s) is selected. From the amount of F(s), the frequency response |*F*(ǵ)| that corresponds to the measurements is obtained:

$$|F(\omega)| = \frac{b\hat{c}}{\sqrt{(a^2+\omega^2)[(a+b)^2+\omega^2]}} \qquad (8)$$

Many interference events f(t) were superimposed on t_o as random variable within the time window T preset by the number of channels. The superposition of incoherent pulses on the time scale leads, in the frequency response, to a quadratic addition of the individual amounts. The superposition of i_o pulses f(t) with the height $\hat{c} / \sqrt{i_0}$ leads to the same frequency response |*F*(ǵ)| as shown in Fig. 10. The FFT curves were smoothed with a 9th degree polynomial whose parameters were determined with a linear least-squares-fit from the FFT channels. The number of generating pulses can no longer be determined from frequency response measurements.

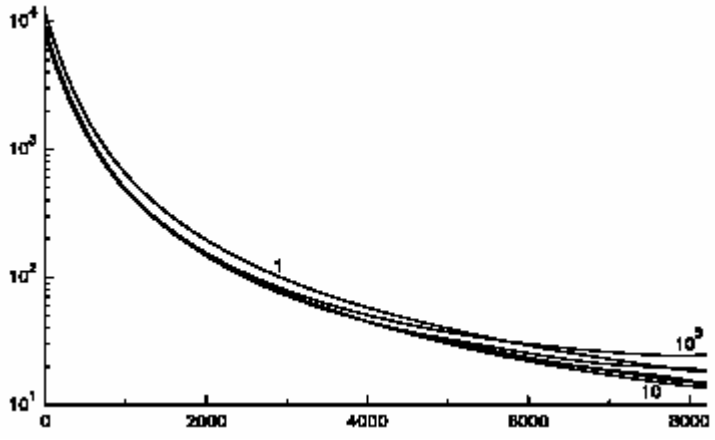

Fig. 10: Frequency response |F|(*k* ǵ) for the superposition of i_o pulses; linear least-squares-fit with 9th degree polynomial, 32768 channels; Parameter i_o = 1, 10, 10^2, 10^3, 10^4, 10^5; pulse function: $e^{-a\,t}(1 - e^{-b\,t})$; a = 1; b = 4

8.4.1 Aliasing

An FFT frequency spectrum of a continuous function f(t) is always limited by the scanning in discrete time steps ǂ*t*. In the process,the frequency spectrum above the Nyquist frequency $f_c = \frac{1}{2 \div t}$ is incorrectly attributed to the lower frequency symmetrically with f_c – the aliasing effect.
In Fig. 11, the FFT frequency response therefore always lies above the frequency response |F(ǵ)| according to equation 8. Furthermore, in the comparison the transformation rule regarding time t, angular frequency ǵ and the channel index i must be observed:

$$t = k\ 2\pi\ \frac{i-1}{2N};\ i = 1..2N\ \rightarrow \omega = \frac{i-1}{k};\ i = 1..N/2;\ N = 4096$$

The frequency spectrum is independent of the time offset f_o. This property of the amplitude spectrum also applies in the two-dimensional case and permits interesting applications in image processing.

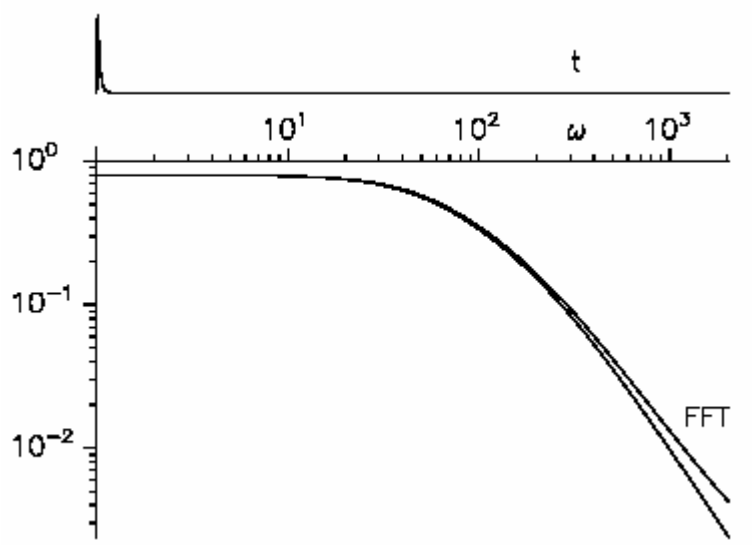

Fig. 11: |*F*(ǵ)|; parameters: k = 50, a = 1, b =4, N = 4096, t_o = 0

8.4.2 Comparison in the time and frequency area

Of interest now with regard to time and frequency is the comparison of a single pulse (contact line arcing) with the superposition of many pulses (in-house interference level). To this end, a single pulse with a height of $\sqrt{500}$ ň as well as the superposition of 500 pulses with a height of ň on the time and frequency scale are shown in Fig. 14 and 15. For the FFT calculation, the subprogramme *four1* from [3] with 32768 time channels was used. It can be seen that with a suitably selected discriminator threshold, the 500 interference events can be easily eliminated, while the individual interference pulse of the tram passes the threshold with no trouble at all and results in an incorrect reading – this with an otherwise identical frequency spectrum. The frequency response of many pulses with statistically distributed start times ensuing from the FTT calculations is naturally subject to wide variations. Nevertheless, the mean value of the FFT curve in Fig. 15 coincides with |F(ǵ)| after equation 8; deviations are due purely to the aliasing effect. The number of pulses can even be raised to 10^5 without too much of an effect on the frequency response, as Fig. 10 shows. In the time diagram the superposition of 10^5 pulses already raises the zero level strongly to 64% of the pulse height of the individual pulse.

If the single pulse ň as an interference event is added to 10^5 pulses with the height ň $\sqrt{10^5}$ on the time scale, the interference pulse still dominates as before. With the superposition of many pulses in many channels, the performance limits of the computer are soon reached. Independently of the FFT calculations, analytically derived equations are useful for extrapolation to the actual experiment.

8.4.3 Pulse function y(t)

For a single pulse, the FFT calculation is based on the following pulse function:

$$y(t) = e^{-t/\tau}(1 - e^{-4t/\tau})$$

For the evaluation, the maximum value ƨ and the steady component $y_=$ of y(t) are needed. By differentiation of y, the pulse height is first obtained:

$$\frac{dy}{dt} = -\frac{1}{\tau}e^{-t/\tau}(1 - 5e^{-4t/\tau}) = 0 \rightarrow \frac{t}{\tau} = \frac{ln\ 5}{4}$$

$$\rightarrow \hat{y} = e^{-\frac{ln\ 5}{4}}(1 - e^{-ln\ 5}) = \frac{4}{5}e^{-\frac{ln\ 5}{4}} = \frac{4}{5\sqrt[4]{5}}$$

When many such pulses are superimposed, the background noise level is shifted upward on the time scale with the width T. The shift $y_=$ (steady component of y) is obtained by integration over the pulse function:

$$\int_0^\infty e^{-t/\tau}(1 - e^{-4t/\tau})\ dt = \left[-\tau e^{-t/\tau} + \frac{\tau}{5}e^{-5t/\tau}\right]_0^\infty = \frac{4}{5}\tau = y_=T$$

8.4.4 Superposition of many pulses

If for the noise level n pulses of height $1/\sqrt{n}$ are superposed, the frequency response level does not change, as the FFT calculations show. On the time scale the superposition in the time window T leads to an increase of the level by the value

$$\frac{n}{\sqrt{n}}y_= = \sqrt{n}\frac{4}{5}\frac{\tau}{T}$$

A superposition of n pulses with height $1/\sqrt{n}$ can raise the level so much on the time scale that the height ƨ of the single pulse is reached.

$$\sqrt{n}\frac{4}{5}\frac{\tau}{T} = \frac{4}{5\sqrt[4]{5}} \rightarrow n_{max} = \frac{1}{\sqrt{5}}\left(\frac{T}{\tau}\right)^2 \qquad (9)$$

In the FFT calculations, t = 0.0225i (k = 117) was set with i as the run index in a field of 32768 cells. This gives the values T/ǰ = 0.0225 * 32768 = 737.28 and n_{max} = 2.4 105 from equation 9. This analytically determined numerical value is fully confirmed in the FFT calculations; in terms of computing time, the superposition of 2 105 pulses can only just be performed with today's computers.

8.4.5 Correction of the measuring level

As a function of n, the amplitude height decreases with $1/\sqrt{n}$; the steady component increases by $\sqrt{n}$. The function $y_m = y = + ƨ$ first decreases and the increases again. The position of the minimum is given by the differentiation:

$$y_m = b\sqrt{n} + \frac{a}{\sqrt{n}};\ a = \frac{4}{5\sqrt[4]{5}};\ b = \frac{4}{5}\frac{\tau}{T};\ \frac{dy_m}{dn} = \frac{b}{2\sqrt{n}} - \frac{a}{2\sqrt{n^3}} = 0$$

$$n_{min} = \frac{a}{b} = \frac{T}{\tau\sqrt[4]{5}};\ y_{min} = b\sqrt{\frac{a}{b}} + a\sqrt{\frac{b}{a}} = 2\sqrt{ab} \qquad (10)$$

If ƨ is understood to be the height of the interference pulse due to the spark discharge and y_{min} to be the in-house noise level, then the two frequency responses for the spark discharge and the in-house noise level correspond completely. However, the many laboratory interference pulses can be easily suppressed by means of a simple threshold discriminator: the measurement of the laboratory noise level remains totally unaffected. As y_{min} < ƨ, the laboratory noise in the frequency

response can even be increased by a factor of y_v without any change in this advantageous measuring situation.

Interference occurs only if $y_v y_{min} = 2$.

$$y_v = \frac{\hat{y}}{y_{min}} = \frac{a+b}{2\sqrt{ab}} = \frac{1}{2}(1+\frac{a}{b})\sqrt{\frac{b}{a}} \approx \frac{1}{2}\sqrt{\frac{a}{b}} = \frac{1}{2}\sqrt{n_{min}} \; mit \; \frac{a}{b} \gg 1 \qquad (11)$$

y_v can be interpreted as a numerical value by which the laboratory noise level must be corrected upward in the frequency response measurements so that the interference influences of the laboratory and the tram can be described as equal on the time scale.

An FFT calculation with 32768 channels allows, with a decay time of ǰ = 100 ns, the mapping of a time window of *T* = 73.7µs. The bandwidth ǂ*f* = 10 kHz of the selective receiver used corresponds to an integration time of T_I = 100 µs. The maximum of the signal is displayed within the measuring time T_M = 1s after the sample & hold. A simulation of the actual experiment would therefore require many more channels and would require a correspondingly greater calculation effort. The numerical calculation is not even necessary, however, because the calculation can also be performed analytically by making use of the given equations. In the spark discharge, the process of charge carrier multiplication occurs in the vicinity of contact wire surfaces with high field strengths. Areas with high field strengths are already formed purely coincidentally as a result of the contact wire geometry. If, owing to electrical insulation, a sudden power drop occurs at a point on the contact wire (dI/dt ш Ð), the induced voltage U_i = L dI/dt additionally ensures high field strengths. Assuming for such a discharge process a not unreasonable rise time of ǰ = 20 ns gives T =1s according to equation 10 and 11 n_{min} = 3.3 107 and y_v = 2891. In this calculation, ǰ remains the big unknown factor that can only be estimated roughly from the measurements carried out in [4]. The random coincidence of several pulses (pile-up) has also remained unconsidered. In digital measuring technology, special circuits (pile-up rejector) can certainly be used to protect electronic counters against such pulses.

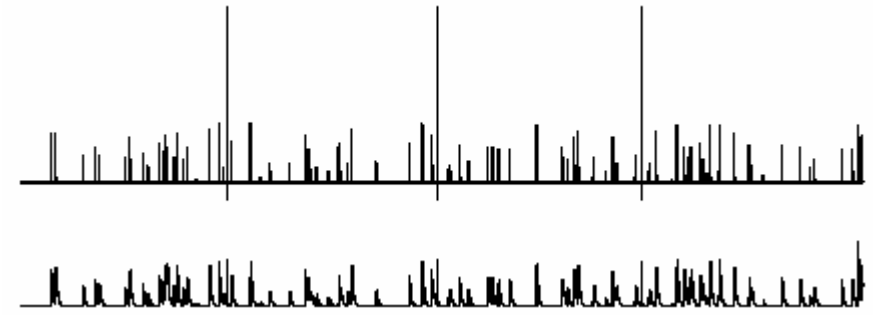

Fig. 12: Pulse diagram before (bottom) and after (top) the differentiating circuit

8.4.6 Differentiating network at input

So far it has been shown that for the same frequency response, few interference pulses of the tramway have high pulse heights and are therefore able to disturb modern electronic measuring systems. However, interference cannot be ruled out either if the height of the interference pulses is low, but they occur rapidly. The measuring pulses are often processed before the discriminator in a differentiating network in which the height of rapid pulses is increased. In Fig. 12 three rapid interference pulses (a = 5,b = 20) on the laboratory spectrum, consisting of 100 pulses (a = 1, b = 4) were added up. Before the 100 pulses, pulse heights and starting time t_0 were cubed. As the three interference pulses are already hardly apparent in the time diagram, they naturally disappear completely in the frequency response because of the quadratic addition of the 100

pulses. If a differentiation network is used for pulse shaping, they may however still cause interference, as Fig. 12 demonstrates.

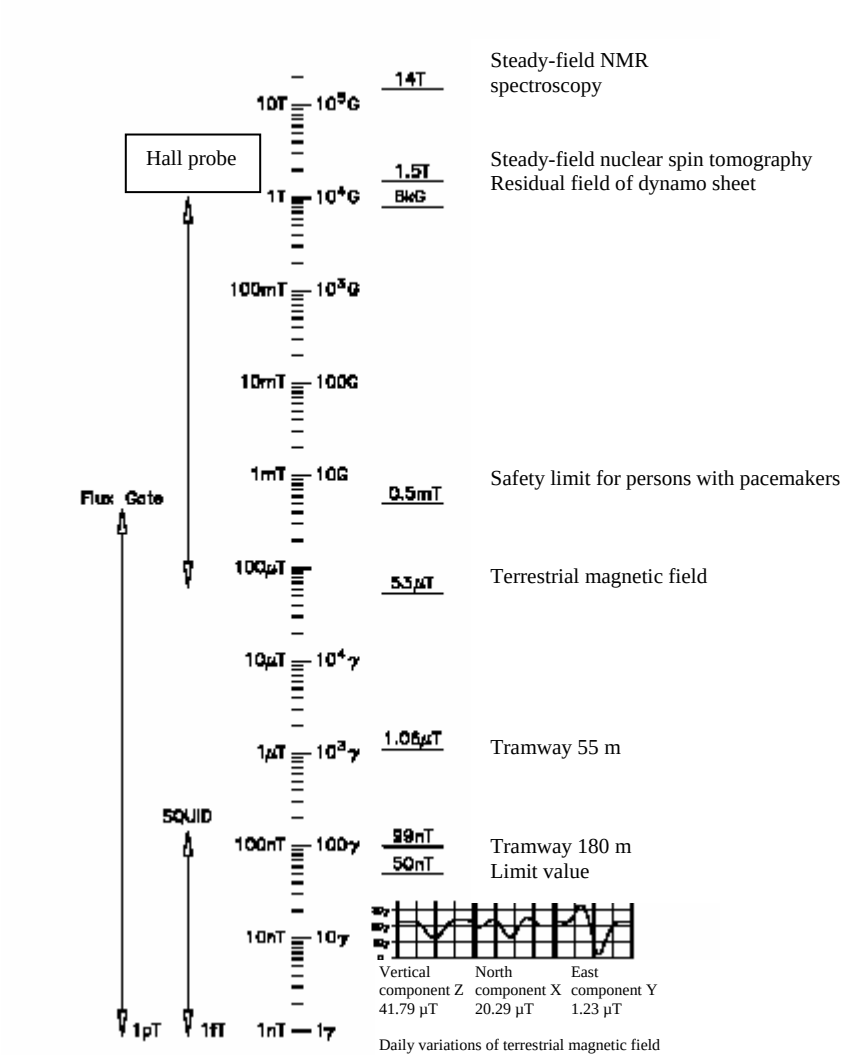

Fig. 13: Limit value, tramway emission values, field-value reference points for orientation and measuring ranges of magnetic-field probes

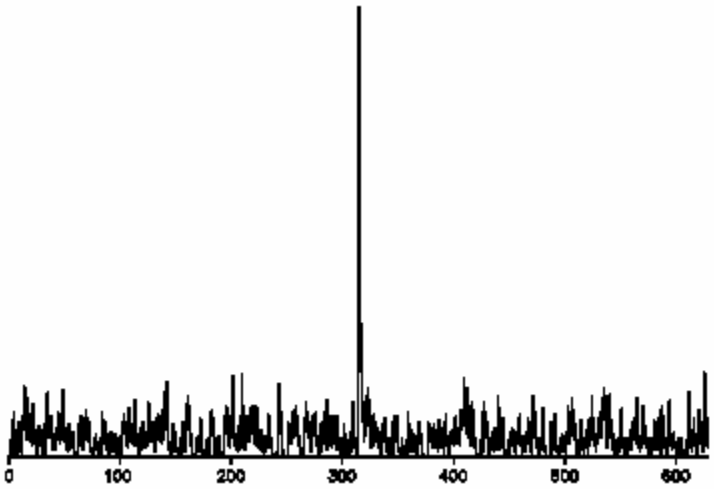

Fig. 14: Time diagram f(t) as superposition of 500 pulses with height 1 and 1 pulse with height $\sqrt{500}$; parameters: k = 100, a = 1, b = 4, 32768 channels

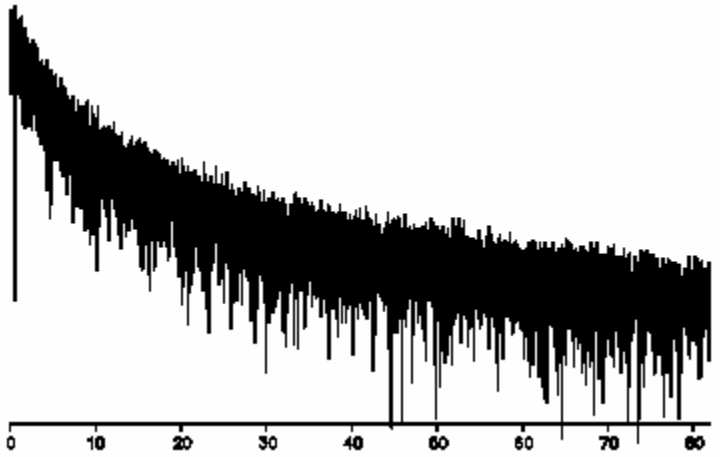

Fig. 15: Frequency response $|F|(\acute{g})$; superposition von 500 pulses; parameters: k = 100, a = 1, b = 4, 32768 channels; logarithmic ordinate scale

References

[1] L. Trahms, Magnetfeldsensoren für die medizinische Meßtechnik, Technisches Messen 61 (1994), 461
[2] L. Trahms, Biomagnetic Instrumentation, to be published, 1997
[3] Press, Teukolsky, Vetterling, Flannery. Numerical Recipes - The Art of Scientific Computing, Second Edition. Cambridge University Press, 1992
[4] D. Peier, Bewertung der Elektromagnetischen Verträglichkeit bei der Planung einer Stadtbahntrasse im Bereich der Universität Bielefeld, 1993

Appendix E

Electric and Magnetic Fields
of
Railway Installations

SIEMENS

Electric and magnetic fields of railway installations

Publication 09/2004

Translation of Publication eb – Elektrische Bahnen 96 (1988)
Braun W., Meisel R., Schneider, E., Zachmeier, M.:
Elektrische und magnetische Felder in der Bahnstromversorgung
In: Elektrische Bahnen 96 (1998)

Siemens AG
Transportation Systems
Electrification

Copyright © Siemens AG 2002. All rights reserved.

Herausgegeben von/Issued by:

Siemens AG
Transportation Systems
Electrification

P.O. Box 3240
D-91050 Erlangen, Germany

E-Mail: techcom.tsel@ts.siemens.de

Änderungen vorbehalten! / Subject to change without notice!

© Siemens AG 2002

HINWEIS / NOTE

Weitergabe sowie Vervielfachung dieser Unterlage, Verwertung und Mitteilung ihres Inhalts sind nicht gestattet, soweit nicht ausdrücklich zugestanden. Zuwiderhandlungen verpflichten zu Schadenersatz. Alle Rechte vorbehalten, insbesondere für den Fall der Patenterteilung oder Gebrauchsmustereintragung.

The reproduction, transmission or use of this document or its contents is not permitted without express written authority. Offenders will be liable for damages. All rights, including rights created by patent grant or registration of a utility model or design, are reserved.

Author

Dipl.-Ing. Wolfgang Braun

Graduated as Electrical Engineer for Electrical Power Systems at Technical University Würzburg-Schweinfurt. Since 1997 Siemens Transportation Systems, Electrification, System design for Traction Power Supply.

Address: Siemens AG, TS EL EN, POB 3240, D-91050 Erlangen

Phone: +49 9131 7 44252, Fax: +49 9131 7 24494

e-mail: wolfgang.a.braun@siemens.com

Dipl.-Ing. Roland Meisel

Graduated as Electrical Engineer at Friedrich-Alexander-University Erlangen-Nuremberg. Since 1996 Siemens Transportation Systems, Electrification, System design for Traction Power Supply.

Address: Siemens AG, TS EL TK, POB 3240, D-91050 Erlangen

Phone: +49 9131 7 44254, Fax: +49 9131 7 28364

e-mail: roland.meisel@siemens.com

Dr.-Ing. Egid Schneider

1979 graduated as Electrical Engineer at Friedrich-Alexander-University Erlangen-Nuremberg. 1988 Dr.-Degree in High Voltage Direct Current Transmission. In the following time Siemens Power Transmission and Distribution. Since 1991 Siemens Transportation Systems, Electrifications, Head of Sector System design for Traction Power Supply.

Address: Siemens AG, TS EL EN, POB 3240, D-91050 Erlangen

Phone: +49 9131 7 28577, Fax: +49 9131 828 28577

e-mail: Egid.Schneider@siemens.com

Dipl.-Ing. Markus Zachmeier

Graduated as Electrical Engineer at Friedrich-Alexander-University Erlangen-Nuremberg. Since 1994 Siemens Transportation Systems, Electrification, System design for Traction Power Supply.

Address: Siemens AG, TS EL EN, POB 3240, D-91050 Erlangen

Phone: +49 9131 7 26712, Fax: +49 9131 7 28364

e-mail: markus.zachmeier@siemens.com

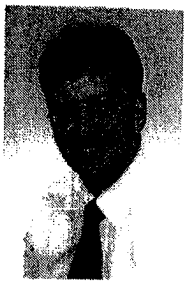

Zusammenfassung

Der Aufsatz beschreibt Berechnungsmethoden für elektrische und magnetische Felder im Umfeld elektrischer Bahnstrecken, gibt typische Werte für unterschiedliche Bahnstromversorgungssysteme an, vergleicht diese mit Vorsorgewerten und Grenzwerten nach dem derzeitigen Stand der Normung und Gesetzgebung und zeigt Wege zur Reduktion der Feldstärken, die sich mit vertretbarem Aufwand beim heutigem Stand der Technik umsetzen lassen.

Summary

This paper deals with calculation methods for electric and magnetic fields in the vicinity of electric railways, gives typical values for different traction supply systems, compares them with precaution values and limit values based on recent standards and laws and shows possibilities to reduce the field intensities, which can be realised with present technologies.

Résumé

L'article décrit les méthodes de calculation des champs électriques et magnétiques aux environs des lignes ferroviaires électrifiées, indique les valeurs typiques pour différent systèmes d'alimentation en energie de traction. Il compare celles-ci avec des valeurs de précaution et des valeurs limites sur la base des normes et de la législation en vigueur et démontre des possibilités pour réduire les intensités des champs en pouvant être réalisées à l'aide de la technologie actuelle.

1 Introduction

Increasing importance is being attached to the fields in electrical power systems to make power transmission systems more acceptable to public opinion. This includes high-voltage transmission lines as well as overhead contact line systems of mass transit systems and main line railways. These generate electric and magnetic fields which depend on the operating voltages and currents. The approval procedures for new projects and extension of existing lines require that the operator clearly indicates the electric and magnetic field strengths which will occur during operation. These values are useful for estimating the possible interference in electronic equipment and for comparison with the precautionary values for safety of persons. More detailed studies are necessary if the route passes through areas where sensitive medical diagnostic equipment is installed, research laboratories, certain industrial installations as well as residential areas.

Reliable results of calculations form the basis for reliable planning values. A wide range of programs for calculating the field strengths of transmission lines from simple configurations up to multisystem three-phase transmission lines are commercially available.

Because of the asymmetrical operation to earth and the number of feeding and return conductors involved, the calculation of magnetic field strengths of traction systems – particularly AC traction power supply systems requires the current distribution between the individual conductors. For this reason, a program for the calculation of the electric and magnetic fields of a traction power supply system must include calculation of the current distribution taking into consideration the coupling between all the feeding and return conductors and the peculiarities of railway lines.

2 Natural and technical fields

The natural fields are superimposed on the electric and magnetic fields of the power supply system.

At low frequencies, the electric and magnetic fields are not correlated with each other. This makes it possible to calculate the electric and magnetic fields separately for power frequencies [1].

2.1 Electric field

An *electric field* is created by the charge transfer between two poles. The field lines begin at the positive electrode and end at the negative electrode. It is called a source field.

The *electric field strength* E is specified in kV/m and defines the force exerted on an electrical charge carrier. All values of E in this text and tables are r.m.s. values.

The natural *electric field* varies widely in time and space as a result of varying atmospheric conditions. It can reach values up to 20 kV/m during a thunderstorm.

The values of electric fields generated by technical equipment depend on the voltage, the arrangement of conductors and the distance from the live conductors. The field under a 380 kV overhead line can reach values of up to 10 kV/m. A maximum field strength of maximum 1.5 kV/m under a single-phase 15 kV AC overhead contact line and 2.5 kV/m under a single-phase, 25 kV AC overhead contact line are possible.

Electric fields can be easily shielded. E.g. the cable shield prevents a cable from emitting an electric field and the metal cover of a conductor rail acts as a screen. In the case of a vehicle, the metal body also functions as a screen.

2.2 Magnetic field

The *magnetic field* of an electrical conductor is generated by the current flowing through it. The magnetic field lines surround the conductor through which current is flowing. It is defined as a circuital vector field.

The *magnetic field strength* H is specified in A/m and is independent from material characteristics. On the other hand, the magnetic flux density B, also called magnetic induction, defines the effect of magnetic fields in materials and media. The unit of magnetic flux density is 1 Tesla = 1 Vs/m². The following formula is used for conversion:

$B = \mu_0 \cdot \mu_r \cdot H$

where the permeability constant $\mu_0 = 1.25664 \cdot 10^{-6}$ Vs/Am.

The relative permeability of air is $\mu_r = 1$. In this case the following relation between the magnetic field strength H and the magnetic flux B applies:

1 A/m = 1,26 µT

Some of the literature, standards and recommendations use the term field strength, others use the term flux density. In this paper, we consistently use the term flux density B for the diagrams and tables. All values of B are r.m.s. values.

The natural DC magnetic field of the earth varies with the latitude. It is approximately 48 µT in Central Europe. It varies slightly as a result of variations in the atmosphere and inside the earth.

Technical magnetic fields are a function of the current following through the conductor, the conductor configuration and the distance from the conductors. Strong DC

fields of 0.5 T are generated in magneto-resonance imaging for medical diagnostics. Field strengths of up to 100 µT can be expected under the overhead traction line of single-phase AC railways. In DC railway systems with a conductor rail, DC fields of up to 500 µT can be caused by the high operating currents.

The screening of magnetic fields is practically impossible in the case of widely spread-out plants such as traction power supply systems. Limited local measures such as screening of monitors with high-permeability materials are possible. Such screening measures are, however, very expensive and have only a limited effect against DC fields.

3 Calculation of electric and magnetic fields

Siemens AG has developed the SITRAS®-EMF 2.0 planning tool for calculation of the electric and magnetic fields of high-voltage transmission lines and overhead contact lines of railway systems. Fig. 1 shows the program structure and Fig. 2 the Windows Graphic User Interface. The following calculation functions are integrated in the program:

- Electrical characteristics, self and mutual impedances of various line configurations
- Current distribution in the feeding and return conductors with influence of the earth current
- Electric field strengths
- Magnetic field strengths of railway lines and, in addition
- Magnetic field strengths of individual conductor configurations.

Due to the high operating currents and relatively low transmission voltage of traction systems, the magnetic fields have a greater significance than the electric fields. Exact knowledge of the operating currents and their distribution between the various conductors is absolutely necessary for correct calculation of the magnetic field strength.

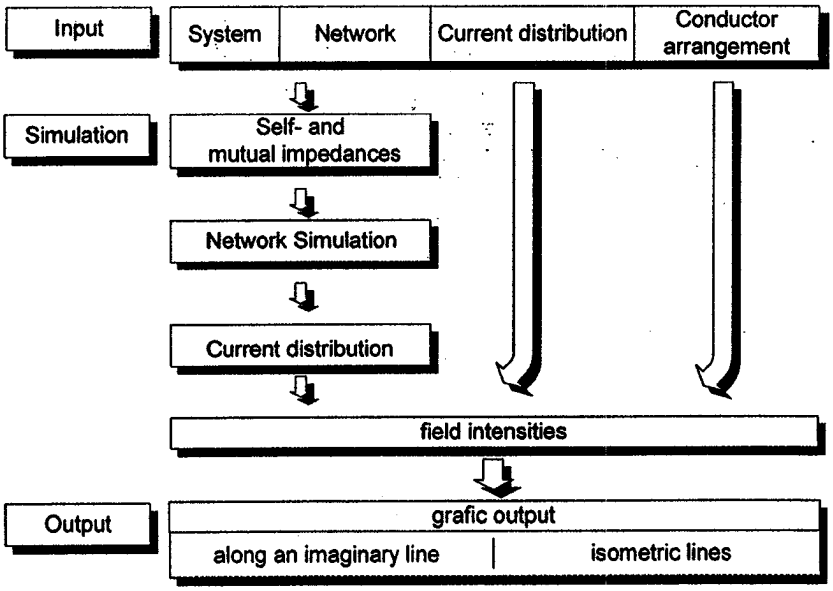

Figure 1: Flow chart for field calculation

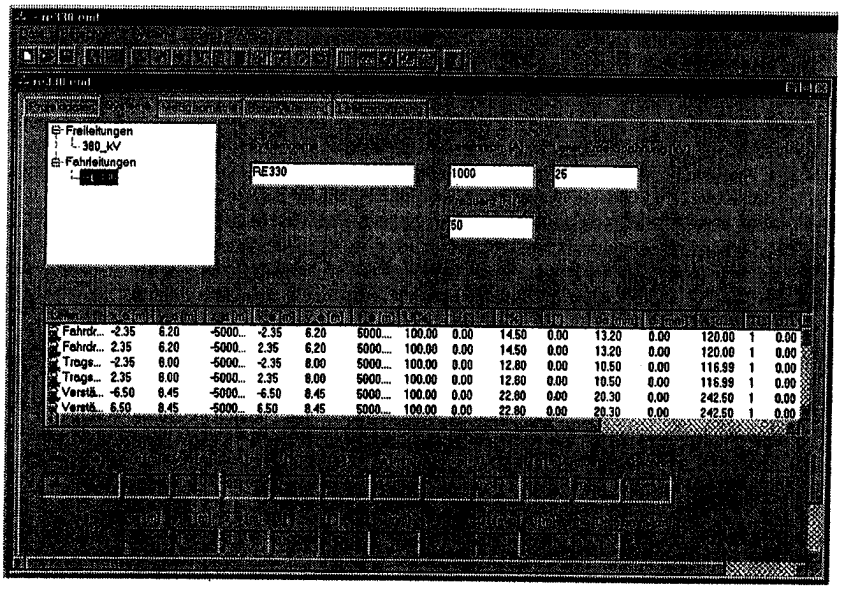

Figure 2: User interface of SITRAS® EMF

The operating currents depend on the operation concept and the resulting electrical design of the route. They are calculated by programs for network calculation with simulated train operation [2].

The current distribution is determined by interconnection of the conductors and by the self and mutual impedances of the incoming feeders, overhead contact lines, reinforcing conductors, return conductors, the running rails and the earth return. Whereas, the current distribution in DC traction systems is mainly determined by the conductivity of the individual conductors, the current distribution in AC traction systems is decisively defined by the couplings between the various conductors. The self and mutual impedances are the result of the conductor material data, the conductor arrangement and soil resistivity. For railway lines normally infinitely long parallel conductors can be assumed, so that the mathematical problem can be reduced to a two-dimensional field problem [3], [4], [5]. SITRAS-EMF calculates the impedances of all current-carrying conductors and transfers these, together with the interconnection data to the network calculation program for calculating the current distribution.

A two-dimensional representation is the best method for assessing the fields along overhead contact lines. For this reason, the fields are calculated at points along freely specified lines or planes at a right angle to the route. The results are shown as function values along the specified lines or as isometric lines (Figs. 3 & 9).

For special problems connected with interference caused by conductor arrangements of finite length as well as crossings and sharp curves, specially in mass transit systems, it is also possible to calculate the magnetic fields of skewed or inclined systems at points along imaginary lines or areas. This requires complicated modelling and data input and is a special function of the SITRAS-EMF program.

4 Typical fields of railway systems

4.1 DC Systems

Power is supplied to DC traction systems either by an overhead contact line or by a conductor rail. The return path is provided either by the running rails and/or an additional return conductor.

The strength of the magnetic field for a given current can vary widely depending on the conductor configuration.

Fig. 3 shows the isomagnetic lines close to and further away from overhead contact line and conductor rail installations for a total current of 1000 Amperes. Each running rail carries 25% return current assuming good insulation against earth and good interconnection of the rails.

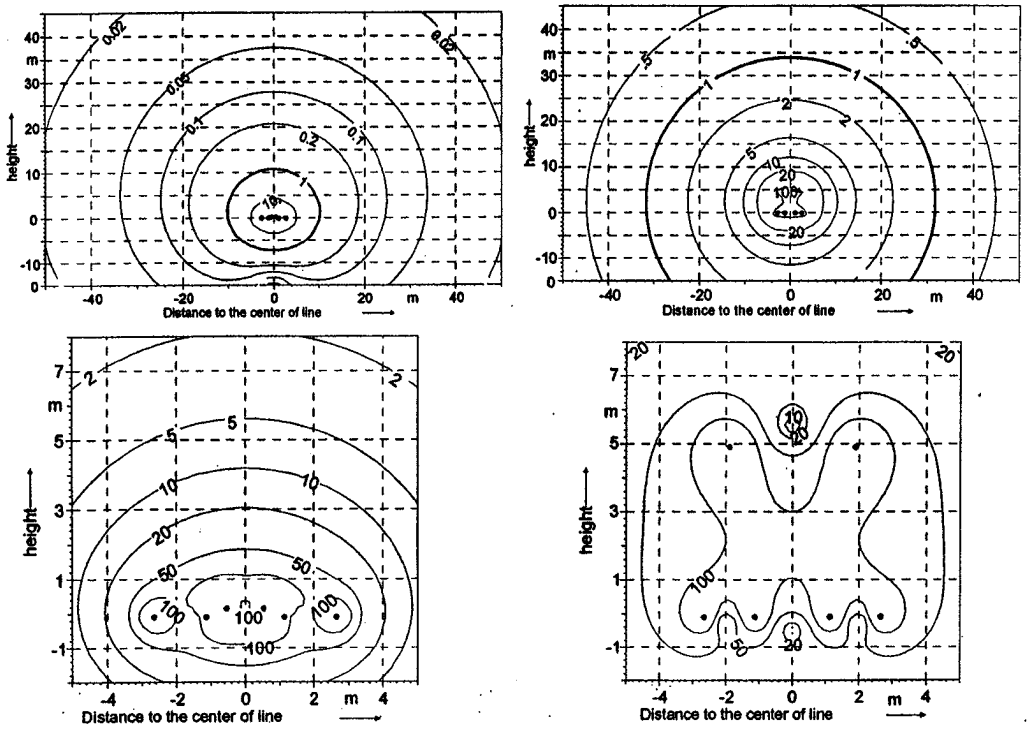

Figure 3: Magnetic flux density B in mT of a two-track DC traction system with conductor rail (left) and overhead contact line (right) both at 1000 A total current for the far range (top) and near range (bottom)

The magnetic induction in the vicinity of the overhead contact line above the running rails is partly more than double the value measured in a conductor rail system at comparative current values. Farther away, i.e. approximately 5 m away from the center axis of the line, the field of a overhead contact line system is 10 – 20 times higher than that of a conductor rail system.

Tables 1 and 2 show a comparison of electric and magnetic field strengths of overhead contact line and conductor rail systems.

Distance to track centerline	1 m V/m	10 m V/m	100 m V/m
Overhead contact line	80	15	0.5
Conductor rail	105	12	0.3

Table 1: Electric field strength *E* of 750 V DC traction systems, 1 m above the top of rail (TOR)

Distance to track centerline	1 m µT	10 m µT	100 m µT
Overhead contact line	120	10	0.1
Conductor rail	120	1	0.005

Table 2: Magnetic flux density *B* of DC traction systems with a total current of 1 kA, 1 m above the top of rail (TOR) (Fig. 3)

4.2 AC Systems

AC systems are primarily used for main line railways. Three types of systems are used world-wide, namely,

- Rail return system
- Autotransformer system and
- Boostertransformer system.

The basic principles of operation and the variants are described in [6].

Fig. 4 shows all three systems one above the other with a train located at kilometre 30 in all three cases. The sectional view shows the typical layout of a two-track high-capacity route with UIC 60 running rail, with overhead contact line system (here type Re 330 of the Deutschen Bahn (DB)), contact wire RiM 120, messenger wire Bz II 120 and reinforcing conductor Al 240. In case a, this is permanently connected to the overhead contact line as a reinforcing conductor; an additional Al 240 return conductor is also used. In case b, this is used as a so-called negative feeder and in case c as a return conductor; here, however, an earth conductor St 120 is suspended from the poles instead of the return conductor.

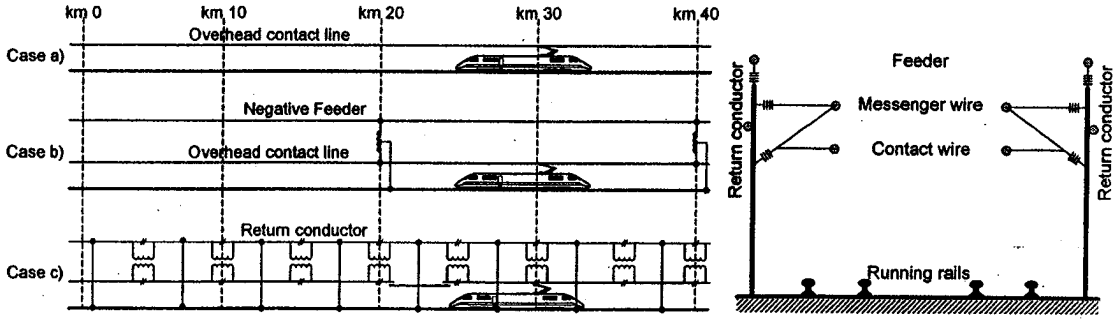

Figure 4: Schematic diagrams of different AC traction power supply systems on a typical route (right).
Case a (top) with return path via running rails and return conductor
Case b (middle) with autotransformers
Case c (bottom) with booster transformers

In case a the return path for the current to the substation is formed by the running rails, the return conductor and the soil. At the transition area in the vicinity of the vehicle and the substation, the return current mainly flows through the running rails. The magnetic field strength here is lower than in the middle range where a larger part of the return current flows through the soil.

In case b, power is transmitted on a two-pole basis in which case the voltage between the overhead contact line and the *negative feeder* is usually double the rated voltage. The autotransformers along the route – at km 20 and km 40 in the figure – step down the voltage to the value required by the vehicle. Between them, the return current path is similar to case a, when fed from both sides.

In case c, the traction current flows to the vehicle at the disconnecting points in the overhead contact line through the primary winding of the booster transformers, here located at 5 km intervals. Their secondary windings force the return current into the return conductor so that there is practically no current flowing through the running rails at large distances from the vehicle.

Under identical operating conditions, the magnetic field strengths are different in the three systems in different sections of the route due to the differing current distributions.

Tables 3 and 4 show a comparison of the general values of the electric and magnetic field strengths. Fig. 5 shows the magnetic fields at points along an imaginary line rectangle to the line, 1 m above the top of the rail at km 10 and km 28.

Distance to track centerline	1 m kV/m	10 m kV/m	100 m kV/m
Case a	2.2	0.6	0.01
Case b	1.8	0.1	0.001
Case c	2.2	0.6	0.01

Table 3: Electric field strength *E* of 25 kV AC traction systems (cases a and c) and 2x25 kV (case b), 1 m above the top of rail (Fig. 4)

Distance to track centerline	1 m µT		10 m µT		100 m µT	
	km 10	km 28	km 10	km 28	km 10	km 28
Case a	55	55	5	5	0.4	0.4
Case b	20	40	2	3.5	0.05	0.25
Case c	20	65	6	7	0.04	0.3

Table 4: Magnetic flux density *B* of AC traction systems with a total current of 1 kA, 1 m above the top of rail (TOR) (Fig. 4)

The autotransformer system shows the lowest values of all three cases. The boostertransformer system has similarly low values of the magnetic field as the autotransformer system in a line section without vehicle at km 10. In a section with a vehicle at km 28, the booster transformer system has the highest magnetic field values as no current flows there in the return conductor.

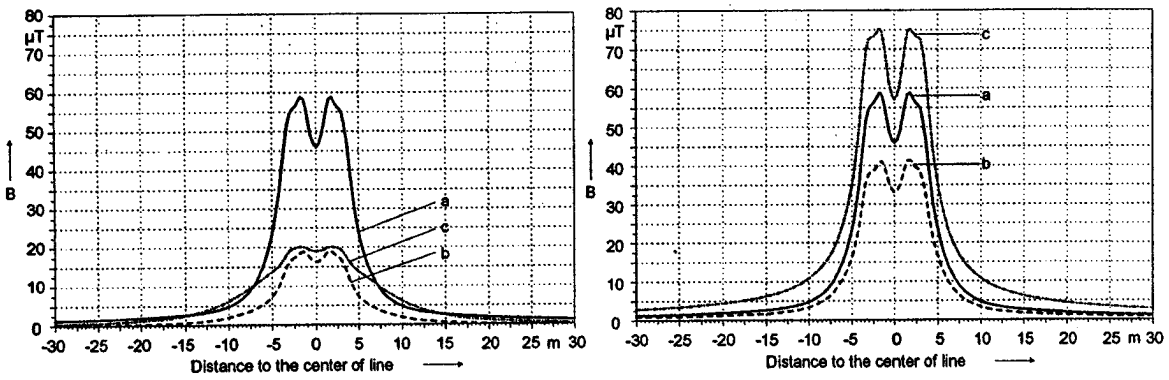

Figure 5: Magnetic flux density *B*, 1 m above the top of rail (TOR) with 1000 A total current, for the three systems of Fig. 4 at km 10 (left) and at km 28 (right).
a) with return path via running rails and return conductor
b) with autotransformers
c) with boostertransformers

In high-capacity traffic, a number of vehicles may be operating in a section fed by the substation; the magnetic fields here can vary widely due to the different current directions and distribution.

5 Measurement of magnetic fields

The measurement of magnetic fields is necessary for assessing the performance of existing systems as well as for verification of computer models. They are also meaningful in cases where calculations would be too expensive and time-consuming.

The results of measurements in an AC traction system are shown in [7] and compared with calculations.

When measuring DC fields, it should be noted that the natural magnetic field of the earth is superimposed on the field being measured. This must be taken care of during evaluation of the measured values with the three directional co-ordinates.

Results of calculations and measurements carried out by Siemens AG on a two-track, DC traction system with a conductor rail are shown in Fig. 6. An return cable insulated versus earth was laid parallel to the four running rails. The values were measured for a traction current of 2000 A which is typical for such an installation. Each of the four running rails carried 21% of the return current; 16% was carried by the additional return conductor. The measured and calculated values coincided well with each other.

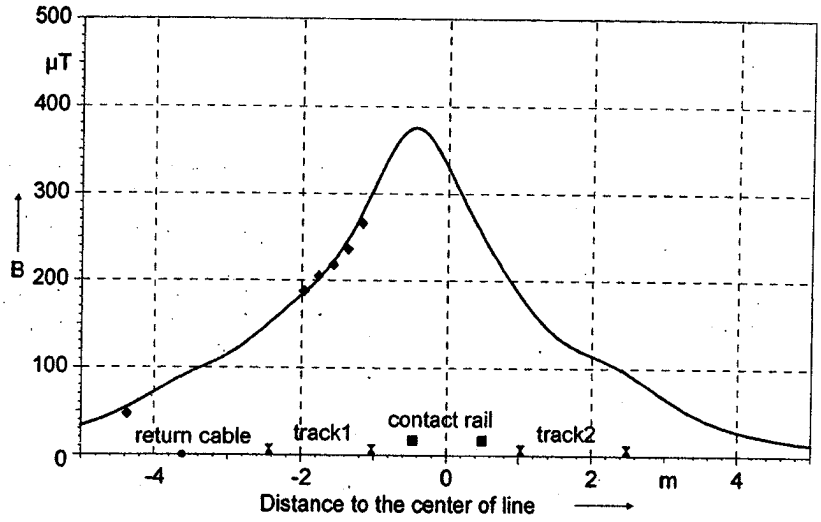

Figure 6: Magnetic flux density *B* 1 m above the top of rail (TOR) for 2000 A total current of a two-track DC traction system with conductor rails and additional return conductor.
Calculation diagram and measurement dots.

The calculation of magnetic fields in substations is very complex because of the complicated cabling and the different types of equipment. Measurements provide quicker and more accurate results.

For this reason, the DC and AC fields were measured in typical underground railway and tramway substations. Simultaneously, the currents in the three-phase incoming feeders and the DC currents were also recorded in order to correlate the fields with the currents.

Fig. 7 shows the measured values for the 50 Hz field in an underground substation. The measured point was 4.5 m from a 2.2 MVA rectifier transformer; the corresponding DC current during train operation is also shown for comparison. In a tramway substation, a maximum 50 Hz induction of 55 µT was measured at a distance of 1 m from the rectifier transformer for a DC current of 600 A.

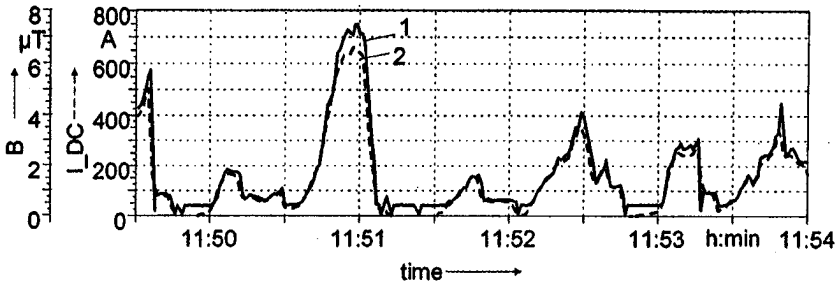

Figure 7: Measurements inside of an underground mass transit substation
1 - Magnetic 50-Hz-flux density B_{AC}
2 - Sum of rectifier currents I_{DC}

The highest DC fields occurred in underground substations directly at the incoming feeder panels; in tramway substations it was in the vicinity of the pole with feeding isolator. The peak values varied between 110 µT and 340 µT.

6 State of standards and mandatory regulations

The increasing discussion on magnetic fields is having its effect on standards and mandatory regulations.

In Germany, the electromagnetic field emitted by an electrical installation with a rated voltage above 1000 V is governed since 1997 by the 26th Directive to implementation of the Federal Emission Protection Code (26.BImSchV, Bundes-Immisionsschutzgesetz) [8]. This directive also applies to AC traction systems, does not however make any statements with respect to DC power supplies. The limit values specified in Tables 5 to 8 may be exceeded by 100% both, for a short time as well as in the near vicinity of the installation.

	26.BImSchV kV/m	ICNIRP/WHO Recommendations kV/m	VDE V 0848-4/A3 EN 50061/A1 kV/m
Area 1		-	30
Area 2	-	-	20
Pacemaker	-	-	20

Table 5: Permissible values of the DC electric field strength *E*. See text for areas.

	26.BImSchV mT	ICNIRP/WHO Recommendations mT	VDE V 0848-4/A3 EN 50061 mT
Area 1		200	67.9
Area 2	-	40	21.22
Pacemaker	-	0.5	0.5 /1[1)]

[1)] VDE V 0848-4/A3 specifies 0.5 mT as the permissible value.
As per EN 50061, static magnetic fields up to 1 mT should not cause any interference with pacemakers. After exposition to a field of up to 10 mT, the pacemaker must function correctly without renewed setting

Table 6: Permissible values of the DC magnetic field strength *B*. See text for areas.

	26.BImSchV kV/m	ICNIRP/WHO Recommendations kV/m	VDE V 0848-4/A3 EN 50061 kV/m
Area 1	5	10	[1]
Area 2		5	[1]
Pacemaker	-	2.5	7.07

[1] The values specified in VDE V 0848-4/A3 are not valid any more !

Table 7: Permissible values of the AC, 50 Hz electric field strength *E*. See text for areas.

	26.BImSchV mT	ICNIRP/WHO Recommendations mT	VDE V 0848-4/A3 EN 50061 mT
Area 1	0.1	0.5	[1]
Area 2		0.1	[1]
Pacemaker	-	0.1 – 0.2	0.053[2]

[1] The values specified in VDE V 0848-4/A3 are not valid any more !
[2] It is however stated that under realistic conditions, interference with pacemakers is not likely at magnetic flux densities below 0.1 to 0.2 mT.

Table 8: Permissible values of the AC, 50 Hz magnetic field strength *B*. See text for areas.

The preliminary version of VDE V 0848-4/A3 Standard of 1995 differs from the 26th Directive in that it defines different areas of exposure. Area 1 includes all controlled areas, e.g. operating rooms and generally accessible areas in which the method of operation or the reason of the stay is such as to ensure that exposure is restricted to a short period only. The limit values for area 2 are lower to ensure protection of certain groups of persons; this includes residential areas, sport and recreational areas and operating rooms in which no technical fields are expected.

This preliminary standard should not be used any more for AC traction systems as the 26th Directive has now laid down new values. The permissible values for DC fields however still hold good as also those for persons having a pacemaker. The values in Tables 5 to 8 for areas 1 and 2 apply only for continuous stay in the area. For shorter periods, the values can be increased by a factor of 3. The values for pacemakers have been derived from the EMC requirements for these devices as per EN 50061 [9]

Similiar to VDE V 0848-4/A3, the rules of the Employer's Liability Insurance Association (Berufsgenossenschaft der Feinmechanik und Elektrotechnik) specify different permissible values than the 26th Directive. For this reason, new accident prevention rules are being worked out in order to specify uniform values.

Both, the values specified in VDE V 0848-4/A3 as also the limits in the Guidelines of the International Commission on Non-Ionizing Radiation Protection (ICNIRP) and the World Health Organisation (WHO) are precautionary values. A basic value of the body current density of 10 mA/m² is accepted as it lies in the range of the natural body current density and no negative effects on health have been proven. This basic value together with a safety factor have been used to derive the permissible values in the ICNIRP/WHO recommendations for magnetic flux density. The ICNIRP/WHO recommendations differentiate between occupational, area 1, for persons who are professionally in contact with electrical equipment and general public, area 2. Additional values, at which no interference with pacemakers is expected are also specified [10], [11]. The values in Tables 5 to 8 for areas 1 and 2 are for continuous stay in the area. The values can be increased by a factor of 10 for shorter periods.

Planning of electric traction systems must also take into account the electromagnetic compatibility with electronic equipment. Magnetic fields can cause interference with electrical and electronic equipment such as monitors and medical diagnostic equipment [12], [13]. According to the law on electromagnetic compatibility of equipment (EMVG) dated 30th August 1995 [14], electrical devices, systems and plants must be installed and operated so that they cause no interference with other equipment nor are they subject to interference from other equipment. This basic requirement is considered as fulfilled if the concerned device fulfils the relevant harmonised European standards. The relevant preliminary European

standard for electromagnetic compatibility of railway systems is quoted in [15]. Limit values for magnetic fields of traction systems are under discussion.

7 Measures for reducing the magnetic field

The magnetic fields of traction systems are based on the superimposition of the fields of the feeding and return conductors. If a number of conductors are used, all the feeding conductors and all the return conductors can be combined into one equivalent conductor respectively. The resulting magnetic field is then at a minimum when both equivalent conductors are identical. If optimum matching of the conductor arrangement is not possible due to structural limitations, additional current-carrying conductors can be laid to reduce the resulting magnetic fields.

Fig. 8 shows the example of an installation with a conductor rail in which a suppression cable is used to reduce the magnetic field. Unfavourable conditions exist when the feeding current is carried by only one conductor rail whereas the return path connections are such that the return current is conducted by all four running rails. A reinforcing cable is laid as a suppression conductor for the conductor rail of track B in the cable trough of track A. The cross-section is selected to obtain a distribution of the feeding current which will minimise the magnetic field in the far range. This can be seen in Fig. 8.

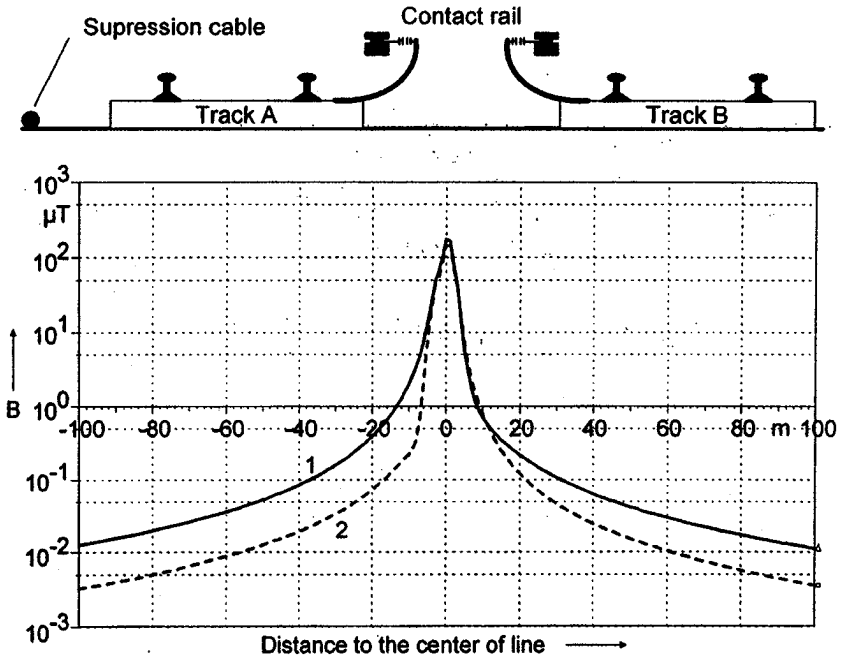

Figure 8: Magnetic flux density *B*, 1 m above the top of rail for 1000 A two-track DC system with conductor rails.
1 - without suppression cable
2 - with suppression cable

In AC traction systems, the additional return conductors on the poles reduce the magnetic fields by approximately 50 % on an open line. In addition, return conductors are also used to reduce the interference in tunnels. Calculations carried out by Siemens AG have shown that, if properly arranged, they can have the same reducing influence as the current-carrying reinforcement of the tunnel (Fig. 9). The longitudinal welding of the reinforcement along the length of the tunnel can thus be avoided. This procedure has also been approved by the DB [16].

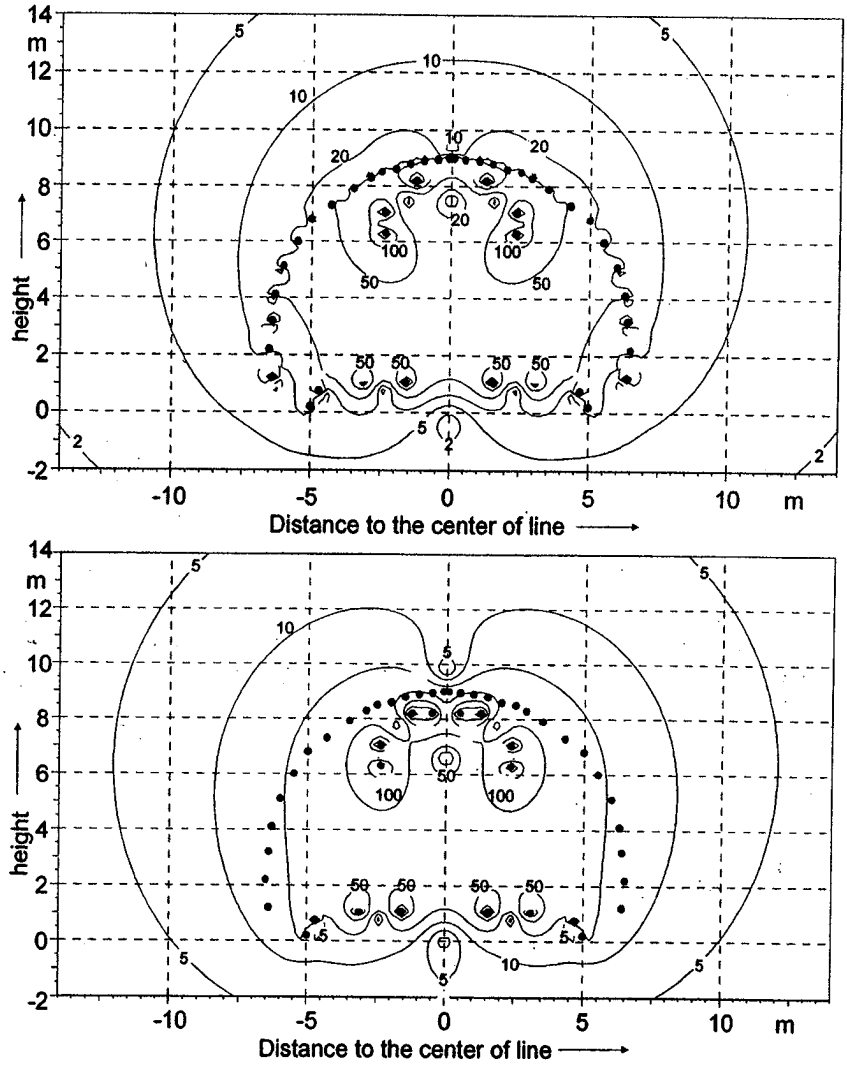

Figure 9: Magnetic flux density *B* in µT of an AC two-track tunnel system for 1000 A total current.
top Return path via tunnel reinforcement
bottom Return path via return conductors close to reinforcing conductors

8 Conclusions

Calculations of the electric and magnetic fields of various traction power supply systems show that the fields of contact line systems are significantly below the precautionary and limit values for protection of persons as prescribed by national and international laws, standards and recommendations. Measurements have confirmed the results of calculations.

In contrast, far lower values of magnetic fields can cause interference with electronic equipment. Therefore, interference with such equipment in the immediate vicinity of traction systems is not out of the question. Reliable calculation of the magnetic fields is of great importance for the planning and design of electric railway systems as this forms the basis for design of power supply systems.

9 Bibliography

[1] *Kröger, R. / Unbehauen, R.:* Elektrodynamik (Electrodynamics). Stuttgart: Teubner, 1990

[2] *Edel, R.; Schneider, E.; Schweller, M.:* Systemauslegung der Bahnstromversorgung (System design of traction power supply). In: Elektrische Bahnen 96 (1998), H.7, S. 213-221

[3] *Carson, J. R.:* Wave Propagation in Overhead Wires with Ground Return. In: Bell. Syst. techn. (1926), vol. 5., p. 539-554.

[4] *Dwight, H. B.:* A precise method of calculation of skin effect in isolated tubes. In: Journal AIEE (1923), p. 827-831

[5] *Pollaczek, F.:* Über das Feld einer unendlich langen wechselstromdurchflossenen Einfachleitung (The field of an infinitely long AC line). In: Elektrische Nachrichtentechnik (1926), S. 339-359.

[6] *Gukow, A.I.; Kießling, F.; Puschmann, R.; Schmieder, A.; Schmidt, P.:* Fahrleitungen elektrischer Bahnen (Contact line systems of electric railways). Stuttgart: Teubner, 1997.

[7] *Zimmert, G.; Hofmann, G.; Jecksties, R.; Kraft, R.; Schneider, E.:* Rückleiter in Oberleitungsanlagen auf der Strecke Magdeburg – Marienborn (Return conductor in the overhead contact line systems on the Magdeburg – Marienborn route). In: Elektrische Bahnen 92 (1994), H.4, S.105-111.

[8] Bundesgesetzblatt: Sechsundzwanzigste Verordnung zur Durchführung des Bundes-Immisionsschutzgesetzes (Verordnung über elektromagnetische Felder - 26. BImSchV). (German Federal Law Gazett: 26th Directive to execution of the Federal Emission Protection Law) Dezember 1996

[9] EN 50061/A1: Sicherheit implantierter Herzschrittmacher, Schutz gegen elektromagnetische Störungen.(Safety of implanted pacemakers, protection against electromagnetic interference) Juli 1996.

[10] ICNIRP Guidelines: Guidelines on limits of exposure to static magnetic fields, International Commission on Non-Ionizing Radiation Protection. 1993.

[11] IRPA/INIRC Guidelines: Interim Guidelines on limits of exposure to 50/60 Hz electric and magnetic fields, International Non-Ionizing Radiation Committee of the International Radiation Protection Association. 1989.

[12] *Kohling, A.; Zimmer, G.:* Beeinflussung von Bildschirmarbeitsplätzen durch Magnetfelder. (Interference to monitors caused by magnetic fields in monitors) in etz 114 (1993) H. 12, S.758-763.

[13] *Angerer, M.:* Auch Bahnstrom lässt den Bildschirm flimmern.(Traction current also causes flicker on the screen) In: Deine Bahn 1996, H.6, S.358-361.

[14] 1.EMVGÄndG, BGBl. I S1118: Gesetz über die elektromagnetische Verträglichkeit von Geräten (EMVG) (Law regarding equipment EMC). August 1995.

[15] ENV 50121, Teil 1 bis 5: Bahnanwendungen, Elektromagnetische Verträglichkeit (ENV 50121, Parts 1 to 5, Railway applications, EMC). Stand Dezember 1997.

[16] DS 997.0223, Geschäftsbereichsrichtlinie DB AG: Oberleitungsanlagen; Bahnerdung bei Bauwerken aus Beton. (Divisional Guidelines, DB AG, Contact line systems, earthing and bonding in concrete structures) Dezember 1996.

Siemens AG
Transportation Systems
Electrification
Postfach 3240
D-91050 Erlangen

E-Mail: electrification@ts.siemens.de

Internet: www.siemens.com/ts

Copyright © Siemens AG 2002. All rights reserved. Änderungen vorbehalten!

Appendix F

Observation of Bielefeld
B-Field Testing, May 2005

APPENDIX F

OBSERVATION OF BIELEFELD B-FIELD TESTING, MAY 2005

Prepared for LTK and Sound Transit

F. Ross Holmstrom, Ph.D.
7 June 2005

INTRODUCTION

On 23-24 May 2005 measurements were made at the University of Bielefeld of stray magnetic fields due to the No. 4 Line of the Bielefeld S-Bahn in Bielefeld, Germany. The measurement sessions were attended by this author, and by Mr. Thomas Heilig of TriMet in Portland, who served in the dual capacities of rail transit electrical power specialist and native German speaking translator.

The stray B-field measurements were made to document the observed fact that B-fields from the tram line do not interfere with research activities in Physics and Chemistry laboratories located 180 meters (590 ft) away from the nearest track.

Observations of the tests and direct communication with the testers and with University of Bielefeld enabled us to acquire more specific information regarding the B-field mitigation circuitry employed in Bielefeld than has been obtained previously.

The detail of the Bielefeld B-field mitigation plan most interesting to this author is the special design of the running rail supports used to reduce ground leakage currents.

The B-field data from the 23-24 May measurements will be available in approx. 2 months, and we have been promised a copy. Mr. Ulrich Bette of the Techniche Akademie Wuppertal, in Wuppertal, Germany who performed the measurements stated that brief examination of B-field levels during the testing indicated that they were consistent with previous measurement results, with stray tram-caused B-fields dropping to the level of background fluctuations at a distance of approx. 40 meters (130 ft) from the nearest track.

HISTORY

Figure 1 shows a map of a portion of the University of Bielefeld campus including the Tram Line No. 4 running NW to SE parallel to N. Universitätstrasse at the top. Physics laboratories are in Buildings D and E, and Chemistry laboratories are in Buildings E and F. This map is designed to show the physical relation of university buildings, tram line, TPSS, B-field mitigation region and roads. Lateral distances and critical building-to-track distances are shown fairly accurately. Other distances are very approximate.

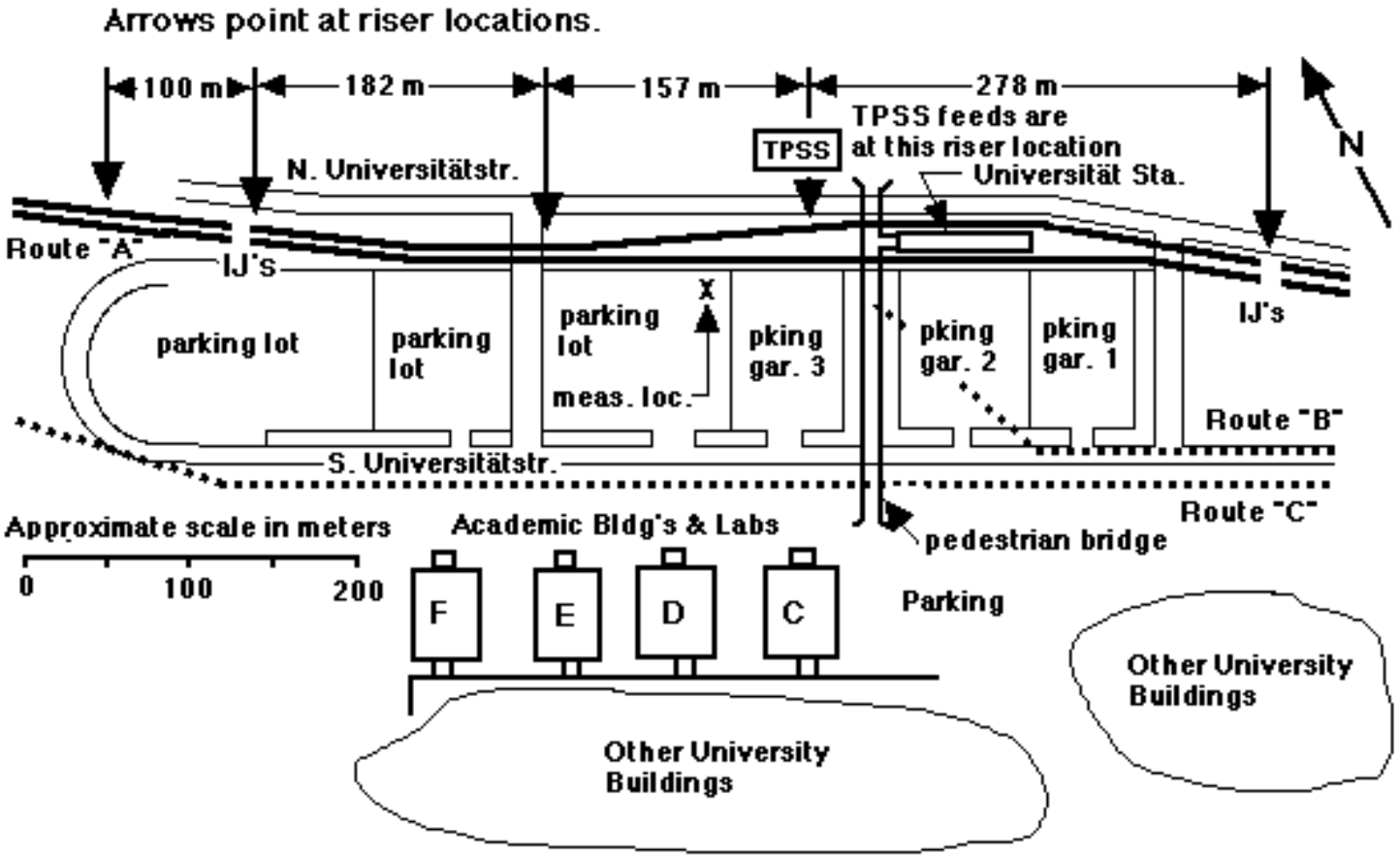

Figure 1. The University of Bielefeld and the adjacent Tram Line No. 4. The nearest track lies 180 meters (590 ft) from research labs in Buildings D, E and F.

The University of Bielefeld was founded in 1969 and construction continued into the 1970's. In the '70's a tram line from Bielefeld to the University was first proposed. One route was considered running along a ROW significantly farther SW of Buildings C, D, E and F than the distance from those buildings to the present ROW. However, this proposal was abandoned because it was not compatible with the desired proximity of a station to several residential areas NW of the campus.

Routes "A" (the one finally chosen), "B" and "C" were examined in greater detail. An organization of students at the University preferred Route "C". They stated that a premium should be placed on the safety of tram riders, especially women, who would have to walk a considerable distance from a Route "A" station to the university buildings, often under conditions of darkness.

Route "B" was abandoned because the University did not want to sacrifice Parking Garage No. 2. Arguments of Physics and Chemistry faculty that stray B-fields from Route C would disrupt research in Buildings D, E and F eventually prevailed. However to increase the safety of tram riders a pedestrian bridge was build linking the tram station to the vicinity of the university buildings. From the station platform one now ascends by elevator or stairs to the bridge one story aboveground and then walks above the eastbound track, past the parking garages under CCTV surveillance and across S. Universitätstrasse to the vicinity of the main university buildings.

To suppress stray B-fields to levels compatible with Physics and Chemistry research in Bldg's D, E and F, the design of the specialized DC propulsion feed circuitry was developed by Mr. Bette, incorporating the now familiar large diameter buried current feed cable beneath each track, with a product of cross section times depth chosen to equal the product of cross section times height of the overhead contact wire.

After the modeling of this design predicted that stray B-field levels would be compatible with research in the laboratories, the tram line was build. It entered service in the late 1990's. Subsequent preliminary B-field measurements, as well as observations in the laboratories, showed that stray B-field levels were consistent with predicted values and that those values did not interfere with research.

Scheduling of the final B-field measurements just made was delayed until an insulated joint was installed in the structure of the pedestrian bridge, to prevent ground leakage currents from entering the bridge at the northern end near the tracks and being conducted to the proximity of the main university buildings. The first insulated structural joint was electrically bridged in some fashion and failed to work. The second insulated joint performed satisfactorily, and the hopefully definitive measurements of stray B-field levels now have been made.

LABORATORY EQUIPMENT

On Mon. 23 May Prof. Willi Schepper of the U. of Bielefeld Physics Dept. joined us briefly and went over the facts regarding physics chemistry labs. We also met Prof. C.R. Rabl, now retired from the Chemistry Dept., who graciously took us to lunch at the Student Union.

The northern walls of Buildings D, E and F (not the protruding stairwells) lie 180 meters from the nearest tram track. The University's maximum stray B-field level due to tram operations is 0.5 mG (50 nT).

Physics lab equipment in Buildings D and E includes scanning electron microscopes and mass spectrometers including time-of-flight mass spectrometers. Much of the physics research involves magnetic materials and devices, including observation of giant magnetoresistance and tunneling magnetoresistance in layered structures. Researchers at U. of Bielefeld also construct and use SQUID B-field sensors and MRI scanners.

Chemistry lab equipment in Buildings E and F includes ultra-high field solution NMR apparatus. Dr. Schepper noted points concerning the operation of the NMR apparatus that we have heard from the UW chemists: B-field fluctuations must not be so rapid as to overwhelm the Deuterium B-field compensation circuitry; and, the low level of B-field fluctuations must be maintained continually over the days required to run individual experiments.

B-FIELD MEASUREMENTS

The measurement location was in the parking lot adjacent to Parking Garage No. 3 in the vicinity of the "X" labeled "meas. loc." in Figure 1. A Hall effect B-field sensor was permanently set up 5 meters from the nearest track to obtain an unambiguous signal from every passing train.

A 3-axis fluxgate magnetometer was set up at a variety of distances from 5 to 40 meters distance from the nearest track and left at each location long enough to record B-fields from the passage of several trains in each direction. This magnetometer was a Bartington Instruments (www.bartington.com) unit capable of sensing B-field fluctuations with 30 pT (0.03 nT= 0.3 μG) noise level and 1 nT (0.01 mG) resolution. For measuring B-field fluctuations the instrument was set up to null out the output signal due to the steady background B-field, and to produce an analog signal out proportional to the fluctuation level. These analog output signals were recorded using data loggers. The data loggers were all time-synchronized so that their stored data could be referenced to the data from the Hall sensor.

At a distance of 40 meters from the track Mr. Bette said that the magnitude of B-field fluctuations from train operation was already lower than the level of fluctuations in the ambient background, so there was little point in continuing observations at greater distances.

TRAIN AND PROPULSION CHARACTERISTICS

Each train operating on the No. 4 line past the university consists of two powered end cars with a trailer car in the middle. The trailer cars do have pantographs to provide auxiliary power. Each powered car draws a maximum of 1.4 kA, for total of 2.8 kA max for the train, which happens to be the same max. train current as for 4-car Link light rail trains. DC voltage is 750 volts.

MITIGATION REGION

The B-field mitigation region near U. of Bielefeld is divided into two portions. The main portion has its SE end at insulated joints 278 meters (912 ft)SE of the TPSS feed point, and its NW end at insulated joints 182 + 157 = 339 meters (1112 ft) NW of the TPSS feed point. A secondary portion runs from thse NW insulated joints for an additional distance of 100 meters (328 ft).

In the main mitigation region a buried primary current cable runs beneath the center line of each track and is connected to that track's OCW by four risers with spacings of 182, 157 and 278 meters as shown in Figure 1. In this region the running rails of the two tracks are not cross bonded and the OCWs are not cross connected.

In the secondary mitigation region the running rails of the two tracks are cross bonded, the OCWs are cross connected, and a single buried cable is used for the ROW, running down the center of the ROW between the tracks.

At each insulated joint location there is a break in the overhead contact wire that is bridged when a pantograph passes. The insulated joints in each pair are also staggered in location to assure that at least one axle of each truck will bridge the IJ pair longitudinally when the pantograph transits the gap immediately above. This design was implemented to diminish RF emissions due to arcing.

The TPSS shown in Figure 1 just north of Parking Garage 3 contains three separate floating and isolated propulsion rectifiers. One of these rectifiers powers the eastbound track in the main mitigation region, and one the westbound track The third powers both tracks in the secondary mitigation region and the electrically connected ROW that continues another 700 meters NW to the end of the line.

Tram Line No. 4 uses a 1 meter buried cable depth. Dual 240 mm^2 buried cables are used with total cross section of 480 mm^2 (947 kCmil).

Risers are composed of triple 95 mm^2 conductors with total cross section of 285 mm^2 (562 kCmil). Each riser conductor has its own clamp contact to the OCW, providing redundancy for this critical connection. Of the 15 clamped riser contacts originally installed only one was bad, and that was caught at the time of installation. All the riser contacts appear to have stayed good subsequently.

Max allowable OCW wear is 20 percent.

GROUND LEAKAGE CURRENT CONTROL

One of our most significant observations at Bielefeld was of a design feature used to diminish ground leakage currents from the running rails. Each running rail rests on a concrete pier approx. 16 inches (40 cm) wide by 16 inches deep that runs longitudinally the length of the line. Each pier contains steel reinforcing rods that are welded together end-to-end to form a continuously conducting metallic path from one end to the other.

The purpose of these continuous conducting paths is to intercept leakage currents from the rails so that they do not leak into the ground. In practice, when propulsion currents in the rails raise the voltage at one end of the rail section and lower the voltage of the other end, current that has leaked out of the running rail and into the re-bar at the high-voltage end will flow down the length of the re-bar and back into the running rail at the other end, thus constraining such leakage currents to take a well-defined path in close proximity to the running rail.

At periodic intervals the re-bar conducting paths are broken and leads are brought up to terminal points at the upper surfaces of the piers. Normally these terminal points are jumpered together. When it is desired to measure the leakage current flowing in the re-bar, the jumpers are replaced by ammeters.

Periodically the rail to re-bar resistance is measured to verify the resistance of the rubber insulating pads between the rails and supporting piers.

Thomas Heilig of Tri Met noted that the provision of longitudinally continuous conducting paths through welded re-bar was a standard practice in US rail transit systems to reduce ground leakage currents in those locations where running rails were mounted on concrete.

Perhaps plans for North Link already call for such conducting re-bar paths. If they do not, they certainly should be considered. In discussions with ST personnel they have noted that the North Link roadbed through the UW campus might include large concrete slabs placed on top of neoprene vibration barriers, with the slabs butted end-to-end clear from Montlake to NE 45th St. In such a case it would be fairly straightforward to include continuously welded re-bar for the length of each slab, bring conductors from the re-bar up to the surface at each end of each slab, and jumper slab-to-slab to provide the continuous circuit.

The inclusion of the conducting paths described above would not change the B-field levels that have predicted to date that assumed zero ground leakage current. However such inclusion probably would decrease the likelihood that any leakage of propulsion current out of the rails would adversely affect UW labs, and would increase the confidence of UW researchers that such ground leakage currents would not interfere with their work.

Measured rail-to-rebar conductance on at-grade sections of the tram line is 26 mS/km for one rail or 52 mS/km for the two rails of one track.. In tunnels away

from stations the figure is lower at 1 to 10 mS/km, and I forgot to ask if this was for one rail or for two. Near stations conductance is higher because of the moisture resulting from cleaning the stations. Observations to date indicate that ground leakage currents have not caused adverse B-field levels at U. of Bielefeld labs.

RAIL TO GROUND VOLTAGE MONITORING

In the propulsion substation on each propulsion circuit there is a relay that is closed, shorting rails to ground, when rail-to-ground voltage exceeds 60 volts in magnitude. After 10 sec it re-opens. But after the third closing, it stays closed.

FURTHER DETAILS

Additional data gathered by Thomas Heilig during the Bielefeld visit is presented here:

Track Structure: Two reinforced concrete beams, 40 by 40 cm, poured in place, re-bar continuously welded. Rebar cross bonded every 100 m. Rail cross bonded every 125m (VDV requirement?). Meter gauge. Direct fixation track, S49 T-rail, using insulated pads. Grass track to base of rail. Grass growing quite high and contacting rail in places.

Eastbound and westbound tracks in mitigation area are electrically not cross bonded

Track-to-rebar resistance was measured at a re-bar cross bond: 31.5 Ohm for single track / two-rail section, total segment length 617 m = 52 mS/km.

Previous measurements were referenced: Similar value was obtained after construction, intermediate measurement during wet conditions showed ~200 mS/km.

Re-bar to earth resistance is very low, earlier measurements showed 25 mili-Ohm for the entire mitigation section (617 m, one track)

Earth gradient potential was measured over a four-hour period during Tuesday's test. A copper-sulfate probe was installed in the earth 1 m south from the southernmost rail. A second probe was installed approximately 40 m further south, a location considered remote earth potential. Typical values observed during train passings were in the plus/minus three mV range. However, the peak values stored during the measurement period were + 72 mV and – 42 mV.

The substation is located near the University passenger station, close to second riser. The second riser is the feed point from the substation.

Four rectifiers/breakers are in the substation:

1. Feeds track-section west of mitigation section
2. Feeds eastbound track in mitigation section
3. Feeds westbound track in mitigation section
4. Feeds track-section east of mitigation section, likely including easternmost mitigated segment.

Main mitigation section is 617 meters long. Insulated joints and bridging section insulators in each track at each end. Insulated joints in the two rails of a track are offset by approximately 4 meters, section insulator located in the middle.

OCS: Fixed tension catenary, messenger wire insulated and non current-carrying. Non-insulated overlap located between riser 2 and riser 3.

Station ground separate from utility ground and university facility ground. Pedestrian bridge between Station and University built with insulated joint, located approximately 30 m South of track. This IJ never worked properly, so it was abandoned and new insulated joints were installed at South end of bridge, at bridge to Parking Garage 3 connection, and at bridge to stairs/elevator connection (directly opposite to Parking Garage 3 connection. The entire bridge is on station ground potential.

Short circuit switches are installed at the University Passenger Station, connecting rail to the station ground in case of a rail-to-earth overvoltage. (see attached brochure from Thomas Schmid from Siemens).

Rail-to-earth monitoring devices are also set up in the same location. Their purpose is to detect a low rail-to-earth resistance. The continuously monitor rail-to-earth voltage and send an alarm if a preset voltage level is not exceeded within a predetermined time period. For the mitigation section, the alarm limit was 3 V (?) in a 72 hour period.

Four fault conditions were set up:

1. Eastbound and westbound OCS and track connected in parallel at the substation.
2. Track sections east and west of the mitigation sections connected with each other at the substation
3. Mitigation area connected to track-section to the west (?)
4. Mitigation area connected to track-section to the east (?)

Measurement location roughly halfway between riser 2 and riser 3.

Cars: Eight-axle M8C and M8D cars, 4 axles powered. MoBiel has 80 power cars and five un-powered four-axle trailers. On the University Line, due to high passenger loads, they usually operate a three-car consist, assembled of two M8 power cars and one 4-axle trailer car in the middle.

CONCLUSIONS

Data gathered during the trip to observe the Bielefeld measurements filled in many of the gaps in our knowledge of the B-field mitigation system employed there.

The amount learned about the rail mounting procedures for combating ground leakage current, including the continuously welded re-bar in the concrete rail supports, was especially gratifying, since we knew nothing about these procedures before our trip.

We will have to wait approx. 2 months to obtain the results of B-field measurements. However, even before that data arrives, the information learned about the rail mounting procedures is very valuable.